Anti-inflammatory actions of boswellic acids: Identification and critical evaluation of molecular targets and signaling pathways

Entzündungshemmende Wirkungen von Boswelliasäuren: Identifizierung und kritische Evaluierung molekularer Targets und Signalwege

D I S S E R T A T I O N

der Fakultät für Chemie und Pharmazie
der Eberhard Karls Universität Tübingen

zur Erlangung des Grades eines Doktors
der Naturwissenschaften

2009

vorgelegt von

Ulf Siemoneit

Tag der mündlichen Prüfung: 24. April 2009

Dekan: Prof. Dr. L. Wesemann

Erster Berichterstatter: Prof. Dr. O. Werz

Zweiter Berichterstatter: Prof. Dr. S. Laufer

“Wege entstehen dadurch, dass man sie geht.” (Franz Kafka)

TABLE OF CONTENTS

INDEX OF FIGURES

INDEX OF TABLES

1 ABBREVIATIONS

[^{3}H]-AA	tritium labeled arachidonic acid
(A)KBA	(3-*O*-acetyl)-11-keto boswellic acid
(A)β-BA	(3-*O*-acetyl)-β-boswellic acid
(K)BA-Seph	11-(keto)-β-boswellic acid coupled to Sepharose
$[Ca^{2+}]_i$	intracellular Ca^{2+} concentration
12-HHT	12(S)-hydroxy-5-cis-8,10-trans-heptadecatrienoic acid
ADP/ATP	adenosine diphosphate/adenosine triphosphate
Akt/PKB	protein kinase B
ANOVA	Analysis of variance between groups
AUC	area under the curve
B. spec.	*Boswellia species*
BAs	boswellic acids
BSA	bovine serum albumin
$CaCl_2$	calcium chloride
CDC	cinnamyl-3,4-dihydroxy-alpha-cyanocinnamate
COX	cyclooxygenase
cPGES	cytosolic prostaglandin E_2-synthase
CYP450	cytochrome P450
DAG	diacylglycerol
DMSO	dimethylsulfoxide
DTT	dithiothreitol
E. coli	*Escherichia coli*
EDTA	ethylenediaminetetraacetate
EET	epoxyeicosatrienoic acid
ELISA	enzyme-linked immunosorbent assay
ERK	extracellular signal-regulated kinase
FCS	fetal calf serum
FLAP	5-lipoxygenase-activating protein
fMLP	N-formyl-methionyl-leucyl-phenylalanine
GPCR	G protein-coupled receptor

GSH	glutathione
H(P)ETE	hydro(per)oxy-eicosatetraenoic acid
HEPES	N-2-Hydroxyethylpiperazine-N'-2-ethanesulfonic acid
HLE	human leukocyte elastase
HPLC	high pressure liquid chromatography
i.p.	intraperitoneal
IgG / IgM	immunoglobuline G/M
IKK	IκB-kinase
IL	interleukin
IP3	inositoltrisphosphate
LB-medium	Luria Broth base - medium
LO	lipoyxgenase
LPS	lipopolysaccharide
LT	leukotriene
MAPEG	membrane-associated proteins involved in eicosanoid and glutathione metabolism
MAPK	mitogen-activated protein kinase
MK-886	(3-[1-(4-chlorobenzyl)-3-t-butyl-thio-5-isopropylindol-2-yl]-2,2-dimethylpropanoic acid)
MM6	human monocytic-like cell line
mPGES	mircosomal prostaglandin E_2-synthase
MQ	Milli Q water
MS	mass spectrometry
NFκB	nuclear factor κ B
NSAIDs	non-steroidal anti-inflammatory drugs
OA	osteoarthritis
OD	optical density
p12-LO	platelet-type 12-lipoxygenase
PAF	platelet-activating factor
PAR	protease-activated receptor
PBS	phosphate-buffered saline
PC	phosphatidylcholine
PDGF	platelet-derived growth factor

PG	prostaglandin
PG buffer	PBS plus 1 mg/ml glucose
PGC buffer	PG buffer plus 1 mM $CaCl_2$
PGES	prostaglandin E_2-synthase
PI3K	phosphatidylinositol-3 kinase
PIP2	phosphatidylinositol-4,5-trisphosphate
PIP3	phosphatidylinositol-1,4,5-trisphosphate
PLA_2	phospholipase A_2
PLC	phospholipase C
PMNL	polymorphonuclear leukocytes
PMSF	phenylmethylsulfonylfluoride
PRP	platelet rich plasma
pTyr	phosphor-tyrosine
RA	rheumatoid arthritis
ROS	reactive oxygen species
RP	reversed phase
RT	room temperature
RTK	receptor tyrosine kinases
RU	response units
SDS	sodium dodecylsulfate
SDS-b	2× SDS loading buffer
SDS-PAGE	SDS-polyacrylamide gel electrophoresis
Seph	EAH-Sepharose 4B
SPR	surface plasmon resonance
TBS	tris-buffered saline
TFA	trifluoro acetic acid
TNFα	tumor necrosis factor alpha
TXA_2	thromboxane A_2
w/o	without
WB	Western blot

2 INTRODUCTION

2.1 Boswellic acids

2.1.1 Origin and historical background

Frankincense (also termed olibanum or salai guggal) is the natural oleum gum resin obtained from *Boswellia species* (*B. spec.*), including *B. carterii, B. sacra, and B. serrata* belonging to the family of Burseraceae. The "boswellia tree" (**Figure 2.1**) is native to Arabia (Yemen and Oman), East Africa (Eritrea, Somali and Sudan) and India. Frankincense has a long tradition for use e.g., in religious ceremonies, perfume production and its medicinal properties are reported since millennia, firstly described in the Ebers papyrus, 16 th century BC [1] and also mentioned in scripts of Hippocrates and Celcus [2]. Lipophilic preparations of frankincense (mainly derived from *B. serrata*) are traditionally applied in the Indian ayurvedic medicine with various therapeutic indications including diarrhea, cardiotonic actions and mainly inflammatory-related disorders. Indeed, analgesic, anti-inflammatory and antiarthritic effects of *B. spec.* extracts in animals were published in initial studies [3, 4]. In the last two decades cumulating evidence from experimental animal models and human clinical studies confirmed an anti-inflammatory, immunomodulatory and anti-tumor potential of frankincense preparations (for review see [5, 6]). Today, the dried gum resin from *B. serrata* is listed as a monograph in the European Pharmacopoeia (6.0) and a dried ethanolic extract of *B. serrata* resin (H15® Gufic), approved in a part from Switzerland, was designated by the EMEA (European Agency for the evaluation of Medicinal Products) in 2002 as an orphan drug for the treatment of peritumoral brain edema.

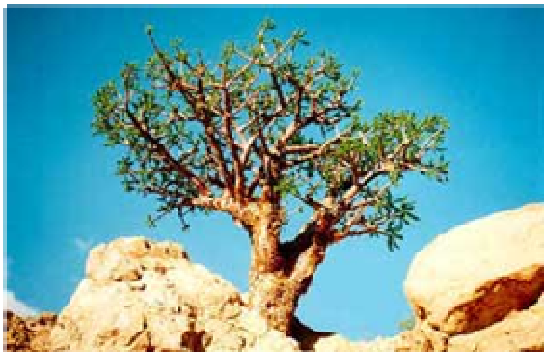

Figure 2.1: *Boswellia serrata* tree (left) **and frankincense** (right)**.**

The gum resin of *B. serrata* is composed of ~10% volatile oil (mono- and sesquiterpenes), ~15-20% water-soluble gum (polysaccharides) and lipophilic di- and triterpenes (~ 70%) [5]. Within the lipophilic fraction of frankincense, the pentacyclic triterpenes boswellic acids (BAs) were identified as the major constituents [7] (**Table 2.1**) and are regarded as the pharmacological principles of these preparations. Note that also structurally related amyrins and ursolic acid were detected in considerable amounts.

Table 2.1: Contents of various BAs in the dry extract of *B. serrata* gum resin (adopted from [7])**.**

Compound	Content in %
β-BA	18.2
Aβ-BA	10.5
KBA	6.1
AKBA	3.7
α-BA	13.2

BAs (**Figure 2.2**) exist in a α- (geminal methyl groups C-20) or β-configuration (vicinal methyl groups C-19/C-20) and several pharmacological studies confirmed a superior effectiveness of β-configurated BAs (β-BAs) over the α-form [6]. Further structurally variation is given by the occurrence of a carbonyl moiety at position C-11, yielding 11-keto-BAs and the presence of an acetyl group at the hydroxyl function at C-3. It was reported that these structural differences are crucial determinants for the potency of BAs to interfere with several targets or signaling pathways [9-11]. The related pentacyclic triterpene α-amyrin lacks essential functional characteristics, namely the 4-carboxylic group. These properties render α-amyrin a useful pharmacological tool, serving as negative control.

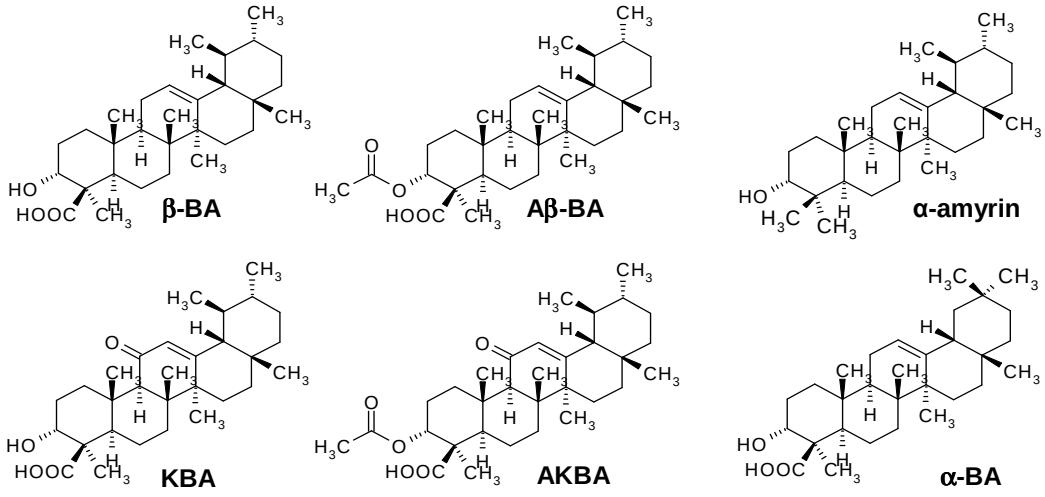

Figure 2.2: Chemical structures of BAs and α-amyrin
β-BA (β-boswellic acid); Aβ-BA (3-*O*-acetyl-β-boswellic acid); KBA (11-keto-β-boswellic acid) AKBA (3-*O*-acetyl-11-keto-β-boswellic acid); α-BA (α-boswellic acid).

2.1.2 Pharmacokinetic properties of BAs

Since the bioavailability reflects the extent of therapeutically active drug that reaches systemic circulation and its disposability at the site of action, pharmacokinetic knowledge of a given drug is a crucial factor to evaluate its pharmacological efficacy [12]. Initial pharmacokinetic studies conducted in humans revealed comparably low concentrations of 11-keto-BAs in plasma [13, 14]. After single dose application of up to 1600 mg *B. spec.* extract, plasma levels of max. 2 µM KBA and no detectable amounts of AKBA were found, whereas BAs lacking the 11-oxo moiety were not determined. The plasma concentration of KBA declined with an elimination half life of approx. 6 h, indicating the prerequisite of a repeated application per day. A detailed analysis of pentacyclic triterpenes, including all four major β-BAs performed by Buechele and Simmet [7] revealed plasma levels as follows: 0.1 µM AKBA, 0.34 µM KBA, 2.4 µM Aβ-BA and 10.1 µM β-BA. Notably, these plasma levels were detected after the daily intake of 4 × 786 mg *B. serrata* extract for 10 days. Finally it was found that administration of a *B. spec.* extract concomitantly with a high-fat meal led to approx. 3-fold increased bioavailability of β-configurated BAs [15]. Ongoing efforts to address factors responsible for the poor bioavailability of 11-keto-BAs demonstrated an extensive phase I metabolism for KBA *in vitro* and *in vivo*. In contrast, AKBA was metabolically unaffected and a deacetylation to KBA was excluded [16]. Moreover, poor permeability for both 11-keto-BAs in the Caco-2 model became evident and in contrast to a previous study [17], AKBA and KBA were not identified as substrates of P-glycoprotein [18]. Nonetheless, an interference with the activity of organic anion transporter $B_1$13 and multidrug resistance protein 2 in a cellular model was observed [18]. Since nonselective interference of BAs with cytochrome P450 (CYP450) enzymes has been demonstrated before [19], pharmacologically relevant interactions with other anionic substances (e.g. bile acids or drugs) should be considered while administering *B. spec.* extracts to humans.

2.1.3 Therapeutic value of BAs in disease treatment

As mentioned above, multiple experimental animal models indicate a beneficial impact of isolated BAs or frankincense preparations containing BAs for the treatment of inflammation-related disorders such as atherosclerosis [20], arthritis [21-23], ileitis [24], colitis [25-27], hepatitis [28, 29], autoimmune encephalomyelitis [30], gastric ulcer [31]. Also cancer [32, 33], pain [3, 34], hyperlipidemia [35], allergy [36] and diabetes [37] were modulated.

The clinical effectiveness of diverse *B. serrata* preparations has been studied in several human trials. At least the methodological quality of these studies differs concerning number of patients, content and strength of medication as well as placebo control or comparison against active treatments [38], thus, hampering explicit evaluation. Promising effects of *B. spec.* extracts were reported for the treatment of osteoarthritis (OA) manifested in reduced pain and increase in knee flexion [39, 40], and more recently a significant decrease in the WOMAC (Western Ontario Mac Master) Index was reported for the OA-suffering collective versus the placebo group [41, 42]. However, a clinical trial analyzing the impact of H15® treatment in addition with steroids and/or nonsteroidal anti-inflammatory drugs (NSAIDs) on rheumatoid arthritis (RA) revealed no significant reduction of efficacy parameters (e.g. pain) [43].

Patients suffering from chronic inflammatory bowel diseases encompassing ulcerative colitis, Crohn`s disease and collagenous colitis were treated with H15® or other *B. serrata* preparations and a remarkable improvement in disease parameters (stool frequency, histopathology, remission and Crohn`s Disease Activity index) confirmed clinical relevance, being almost equipotent or even superior to sulfasalazine or mesalazine [44-46]. In 1998, a trial with bronchial asthma patients [47] reported clinical relevance (70% remission) for the *B. spec.* extract-treated collective. The efficacy of H15® administration for several months in patients suffering from intracranial tumors [48] or glioblastoma and leukoencephalopathy [49] was investigated. In both studies no anti-proliferative or anti-neoplastic effects were observed but tumor-associated progressive edema was significantly attenuated [49]. Moreover, for some patients amelioration in health parameters and neurological symptoms was registered suggesting beneficial effects for H15® application in central nervous system tumors. These results eventually led to the orphan drug status of H15® for the treatment of peritumoral brain edema (see above). Side effects of *B. spec.* extracts in all clinical trials were minute and not different from those noted in placebo groups. No markedly differences in safety and laboratory (hematological, biochemical or histological) parameters were evident during the studies [39, 41, 50] and recently, moderate to low toxicity for *B. serrata* extracts and AKBA on the skin after topical application was demonstrated [51].

All trials conducted to demonstrate effectiveness of *B. serrata* preparations were carried out with small patient numbers, sometimes even lacking essential study parameters, and except for OA

independent replications are still missing. Nevertheless, these data together imply an efficacy and therapeutic value of *B. spec.* extracts to treat various diseases caused or maintained by inflammatory processes but additional well-controlled investigations are required to warrant treatment with *B. spec.* extracts or purified BAs a convincing therapy.

2.1.4 Pharmacological actions and proposed molecular targets of BAs

In order to identify pharmacological principles and mechanisms of action of frankincense responsible for the effectiveness observed in clinical trials and in experimental animal models multitude of experiments on the cellular and molecular level employing isolated BAs, mixtures of them or crude B. spec. extracts were performed. It should be emphasize that in general AKBA was assumed to be the most potent and pharmacologically relevant BA analogue and many studies neglected other natural occurring BAs as potential key players. Initially, frankincense extracts were found to inhibit leukotriene (LT)B4 formation in activated rat polymorphonuclear leukocytes (PMNL) [52] and also isolated BAs blocked LT formation in this assay [53]. Since BAs interfere with 5-lipoxygenase (5-LO), the key enzyme in LT biosynthesis [54-57], a molecular mechanism underlying the anti-inflammatory effectiveness of frankincense preparations was proposed. Among the four major β-configurated BAs from frankincense, AKBA is the most potent analogue with IC_{50} values in the range of 1.5 to 50 µM, depending on the assay conditions (e.g. species, cell type, cell-free or cell-based assays, stimuli etc.) described by [57] and this study. AKBA seemingly belongs to the class of nonredox-type 5-LO inhibitors [53] and interferes in the presence of Ca^{2+} with a fatty acid-binding site of 5-LO distinct from the substrate binding cleft which was shown using a photoaffinity analogue of AKBA [55]. The interference with other arachidonic acid (AA) metabolizing enzymes such as 12-lipoxygenase (12-LO) or cyclooxygenase (COX) has long been excluded [53] but was later reconciled by Poeckel et al. [8] for platelet-type (p)12-LO and by Frank and Unger [19] for CYP450 enzymes and in this thesis for COX-1.

Further attempts to elucidate molecular targets of BAs identified the human leukocyte elastase (HLE). HLE release from PMNL is activated through a broad range of stimuli and connected to a variety of inflammatory and hypersensitivity-related disorders. Direct inhibition of HLE activity was found for AKBA (IC_{50} = 15 µM) but also β-BA and other related pentacyclic triterpenes including amyrin and ursolic acid ($IC_{50} \leq 2$ µM) were active [58, 59]. Recently, nonselective inhibition of recombinant CYP enzymes (CYP 2C8, 2C9, 3A4) by AKBA, KBA and β-BA in the range of 5-10 µM [19] as well as for several B. spec. extracts has been described, indicating a possible influence on drug metabolism in vivo.

In addition, key players of intracellular signaling such as protein kinase B (PKB/Akt) and the mitogen-activated protein kinases (MAPK) ERK1/2 and p38 MAPK were objects of intensive investigations. It was found that AKBA (> 15 µM) impaired ERK1/2 activation in platelet-derived growth factor (PDGF)-stimulated meningioma cells [60] but failed to do so in tumor necrosis factor (TNF)-α activated human myeloid cells [61]. Interestingly, in lipopolysaccharide (LPS)-challenged peripheral blood mononuclear cells (PBMC) the extract of *B. serrata* prevented phosphorylation of the MAPKs c-Jun *N*-terminal kinase (JNK) and $p38^{MAPK}$ while no inhibition was seen for ERK phosphorylation [62]. In MM6 cells AKBA (30 µM) markedly attenuated fMLP-induced phosphorylation of $p38^{MAPK}$ and in contrast also impaired activation of ERK1/2 which was accompanied by decreased basal and agonist-induced intracellular Ca^{2+} levels [10]. Whereas in human PMNL, 11-keto-BAs (30 µM) induced Ca^{2+} mobilization, activated $p38^{MAPK}$ and ERK1/2, evoked reactive oxygen species (ROS) formation, and caused AA-release, BAs lacking the 11-keto moiety were less effective [9, 63]. Also in human platelets, BAs differentially interfered with cellular signaling pathways. Thus, BAs lacking the 11-oxo moiety (i.e. β-BA) exhibited agonistic effects on Ca^{2+} mobilization, induced phosphorylation of Akt, $p38^{MAPK}$ and ERK1/2 and caused liberation of AA, generation of thrombin and delayed platelet aggregation. In contrast, the 11-keto analogues, AKBA and KBA were hardly effective or even failed at all in this respect [64 and this study]. The effect of BAs on AA-release and p12-LO activity in human platelets was studied in more detail. Whereas both, β-BA and AKBA enhanced the release of AA via cytosolic phospholipase A_2, the former generation of the p12-LO product 12-hydro(per)oxy-eicosatetraenoic acid (12-H(P)ETE) was markedly induced only by β-BA and cell-free assays revealed detrimental effects of AKBA (IC_{50} = 17 µM) on 12-H(P)ETE formation. In addition, immobilized KBA selectively precipitated p12-LO from platelet lysates implying p12-LO as a select molecular target of BAs [8] (**Table 2.2**). Regarding the anti-inflammatory potential of 3-*O*-acetyl-BAs (i.e., AKBA and Aβ-BA), the interference with nuclear factor (NF)-κB signaling in peripheral monocytes was reported. Thus, AKBA limited TNF-α signaling presumably by direct interference with inhibitor of NF-κB (IκB)-kinase (IKK) [65], and reduced TNF-α-induced expression of pro-inflammatory matrix metalloproteases and the adhesion receptors VCAM-1 and ICAM-1 in human microvascular cells were reported [66].

Table 2.2: Proposed molecular targets of AKBA (modified according to [6]).

Target	EC_{50}/IC_{50}	Reference
human/rat 5-LO	1.5-50 µM	[53, 54, 57]
HLE	15 µM	[58]
human topoisomersases I/IIa	30 µM	[80]
human recombinant IκB kinase α/β	30 µM	[65]
human recombinant CYP450	5-10 µM	[19]
human p12-LO	15-20 µM	[8]

There are reports about the interference of several BAs with the humoral and cellular immune response such as suppression of leukocyte infiltration [67] and anti-complementary activity through inhibition of C3-convertase [68], modulation of T helper cell cytokine production, and enhanced T-lymphocyte proliferation [69, 70]. Also, numerous studies were performed describing effects of BAs, in particular of AKBA on cell proliferation, differentiation, and cell death. Multiple investigation demonstrated cell growth inhibition by BAs in various leukemia cell lines [71, 72] with an $IC_{50} \approx 30$ µM for AKBA [73], as well as for colon cancer cells and meningioma cells [60, 74]. Effects on cell differentiation were shown for *B. spec.* extracts and isolated BAs [71, 75, 76]. These effects were related to induction of apoptosis [77-79] and continuing analysis revealed the inhibition of topoisomerase I and IIa as responsible molecular targets of BAs with IC_{50} = 1-50 µM, depending on their structure [73, 76, 80]. Further studies elucidated that BAs trigger apoptosis via the caspase 8-mediated pathway [81-83]. However, the expected interaction with the upstream receptor Fas/FasL was excluded [84] and for AKBA the death receptor 5-mediated pathway seemed to be responsible for capase 8 activation in prostate cancer cells [85]. Recently, an inhibitory effect of AKBA (30 µM) on the androgen receptor by interference with SP1 binding activity in prostate cancer cells was reported [86]. Moreover, after AKBA treatment (10-50 µM) gene products connected to cell proliferation (e.g. cyclin-D1) and anti-apoptosis (Bcl-2, Bcl-X_L, survivin, mcl-1) were suppressed. These effects were preferably related to interruption of NF-κB-signaling on the "Akt level" [61] rather then to direct interaction with IKK [87]. Besides interference with the NFκB route repression of signal transducers and activators of transcription (STAT)-3 in multiple myeloma cells via protein tyrosine phosphatase SHP-1 by AKBA was demonstrated [88].
Conclusively, modulation of cell death signaling by BAs shares common apoptotic mediators and functional downstream effectors but remain to be clearly illustrated.

In summary, isolated BAs and diverse *B. spec.* extracts modulate a large number of pivotal cellular and molecular mechanisms involved in inflammation and cancer. Nevertheless, there are

evident discrepancies in the efficacy of purified BAs (also depending on their structure) and the crude *B. spec.* extract. Obviously, there are stimulatory as well as inhibitory effects exerted by the same compound depending on the experimental conditions (e.g. cell type or stimulus). Moreover, the required concentration of AKBA (the most extensive addressed BA) to induce any biological effect is far above the reachable plasma level after oral application of frankincense preparations, and therefore the interference with the assumed targets, especially in a physiological context, remains questionable.

2.2 Inflammation

Inflammation is a biological response of the immune defense against challenges originating from the surrounding environment. Challenge of host tissues due to traumatic, infectious or toxic injury or lesions lead to a complex series of vascular and cellular events carried out by the organism to remove the injury and to initiate the healing process, resulting in the release of different biochemical mediators. These events give in turn rise to the initial cardinal signs of inflammation defined by Celcus AD40: rubor (redness), calor (heat), tumor (swelling) and dolor (pain) [89]. They reflect vasodilatation and its resulting increased blood flow, enhanced permeability of blood vessels and peripheral nervous tissue stimulation. The host protective response is normally followed by a timely resolution of inflammation, which ensures a self-limitation of the process. However, depending on the extent of the insult, prolonged inflammation can lead to a chronic condition and eventually to loss of function (functio laesio), if a complete healing of the tissue fails.

The inflammatory challenge consists of a large and complex regulated number of biochemical events including cellular, molecular and physiological changes in response to the harmful stimuli. They involve the immune system (e.g. complement system), the local vascular system, and cells resident within the injured tissue (e.g. mast cells). These cells produce multiple early inflammatory mediators including cytokines (e.g. interleukin 1 (IL-1), TNF), plasma proteins (bradykinin, thrombin), histamine, and bioactive lipids. These early events enable the successive recruitment of leukocytes (neutrophils, monocytes/macrophages and lymphocytes) from the blood which, in turn, release further pro-inflammatory signals (mediators) [90]. Among these mediators, the lipid metabolites derived from the precursor AA, the so-called eicosanoids, are well established to play key role(s) as signaling molecules in inflammation [91]. Thus, pharmacological modulation of eicosanoid formation is considered as an appropriate intervention with beneficial effects in the treatment of inflammatory disorders including atherosclerosis, inflammatory bowel diseases, asthma, arthritis and also of cancer.

2.2.1 The arachidonic acid cascade

Arachidonic acid (AA) is a carboxylic acid with a 20-carbon chain and four cis-configurated double bonds (all-*cis* 5,8,11,14-eicosatetraenoic acid): the first double bond is located at the sixth carbon from the omega end (20:4;ω-6). The polyunsaturated AA is abundantly incorporated in an esterified form (sn-2) into membranous phospholipids (e.g. phosphatidylcholine (PC) or phosphatidylethanolamine). Cellular activation by an appropriate stimulus (e.g. platelet activation with thrombin) induces the release of AA from cellular membrane phospholipids via

the activity of the enzyme phospholipase A_2 (PLA_2) (see **2.2.2**). Once liberated, free AA functions as a second messenger itself [92], is re-incorporated into phospholipids, or serves as the premier precursor of eicosanoid biosynthesis in mammalian cells. The conversion of AA into eicosanoids is govern by three classes of enzymes (**Figure 2.3**) which initially incorporate oxygen at different positions of the substrate: i) cyclooxygenases (COXs), which initiates the synthesis of prostaglandins (PGs) and thromboxanes (TXs), altogether termed prostanoids; ii) lipoxygenases (LOs), such as 5-LO, which catalyses the formation of leukotrienes (LT) as well as 12- and 15-LOs yielding hydroxy-eicosatetraenoic acids (HETEs); and iii) a class of CYP 450 enzymes which form epoxyeicosatrienoic acids (EETs) [93]. Since, all generated products have different biological activities (physiological or pathophysiological) but originate from the same substrate; AA plays a cardinal role in the regulation of the inflammatory process.

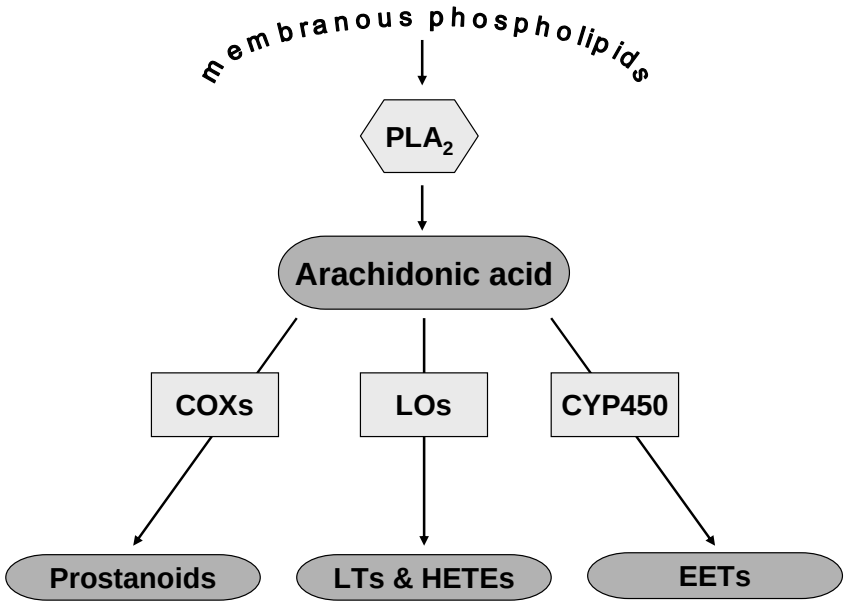

Figure 2.3: Arachidonic acid pathways
Free arachidonic acid is released by phospholipase A_2 (PLA_2) and subjected to further metabolism by cyclooxygenases (COXs), lipoxygenases (LOs) or cytochrome P (CYP)450 enzymes to their respective products. They include prostanoids, leukotrienes (LTs) & hydroxy-eicosatetraenoic acids (HETEs) and epoxyeicosatrienoic acids (EETs).

2.2.2 Phospholipase A_2

The phospholipase A_2 (PLA_2) superfamily constitutes of different enzymes catalyzing the hydrolysis of the fatty acid at the sn-2 position of membrane phospholipids. The products of this reaction *in vivo*, an unsaturated fatty acid and a lysophospholipid, can be further metabolized to important second messengers (e.g. eicosanoids and platelet activating factor (PAF), respectively) with essential (patho)physiological impact. There are five main classes of PLA_2s: secreted (s)PLA_2s; Ca^{2+}-dependent cytosolic (c)PLA_2s; Ca^{2+}-independent (i)PLA_2s; PAF acetylhydrolases, and lysosomal PLA_2s [94]. The cPLA_2s class (Group IV), consists of 6 (α-ζ) subtypes with molecular weights of 61-114 kDa. Within this class, the c$PLA_2\alpha$ is the most extensively studied isoform, first characterized and purified from platelets, macrophage cell lines, and various tissues [95-98]. Due to its exclusive specificity for sn-2 esterified AA, the c$PLA_2\alpha$ is believed to be mainly responsible to provide free AA for eicosanoid (prostanoid and LT) biosynthesis in the cell in response to a variety of extracellular stimuli. Receptor-mediated cellular stimulation by collagen or thrombin as well as receptor-circumventing ionophores (Ca^{2+}-ionophore A23187) causes cPLA_2-depending formation of the eicosanoid-precursor AA. Cellular activation with exogenously applied AA bypasses cPLA_2 activity and the substrate is directly subjected to eicosanoid metabolism via the respective downstream enzymes.

Genetic ablation of c$PLA_2\alpha$ in various animal models or studies with PLA_2 inhibitors resulted in lower production of eicosanoids and related physiological and pathophysiological processes [99]. Besides c$PLA_2\alpha$, members of the low-molecular weight sPLA_2-family have been proposed to participate in cellular eicosanoid generation but clear evidences has not yet provided for such a role [100]. The physiological function of iPLA_2s is considered to lipid remodeling, apoptosis and insulin secretion [101-103]. Lysosomal phospholipase A_2 is an acidic PL that is highly expressed in alveolar macrophages and that may play a role in the catabolism of pulmonary surfactant [104]. PAF acetylhydrolases (which act also in Ca^{2+}-independent manner) catalyze the hydrolysis of phospholipids containing short chain sn-2 acyl groups and thereby inactivate PAF [105].

Regulation of c$PLA_2\alpha$ involves its translocation from the cytosol to membranes to access the substrate. Cellular stimulation induces a rise in $[Ca^{2+}]_i$, where Ca^{2+} binds to the C2 domain of the enzyme and induces translocation to the nuclear envelope and endoplasmatic reticulum (ER). Ca^{2+} largely enhances the affinity of the enzyme for membranes but is not necessary for catalysis [106]. Binding of phosphatidylinositol-(4,5)-bis-phosphate (PIP2) [107] has been shown to significantly activate the enzyme and direct interference with ceramide-1-phosphate [108] reduces dissociation from the membrane surface also in the absence of Ca^{2+}. Moreover, c$PLA_2\alpha$ contains different phosphorylation sites (Ser-505, Ser-515, and Ser-727), which are

phosphorylated by MAPKs, calmodulin kinase II (CamKII) and MAPK-interacting kinase (MNK1), respectively [109]. Phosphorylation events either activate the enzyme or facilitate its translocation to cellular membranes. Taken together, $cPLA_2\alpha$ plays a pivotal role in agonist-induced release of AA as the upstream regulatory enzyme in cellular production of primarily pro-inflammatory bioactive lipid mediators, including PAF, LTs and prostanoids.

2.2.3 Cyclooxygenases and prostanoids

Once AA is liberated by $cPLA_2$, it can be further metabolized via cyclooxygenase (COX) enzymes. In humans, two isoforms of COX exist, namely COX-1 and -2. These enzymes show approx. 65% sequence identity. COX-1 is constitutively expressed in a variety of mammalian cells and tissues [110], such as blood vessel wall, smooth muscle cells, intestinal cells, platelets, renal tubulus and seminal vesicles, and is considered to be mainly responsible for formation of PGs with homeostatic functions. However, strong evidence for its contribution to inflammatory processes has also been provided [111, 112]. In contrast, COX-2 is considered to be inducible and is expressed in response to cytokines (e.g. IL-1β, IL-6, TNFα, lipopolysaccharide (LPS)), growth factors (e.g. PDGF, TGFβ) or others [113]. Nevertheless, constitutively expressed COX-2 was found in brain, kidney, female reproductive tract and evidence for a homeostatic role in the cardiovascular system is given [114, 115]. Expression of the COX-2 gene can be suppressed by anti-inflammatory cytokines (IL-4 or IL-10) and glucocorticoids. Recently, a COX-enzyme derived from a splicing variant of the COX-1 mRNA, termed COX-3, was found in canine and human celebral cortex but its function is still a matter of debate [116].

The reactions catalyzed by COX enzymes comprise the conversion of AA including incorporation of two molecules of O_2 to give the intermediate PGG_2 (cyclooxygenase reaction) and a subsequent peroxidase reaction, which reduces PGG_2 to PGH_2. In turn, PGH_2 is then further metabolized by downstream enzymes into different prostanoids, depending on the cell type (**Figure 2.4**).

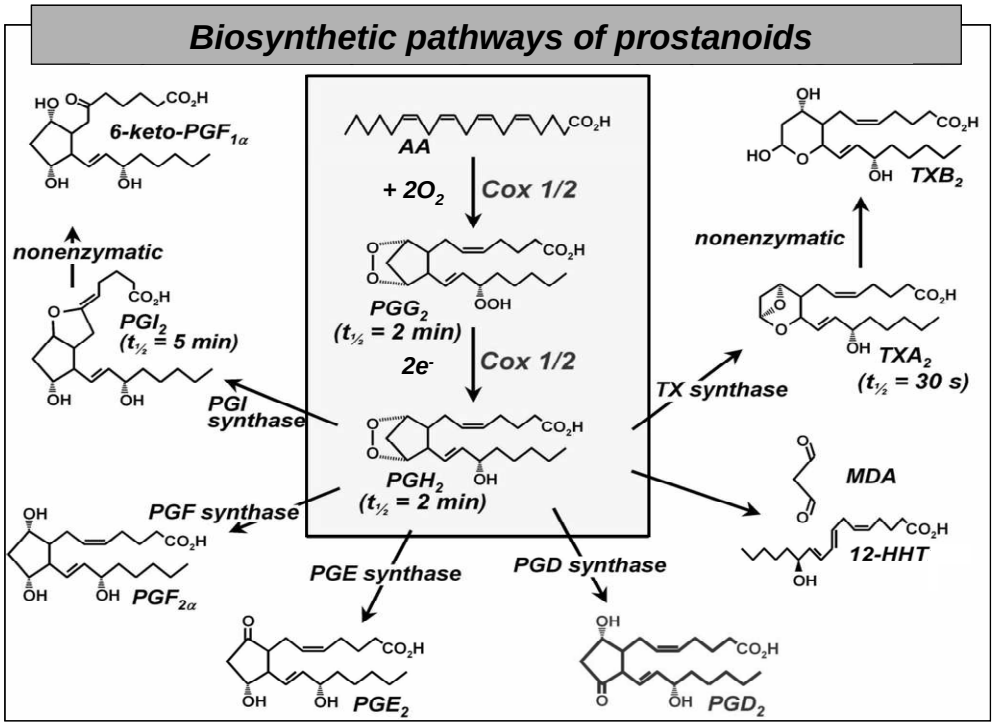

Figure 2.4: Formation of prostanoids derived from arachidonic acid by cyclooxygenase enzymes.
Arachidonic acid (AA), prostaglandin (PG), 12(S)-hydroxy-5-cis-8,10-trans-heptadecatrienoic acid (12-HHT), thromboxane (TX), malonedialdehyde (MDA)

The peroxidase activity is necessary to activate COX reaction and can operate independently of the cyclooxygenase reaction [117, 118] while suicide inactivation is assumed for both, peroxidase and cyclooxygenase activity [119]. COX-2 is known to utilize both, free fatty acids and 2-arachidonyl glycerol as substrates, whereas COX-1 appears to exclusively convert unbound fatty acids, such as free AA [120]. However, AA is the preferential substrate for both isoforms with nearly the same K_m (5 µM). Interestingly, an unusual negative allosteric effect was reported for COX-1 at low AA concentration (≤ 1 µM), which seems to be hydroperoxide-dependent. This might be the reason for the preferred *in vivo* conversion of endogenous substrate amounts (AA ~ 1 µM) by COX-2, when both isoenzymes are expressed in the same cell [121]. In cells expressing COX-1, an immediate pulsatile burst of PG formation occurs in response to an appropriate stimulus (e.g. G protein-coupled receptor (GPCR) agonists) but, at least in certain cells types, a second phase of PG generation 30 - 60 min begins after the initial burst and continues for a few hours. This second more gradual phase involves primarily PGs derived from COX-2 and its expression is in turn partially promoted by the PGs formed via COX-1 [122].

Another important difference between the two COX isoforms is the structure of the active site, a hydrophobic tunnel where the substrate is converted (and where also COX-inhibitors bind). Thus, the COX-2 active site is larger than that of COX-1, due to differences in three amino acids (COX2: Val434, Val523, Arg513; COX-1: Ile434, His513, Ile523) forming a side pocket, and to a different position of a helix in the membrane binding domain (D1 helix), altering the position of Arg120 (responsible for the binding of carboxylic groups of fatty acids and COX-inhibitors)

[123]. In fact, this knowledge led to the development of the COX-2 specific inhibitors (coxibs), e.g. the diarylheterocycle class, including celecoxib and rofecoxib (see below).

Studies on subcellular localization of COX-1/2 showed that both isoforms reside in the ER and nuclear envelope. However, COX-1 seems to be equally distributed, whereas COX-2 localized preferentially (about twofold) at the nuclear envelope [124]. Selective coupling of PLAs to COX enzymes has been reported in several studies [125] but largely depends on expression patterns and the amplitude of the activation of individual PLAs caused by different stimuli. Similarly, attempts to elucidate the coupling of COX isoforms to downstream enzymes of prostanoid formation were carried out. Different functional interferences with PGE synthases [126] (see **2.2.4**), coupling between COX-2 and PGI synthase in the cardiovascular system as well as between COX-1 and TXA_2 synthase in platelets have been shown [127]. However, protein interaction, kinetic properties or simple localization of the terminal synthases might result in selective coupling but still need further elucidation.

De novo synthesized prostanoids, including PGE_2, PGD_2, $PGF_{2\alpha}$, PGI_2 and TXA_2 are widely distributed in a variety of tissues and cells in humans and serve as short-living autocrine or paracrine mediators, acting through specific GPCRs to exert multiple biological functions (**Table 2.3**). However, interactions with nuclear peroxisome proliferator-activated receptors (PPAR) were also reported for certain PGs [128].

Table 2.3: Prostanoid receptor functions and diverse biological activities of prostanoids.

Receptor	Ligand	Signaling	Effect
EP1	PGE_2	$G_q/Ca^{2+}\uparrow$	pain (spinal neurons)
EP2	PGE_2	G_s/cAMP $\uparrow$	maturation for ovulation and fertilization
EP3	PGE_2	G_i/cAMP $\downarrow$	fever (brain); protection of gastric mucosa
EP4	PGE_2	G_s/cAMP $\uparrow$	bone resorption (osteoclast)
DP1	PGD_2	G_s/cAMP $\uparrow$	vasodilatation
DP2	PGD_2	$G_s/cAMP\uparrow$	chemotaxis (Th2 lymphocyte)
FP	$PGD_{2\alpha}$	$G_q/Ca^{2+}\uparrow$	contraction of uterus
$TP_{\alpha/\beta}$	TXA_2	$G_q/Ca^{2+}\uparrow$	vasoconstriction, platelet aggregation
IP	PGI_2	$G_s/cAMP\uparrow$	rennin secretion, vasodilatation, anti-aggregatory

Inhibition of prostanoid formation by targeting COX enzymes is considered a major pharmacological anti-inflammatory intervention. In fact, interference of COX enzymes with NSAIDs targeting both isoforms and the more COX-2 selective coxibs is a common therapeutically strategy to reduce acute and/or chronic inflammatory diseases [129].

Typical NSAIDs inhibit both COX isoforms but generally bind more tightly to COX-1 [130].

Due to competition with AA for binding to the active site, NSAIDs appear to exhibit one of three modes of inhibition: i) rapidly, reversible (e.g. ibuprofen); ii) time-dependent slowly (pseudoirreversible) reversible binding (indomethacin) or iii) rapid, reversible binding followed by covalent modification (aspirin, acetylation at Ser530) [131, 132]. Interestingly, aspirin treated COX-2, in contrast to COX-1 is not simply enzymatically inoperative but is rather able to convert AA to the anti-inflammatory group of lipoxins [133]. Unfortunately, the permanent use of NSAIDs is associated with severe side-effects, mainly gastrotoxicity related to the reduction of COX-1-derived PGE_2 [134]. Search for selective COX-2 inhibitors, in order to improve the safety profile of NSAIDs, led to the development of coxibs. Inhibition of COX-2 activity by these compounds corresponds to a three step-model of interaction leading to time-dependent, pseudoirreversible mechanism, whereas COX-1 is only marginal affected in a rapid and reversible fashion [135]. However the use of coxibs is associated with an increase risk of cardiovascular severe adverse events, mainly due to the suppression of endothelial PGI_2 generated by COX-2 [136] and therefore limiting their use.

In view of the therapeutic benefit, intervention with PG biosynthesis by NSAIDs and coxibs has long been established and still is successfully applied to treat various inflammatory disorders. However, in regard of their severe side effects, compounds interfering with selective terminal PG synthases or PG-receptor antagonists might be of significant advantage.

2.2.4 Microsomal prostaglandin E_2 synthase-1

Among the PGs originating form the COX pathway, PGE_2 acts at least through four different receptors (EP1-4) and regulates key responses in the major human systems including reproductive, gastrointestinal, neuroendocrine and immune functions [137]. In fact, PGE_2 is accepted as a key mediator in fever, pain and inflammatory responses [138]. Isomerization of COX-derived PGH_2 to PGE_2 is catalyzed by PGE_2 synthases (PGES). Many attempts have been attributed to identify and purify these proteins [139, 140]. Meanwhile, three different isoforms have been successfully identified and characterized, namely cytosolic PGE_2 synthase (cPGES), microsomal PGES-1 (mPGES-1) and mPGES-2 [141-144]. The cPGES is a 26 kDa enzyme, constitutively expressed in a variety of tissues (testis, heart, brain and stomach) and preferentially converts PGH_2 derived from COX-1 [141] to maintain homeostatic PGE_2 production. However, initial reports claimed a possible role of this enzyme in inflammation, at least in certain tissues [145]. The mPGES-2 is a 33 kDa enzyme, which is also ubiquitously expressed (brain, heart, skeletal muscle). It is functionally linked to both isoforms of COX enzymes [146] and converts PGH_2 in a glutathione (GSH)-independent manner.

In contrast, mPGES-1 is markedly induced by pro-inflammatory stimuli such as IL-1β, TNFα

and LPS in a variety of cell types including A549 cells, synovial cells, monocytes, human endothelial cells, macrophages, and osteoblasts [147-150] and its induction is suppressed by glucocorticoids and TNFα blockers [150-152]. Low constitutive expression levels of mPGES-1 have been observed in urogenital organs, spleen, stomach and kidney. It has been demonstrated that this enzyme preferentially metabolizes COX-2-derived PGH_2 [141, 153] and requires GSH as cofactor for its catalytically activity [154, 155]. The mPGES-1 is a 16kDa enzyme and is mainly located in the perinuclear membrane and, at least in part, colocalizes with COX-2 [156, 157]. It belongs to the family of "membrane-associated proteins involved in eicosanoid and glutathione metabolism" (MAPEG). Further members of this superfamily are 5-lipoxygenase-activating protein (FLAP), LTC_4 synthase and microsomal glutathione transferases (MGST) 1-3. A recent study by Jegerschöld et al. [158] demonstrated that mPGES-1 is a homotrimer of four transmembrane helix bundles consistent with other structurally characterized MAPEG members. GSH is bound in an u-shape form at the interface between the subunits of the trimer and this binding involves conserved residues of Arg70/Tyr117 and Arg126/Tyr130. A cytoplasmatic cleft between helices 1 and 4 is suggested to form the active site of the enzyme and promote PGH_2 catalysis, which is facilitated by GSH thiolate and Arg126.

Accumulating evidence indicates a pivotal role of mPGES-1 for inflammatory diseases such as arthritis, pain, fever, stroke as well as in cancer [159-162]. As demonstrated in several studies using mPGES-1 deficient mice, inhibition of mPGES-1 provides an efficient pharmacological approach for the treatment of these pathological conditions [153, 163-166] with only marginal effects on the formation of physiologically important and homeostatic PGs. So far, a number of small molecules were described as direct mPGES-1 inhibitors, such as arachidonic acid and 15-deoxy-$\Delta^{12,14}$-PGJ_2 (IC_{50} = 0.5 µM, both) [167], the indole analogue MK-886 (IC_{50} = 1.6 µM) and certain derivatives as well as pirinixic acid derivatives [168-170]. Additionally, some phenanthrene imidazoles including the selective, potent and orally available compound MF63 (IC_{50} = 1 nM) have been described [162, 171].

Since inflammation and related pathophysiological conditions are closely linked to the increased formation of PGE_2 originated from up-regulated mPGES-1 [172], pharmacological intervention with mPGES-1 is assumed to be an attractive alternative to NSAIDs and coxibs with presumably higher safety, due to reduced risk of classical adverse effects of these drugs. Nevertheless, additional experiments and even adequately designed prospective clinical trials are needed to determine a superior effect of selective mPGES-1 inhibitors.

2.2.5 5-Lipoxygenase

Besides biosynthesis of PGs by COX enzymes, AA can be converted through the lipoxygenase (LO) pathway yielding LTs and HETEs. There are have been several LOs described in humans, including 5-LO, p12-LO, epidermis-type 12-LO, and 15-LO-I and -II. Among LO enzymes, the 5-LO seems to play a critical role in the regulation of the inflammatory response and therefore 5-LO-derived LTs are of particular interest. LTs exert physiological roles in innate immune responses, are regarded as pathophysiological mediators in inflammatory associated diseases encompassing asthma, allergic rhinitis, atherosclerosis, myocardial infarction, and stroke [173]. The generation of LT (**Figure 2.5**) in inflammatory cells (neutrophils, macrophages eosinophils and mast cells) is initiated by several immune and pro-inflammatory stimuli. Available amounts of AA are converted via 5-LO into 5-hydro(per)oxy-eicosatetranoic acid (5-H(P)ETE), by incorporation of molecular oxygen (oxygenase activity) and subsequent formation of the unstable epoxide intermediate LTA_4 (LTA_4 synthase activity). The latter can be metabolized by LTA_4 hydrolase to give LTB_4, a potent neutrophil chemoattractant [174, 175] which also mediates adhesion of leukocytes to vascular endothelium, T cell recruitment to inflamed tissues, and causes superoxide release from phagocytes [176, 177]. On the other hand, conjugation of LTA_4 with GSH by LTC_4-synthase (mainly expressed in eosinophils, macrophages and mast cells) may occur, yielding cysteinyl LTs (Cys-LTs), namely LTC_4, LTD_4 and LTE_4 [178]. Cys-LTs are bronchoconstrictive agents and increase vascular permeability, resulting in a pro-inflammatory action. As the prostanoids, also LTs act through specific GPCRs: two receptors for LTB_4 (BLT_1 and BLT_2) and at least two receptors for Cys-LT ($CysLT_1$ and $CysLT_2$) mainly expressed on leukocytes, smooth-muscle cells or endothelial cells [179]. Notably, 5-H(P)ETE is also partially reduced via cellular peroxidases to give its correspondent alcohol 5-HETE and in turn, 5-HETE oxidation leads to 5-oxo-ETE. Both metabolites possess diverse biological functions, including tumor promotion and granulocyte recruitment, respectively [180, 181]. Various studies demonstrated anti-inflammatory properties of LO-derived (5-/12-/15-LO) metabolites, the lipoxins (LXA_4 and LXB_4), suggesting a certain role also in resolution of inflammation [182, 183].

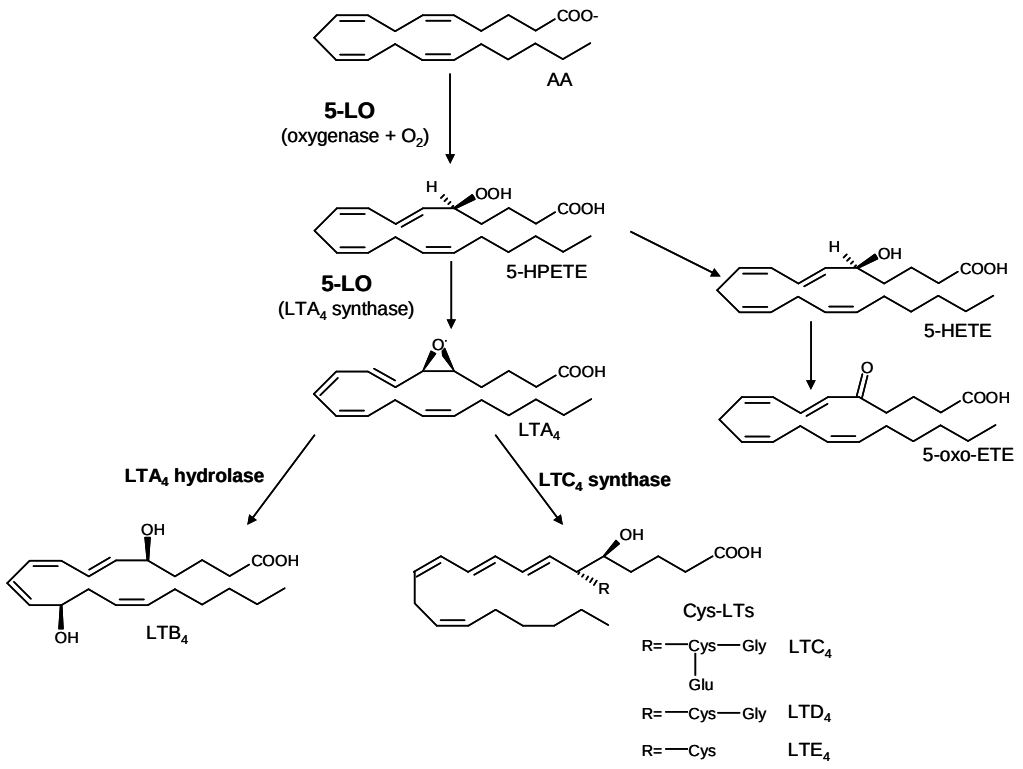

Figure 2.5: Leukotriene biosynthetic pathway
Free arachidonic acid (AA) is subjected to the 5-lipoxygenase (5-LO) pathway. Leukotriene (LT)A_4 hydrolases and LTC_4 synthase; cysteinyl (Cys); glycin (Gly); glutamine (Glu); hydro(per)oxy-eicosatetranoic acid (H(P)ETE)

The 5-LO active site contains a non-heme iron which is essential for the catalytic activity of the enzyme [184, 185]. The iron functions as an electron donor or acceptor during the catalysis, thus, the inactive form of 5-LO contains iron in the ferrous state (Fe^{2+}), and the iron is oxidized to the active (ferric, Fe^{3+}) state by cellular hydroperoxides [186]. Several cofactors and complex activation pathways regulate 5-LO activity. Hence, an increase of intracellular Ca^{2+} strongly stimulate LT formation in intact cells [187] and reversible binding of Ca^{2+} at the C2-like domain of 5-LO enzyme has been confirmed [188]. Binding of Ca^{2+} in turn, supports association of the enzyme with phosphatidylcholine (PC), directing 5-LO towards membranes.

Interference with ATP increases 5-LO activity by stabilizing effects on the enzyme. Besides the catalytic site, 5-LO contains a second putative regulatory fatty-acid-binding site [189]. Glycerides including 1-oleoyl-2acetyl-sn-glycerol (OAG) were reported to activate 5-LO in the absence of Ca^{2+} [190] and binding of coatosin-like protein (CLP) to 5-LO supports Ca^{2+}-induced enzymatic activity [191]. 5-LO is also regulated by phosphorylation by p38 ^{MAPK}-regulated MAPKAP-2/3 (MK-2/3), ERK1/2, CaMKII and PKA [192, 193]. While phosphorylation by MKs and ERKs promote membrane translocation and up-regulate 5-LO product formation [192, 194], PKA-mediated phosphorylation impairs 5-LO activity [195]. In the majority of cells (neutrophils, peritoneal macrophages), 5-LO resides in the cytosol and translocate to the nuclear membrane upon cellular stimulation. After association of 5-LO with the nuclear membrane,

released AA is transferred to 5-LO by FLAP to allow metabolism by 5-LO [196]. FLAP is a member of the MAPEG family and is co-expressed with 5-LO in many tissues. Interestingly, exogenous supply of free AA to the cells (transcellular mechanism or experimental conditions) circumvents FLAP activity and can be metabolized by cytosolic 5-LO [197].

Targeting the biosynthesis of pro-inflammatory LTs is regarded to represent a rational therapeutic goal to block certain allergic and inflammatory diseases. Direct inhibition of 5-LO is achieved by either redox active compounds (phenols e.g., caffeic acid) which reduce the active site iron, iron-ligand inhibitors (BWA4C, zileuton) chelating the active site iron and non-redox type inhibitors (ZM230487) competing with binding of the substrate (AA) to 5-LO. Therein, zileuton is the only compound which entered the market (USA) and is approved for the treatment of asthma. However, it only showed marginal effects in rheumatoid arthritis or inflammatory bowel diseases [198]. An alternative way to suppress LT synthesis is to inhibit FLAP. Using the FLAP inhibitor MK-886, 5-LO product formation is potently attenuated in intact leukocytes but the compound is significantly less efficient (about 500 times) in whole blood and no inhibition of purified 5-LO or LT formation in cell homogenates were observed [199]. Also, addition of exogenous AA to activated cells strongly impairs the potency of MK-886 [57]. Thus, by supplementation of exogenous AA to cells, the possibility is given to circumvent PLA_2 inhibition and to estimate FLAP interference of a given compound [200]. Nevertheless, recent findings concerning FLAP suggest a therapeutic potential of novel FLAP inhibitors [173].

In summary, a complex regulation of 5-LO activity through several cofactors including substrate supply, FLAP, $Ca^{2+}$and phospholipids leading to LT synthesis is established and thus, the efficacy of 5-LO inhibitors, in intact cells as well as in cell-free assays largely depends on the assay conditions.

2.3 Platelet physiology and biochemistry

Platelets are specialized human blood cells derived from megakaryocytes. They are produced in the bone marrow and released into the circulation. Platelets play crucial roles in hemostasis and wound healing as well as they are involved in the pathophysiological processes of thrombosis and inflammation [201]. Injury of a vessel wall exposing the unveiled subendothelial matrix induces platelets to form a hemostatic plug and close the leakage. Also, platelets are accounted for thrombus formation at sites of ruptured atherosclerotic plaques and consequently trigger heart attacks and strokes [202]. The first interaction (adhesion) of platelets is mediated by specific glycoproteins (GP) with the van Willebrand factor (vWF) on the surface of the subendothelium. This interaction enables a firm platelet capture further strengthen by binding of subendothelial collagen to its respective platelet receptors GPIa/IIa and major collagen signaling GPVI receptor [203]. This preliminary stimulation per se together with activation by agents from the surrounding environment (e.g. ADP, thrombin, TXA_2) transduce a rise in intracellular Ca^{2+} concentrations ($[Ca^{2+}]_i$). The increase of $[Ca^{2+}]_i$ is substantially linked to spreading, activation of $cPLA_2$ followed by PG formation (i.e. TXA_2) as well as granule secretion and activation of GPIIb/IIIa (integrin $\alpha_{IIb}\beta_{IIIa}$), causing binding of soluble fibrinogen (inside-out signaling) [204-206]. Secreted products from dense bodies are ADP or serotonin. ADP and TXA_2 exert an important role in additional autocrine/paracrine platelet activation and hemostatic plug growth [207]. The α-granules of platelets contain adhesive proteins (vWF, thrombospondin), mitogenic factors (PDGF and TGF-β), coagulation factors as well as glycoproteins such as P-selectin (CD62) and CD40 ligand. The latter are well recognized to mediate platelet binding to neutrophils and monocytes and to induce inflammatory processes in the microenvironment including VCAM-1 expression, release of tissue factor, enhanced migration of leukocytes as well as an increase in ROS and chemokine production by endothelial cells [208-212].

Activation-induced binding of fibrinogen to GPIIb/IIIa is the primary mechanism of platelet aggregation and the cross-linking of two GPIIb/IIIa molecules on neighboring platelets results in a firm connection and depend on $[Ca^{2+}]_i$ [213]. The increase of $[Ca^{2+}]_i$ also evokes activation of the scramblase enzyme which promotes phospholipid translocation in the cell membrane leading to an anionic membrane surface. This provides binding sites for enzymes and cofactors of coagulation processes in a Ca^{2+}-depending manner, facilitating efficient generation of thrombin and finally of fibrin, to form a stable plug [214] (**Figure 2.6**).

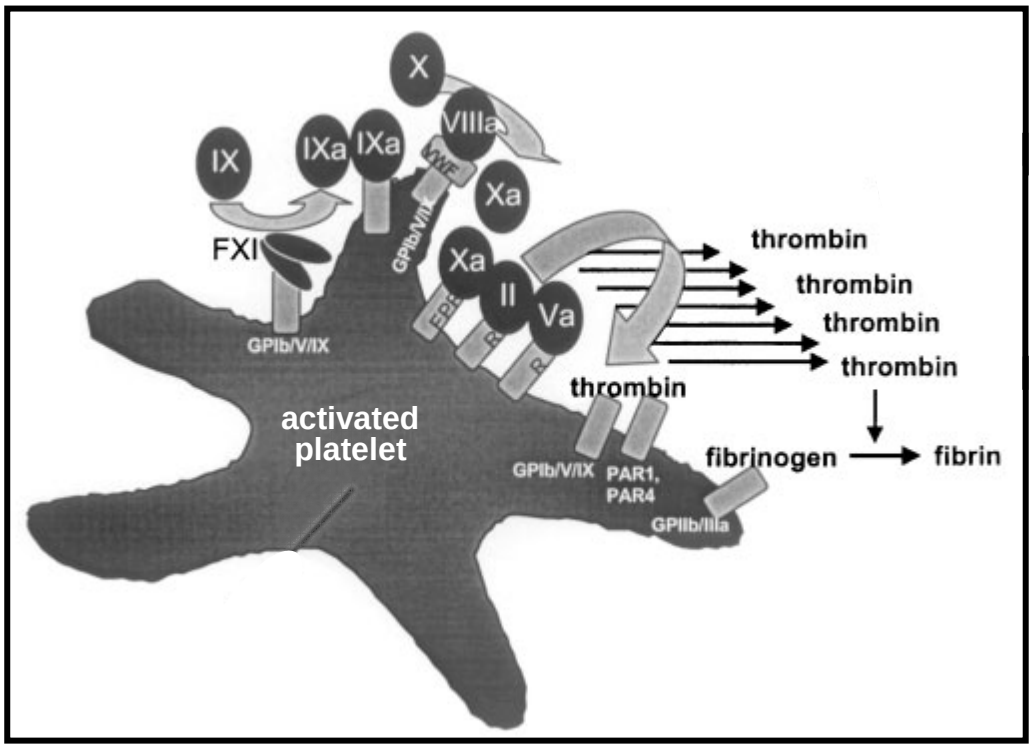

Figure 2.6: Model of platelet-mediated thrombin formation (adopted from [202])
Activated platelets can bind coagulation factors and cofactors via Ca^{2+} and specific receptors. The concerted actions of coagulation factors on the platelet surface lead to a burst of thrombin generation, enabling a stable fibrin clot formation.

Negative regulation of platelet physiology is essential to prevent uncontrolled thrombosis. In this the regard the role of nitric oxid and PGI_2 derived from the endothelium are well established. These mediators induce an intracellular increase of cyclic nucleotides cGMP/cAMP via adenyl and guanyl cyclases, respectively [215] and therefore decrease platelet activity. Antiplatelet agents such as aspirin and ridogrel suppressing TXA_2 activity, clopidogrel affecting ADP receptors and abciximab blocking the GPIIb/IIIa receptor are used to impair platelet activation [216].

Platelet activators such as thrombin or collagen are considered as strong agonists whereas, ADP, serotonin, or TXA_2 require autocrine/paracrine stimulation to induce the entire platelet response [205]. Soluble platelet agonists, including thrombin, PAF, ADP or TXA_2, typically activate specific GPCRs (**Figure 2.7**), leading to the activation of phospholipase (PL)Cβ [217, 218]. PLC catalyses the hydrolysis of PIP2 to inositol trisphosphate (IP3) and diacylglycerol (DAG). Activated IP3 receptors meditate Ca^{2+} mobilization from the intracellular stores (dense tubula system) and this, in turn, leads to massive Ca^{2+} influx from the extracellular space [219]. DAG-mediated activation of protein kinase C (PKC) and downstream effectors also participate in platelet activation process.

The sustained increase of $[Ca^{2+}]_i$ is associated with phosphorylation of myosin-light chain by it respective kinases leading to shape change of platelets as well as the various responses mentioned above including PLA_2-activation, granule secretion, conformational changes and activation of GPIIb/IIIa (integrin $\alpha_{IIb}\beta_{IIIa}$) and providing of catalytically active platelet surfaces.

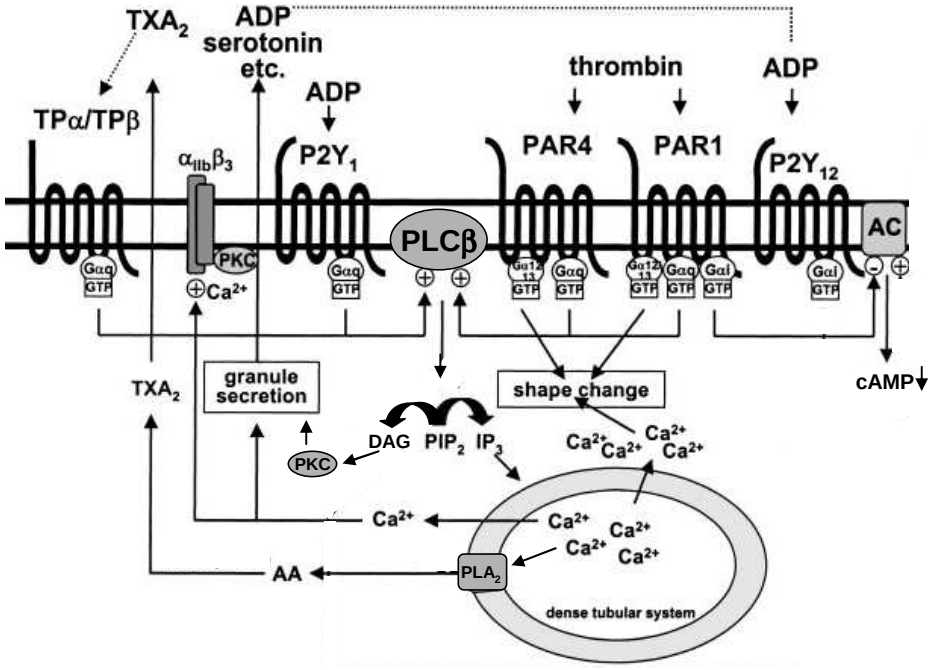

Figure 2.7: G-protein coupled receptor signaling in platelets.
Input signals regulate calcium dynamics and induce secondary pathways potentiating platelet activation. PIP2, phosphatidylinositol-(4,5)-bis-phosphate; IP3, inositol trisphosphate; PAR protease activated receptor; AC, adenylate cyclase; PKC, protein kinase C; [202].

On the other hand, collagen, the most abundant protein of the extracellular matrix, promotes platelet activation through its binding to platelet GPIa/IIa and GPVI. Binding of collagen to GPVI stimulates a non-receptor protein-tyrosine kinase. Cross-linking of GPVI/Fc-receptor γ chain (FcRγ) by collagen ligation results in phosphorylation of the immunoreceptor tyrosine-based activation motif (ITAM) of FcRγ by the Src-kinase family members Lyn and Fyn [220, 221], with subsequent binding and activation of nonreceptor tyrosine kinase Syk. Participation of linker for activation of t cells (LAT) and Src homology 2 domain-containing leukocyte phosphoprotein of 76 kDa (SLP76) results in activation of PLCγ2 (**Figure 2.8**) [222, 223]. LAT also recruits phosphatidylinositol-3 kinase (PI3K) and PI3K-dependent signalling through at least PKB (Akt) contributing to platelet adhesion, spreading and granule secretion [224].

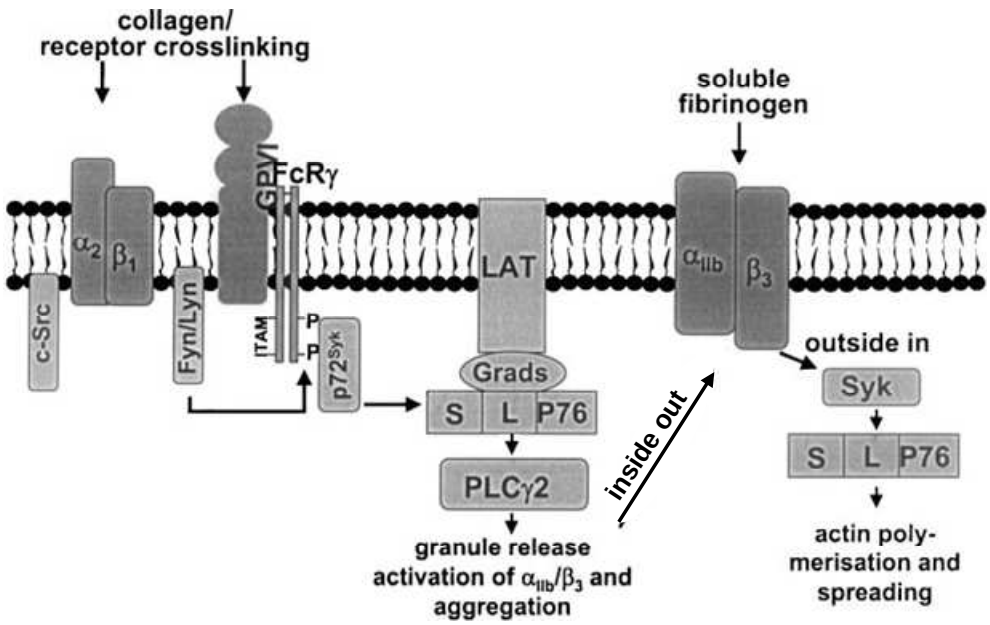

Figure 2.8: Collagen signaling via nonreceptor tyrosine kinase [202]**.**
Tyrosine kinases, c-Src, Lyn/ Fyn; non receptor tyrosine kinase, $p72^{syk}$, syk; adapter molecules LAT, Grads, SLP76.

Stimulation of PLCγ2 leads to IP3 synthesis and the same subsequent downstream pathways are induced as described for Gq-coupled receptors. Notably, activated GPIIb/IIIa enables binding of soluble agonist leading to Syk activation, the so-called outside-in signaling.

Together, Ca^{2+} is a pivotal second messenger in the platelet activation cascade modulating important platelet functions including aggregation, thrombin formation and others. Beside the important role of platelets in hemostasis and thrombosis, it has become evident that platelets also contribute to the progression of inflammation. Therefore, profound knowledge about alterations in character and function of platelets is basically required in the development of anti-inflammatory drugs.

2.4 Aim of this work

In the last decades, a growing public interest for herbal medicine and nature-derived remedies as an alternative therapeutic aspect became more and more evident and therefore, a variety of herbal remedies entered the market. Among those, especially frankincense preparations experienced resurgence. In the traditional medicine from India and China extracts of *B. spec.* have long been recognized for their anti-inflammatory potential and recent clinical trials demonstrated the efficacy of *B. spec.* preparations in the treatment of OA, inflammatory bowel diseases and certain cancer forms. However, for therapeutic use of such crude extracts in the modern phytotherapy it is mandatory to characterize pharmacological principles and molecular mechanisms responsible for their beneficial effects. Thus, BAs were found to be bioactive compounds of frankincense preparations and 5-LO was proposed as a relevant molecular target [53]. Extensive studies on this topic suggested AKBA (the most potent BA analogue in this respect) as a direct and nonredox–type 5-LO inhibitor, responsible for the suppression of pro-inflammatory LT formation observed *in vitro*, whereas interference with other AA-metabolizing enzymes has been excluded. Further investigations, most focused on AKBA or KBA, proposed several other targets including HLE, topoisomerases, IκB kinases, CYP 450 enzymes and p12-LO [58, 80, 65, 19, 8]. These hypotheses constituted attractive models to explain the anti-inflammatory and anti-tumor potential of frankincense preparations but there are serious doubts due to their *in vivo* relevance as the interference of BAs with these targets *in vivo* or in test systems reflecting *in vivo* conditions has been essentially neglected. Moreover, the discrepancies between reachable plasma levels of BAs and the effective concentrations required to affect these targets, questioned the pharmacological relevance.

The aim of this work was to identify novel molecular targets and anti-inflammatory actions of BAs as well as to functionally characterize and evaluate new and existing interactions in view of their biological relevance. To this purpose, putative interferences of BAs with AA-metabolizing enzymes and functional modulation of platelet physiology by BAs were investigated. Preliminary work to characterize cellular and molecular effects of BAs in neutrophils, monocytes and platelets was provided by the thesis of Anja Altmann [225] and was expanded by the work of Daniel Poeckel [226]. The latter specified the identification of p12-LO as a selective molecular target of BAs. Recently, the thesis of Lars Tausch [227] revealed cathepsin G (CatG) as a novel, pharmacologically relevant and anti-inflammatory target of BAs. Partially based on these findings, studies were continued or expanded to other related topics, governing inflammatory processes in humans.

This work investigated the properties of BAs to influence signaling pathways and related functional characteristics of platelets in response to physio-pathophysiological stimuli. Furthermore, COX-1 and mPGES-1 were identified as direct molecular targets of BAs and functional consequences of these results were extensively studied. Detailed biochemical characterizations and critical analysis concerning the pharmacological relevance are provided. Finally, an explicit re-evaluation of the interference between 5-LO and BAs revealed novel aspects regarding the molecular mechanism and *in vivo* relevance of this interaction.

3 MATERIALS & METHODS

3.1 Materials

AA	Sigma-Aldrich (Deideshofen, Germany)
[^{3}H]AA	BioTrend Chemicals (Köln, Germany)
[^{3}H-PGE_2]	Perkin Elmer Life Sciences (Milan, Italy)
11β-PGE_2	BioTrend Chemicals (Köln, Germany)
6-keto-$PGF_{1\alpha}$	Cayman Chemical (Ann Arbor, MI, USA)
α–amyrin	Extrasynthèse (Genay, France)
Anti-mouse-IgG-6-keto-$PGF_{1\alpha}$-antibody	Dr. T. Dingermann (Frankfurt, Germany)
ATP	Roche Diagnostics (Mannheim, Germany)
β-mercaptoethanol	Carl Roth (Karlsruhe, Germany)
Boswellia serrata resin extract (H15® Gufic)	Gufic Chem (Belgaum, Karnataka, India)
Boswellic acids	prepared as described [228]
BWA4C	Dr. L. G. Garland (Wellcome Research Laboratories, London, UK)
Ca^{2+}-ionophore A23187	Sigma-Aldrich (Deideshofen, Germany)
Calcitriol	Dr. H. Wiesinger (Schering, Berlin)
CDC	Biomol (Plymouth Meeting, PA, USA)
Celecoxib	WITEGA Laboratories (Berlin, Germany)
Collagen	Nykomed Pharma (Unterschleißheim, Germany)
Coomassie brilliant blue G250	Applichem (Darmstadt, Germany)
COX-1 (ovine)	Cayman Chemical (Ann Arbor, MI, USA)
COX-2 (human recombinant)	Cayman Chemical (Ann Arbor, MI, USA)
DMEM/High glucose (4.5 g/l) medium	PAA (Coelbe, Germany)
DMSO	Carl Roth (Karlsruhe, Germany)
EAH-Sepharose 4B	GE Healthcare Bio-Sciences (Freiburg, Germany)
Fatty acid-free BSA	Sigma-Aldrich (Deideshofen, Germany)
fMLP	Sigma-Aldrich (Deideshofen, Germany)
Fura-2/AM	Alexis Corp (Lausen, Switzerland)
Insulin	Aventis (Frankfurt, Germany)
IPTG	Applichem (Darmstadt, Germany)
Leupeptin	Applichem (Darmstadt, Germany9

LPS	Sigma-Aldrich (Deideshofen, Germany)
Methanol	Merck (Darmstadt, Germany)
MK-886	BioTrend Chemicals (Köln, Germany)
Nycoprep	PAA (Coelbe, Germany)
Penicillin	PAA (Coelbe, Germany)
PGH_2	Larodan (Malmö, Sweden)
Plastic/PS-materials	Greiner bio-one (Frickenhausen, Germany)
PP2 and PP3	Cayman Chemical (Ann Arbor, MI, USA)
Roti®-Nanoquant	Carl Roth (Karlsruhe, Germany)
SDS	Carl Roth (Karlsruhe, Germany)
Streptomycin	PAA (Coelbe, Germany)
SU5665	Cayman Chemical (Ann Arbor, MI, USA)
Thrombin	Sigma-Aldrich (Deideshofen, Germany)
Trypsin/EDTA solution	PAA (Coelbe, Germany)
Tween 20	Carl Roth (Karlsruhe, Germany)
U-46619	Calbiochem (Bad Soden, Germany)
Ultima Gold™ XR	Perkin Elmer (Boston, MA, USA)
VBSE extract	Pharmasan (Freiburg, Germany)
λ-carrageenan type IV from Gigartina aciculaire & Gigartina pistillata	Sigma-Aldrich (Milan, Italy)

All other chemicals were purchased in analytical grade from Sigma-Aldrich (Deideshofen, Germany) unless stated otherwise.

3.2 Methods

3.2.1 Cell culture

Human cell lines were cultured in incubators (HERAcell, Kendro Laboratory Products, Hanau, Germany) at 37 °C, 6% CO_2 and saturated humidity.

3.2.1.1 Mono Mac 6 cells

Mono Mac 6 (MM6) cells, a human monocyte-like cell line, were obtained form Dr. D. Steinhilber (University Frankfurt, Germany). Cells were maintained in RPMI 1640 medium with glutamine supplemented with 10% (v/v) heat-inactivated fetal calf serum (FCS), penicillin (100 U/ml), streptomycin (100 µg/ml), 1 mM sodium pyruvate, 1× nonessential amino acids, 1 mM oxalacetic acid and 10 µg/ml insulin. Cultures were seeded at a density of 2×10^5/ml.

3.2.1.2 A549 cells

A549 (human lungepithelial carcinoma cell line) cells were obtained from Dr. O. Rådmark (Karolinska Institute, Stockholm, Sweden). Cells were cultured in DMEM/High glucose (4.5 g/l) medium supplemented with FCS (10%, v/v), penicillin (100 U/ml) and streptomycin (100 µg/ml). After 3 days, confluent cells were detached using 1× trypsin/ethylenediaminetetraacetate (EDTA) solution and reseeded at 2×10^6 cells in 20 ml medium.

3.2.2 Cell viability

Cell viability of A549 cells was measured using the colorimetric 3-(4,5-Dimethylthiazol-2-yl)-2,5-diphenyltetrazolium bromide (MTT) dye reduction assay [229] in a 96-well format. Briefly, A549 cells (5×10^4 cells/100 µl medium) were plated into a 96-well microplate and incubated at 37 °C and 6% CO_2 for 16 h. Then, 30 µM of all four BAs and α-amyrin or solvent (DMSO) was added and the samples were incubated for another 5 h, MTT (20 µl, 5 mg/ml) was added and the incubations were continued for 4 h. The formazan product was solubilized with sodium dodecylsulfate (SDS) (10%, (w/v) in 20 mM HCl) and the absorbance of each sample was measured at 595 nm relative to that of vehicle (DMSO)-treated control cells using a multiwell scanning spectrophotometer (Victor^3 plate reader, PerkinElmer, Rodgau-Juegesheim, Germany). Neither α-amyrin nor one of the four β-BAs (30 µM, each) significantly reduced cell viability within 5 h versus DMSO as vehicle, excluding possible acute cytotoxic effects of the compounds

in the cellular assays using A549 cells. Influence on the viability of platelets in response to any agent (BAs, thrombin, or Ca^{2+}-ionophore A23187) could be excluded as described [64]. To exclude acute cytotoxic effects of BAs during preincubation periods in assays using MM6 cells, cell viability was analyzed by light microscopy and trypan blue exclusion. Incubation with 100 µM of any of the BAs at 37 °C for up to 30 min caused no significant change in MM6 cell viability [11].

3.2.3 Isolation of human PMNL from venous blood

Human PMNL were freshly isolated from buffy coats obtained from the Blood Centre, University Hospital Tübingen (Germany). In brief, venous blood from healthy donors was taken and leukocyte concentrates were prepared by centrifugation at 4,000 × g, 20 min, room temperature (RT). Buffy coats were diluted 1:1 (v/v) with phosphate buffered saline pH 7.4 (PBS) and then with ice-cold 5% dextran (w/v in PBS) in a ratio 4:5 (v/v), for 45 min. After dextran sedimentation neutrophils were immediately isolated by centrifugation at 1000 × g, 10 min, RT, w/o brake (Heraeus sepatech, Varifuge 3.0, Hanau , Germany) on Nycoprep cushions, and hypotonic lysis of erythrocytes as described [230]. PMNL (7.5×10^6 cells /ml; purity > 96-97%) were finally resuspended in PBS plus 1 mg/ml glucose (PG buffer) or in PG buffer plus 1 mM $CaCl_2$ (PGC buffer) as indicated.

3.2.4 Isolation of human platelets from venous blood

Platelets were isolated from supernatants after centrifugation of leukocyte concentrates on Nycoprep cushions (see **3.2.3**) to obtain platelet rich plasma (PRP). PRP was then mixed with PBS pH 5.9 (3:2, v/v), centrifuged (1,000 × g, 10 min, RT) and the pelleted platelets were resuspended in PBS pH 5.9/NaCl 0.9% (1:1, v/v) and washed by centrifugation (1,000 × g, 10 min, RT). Preparation of platelets at pH 5.9 is thought to minimize temperature-induced activation. Finally, platelets were resuspended in PG or PGC buffer as specified.

In experiments investigating platelet aggregation, human platelets were freshly isolated from venous blood of healthy donors (Blood Center, University Hospital Tübingen, Germany) who had not taken any medication for at least 10 days. Briefly, venous blood was collected in monovettes (Monovette®, Sarstedt, Nümbrecht, Germany) containing 0.106 mol/l trisodium citrate solution. PRP was obtained after centrifugation of whole blood at 200 × g for 15 min at RT w/o brake and placed into 15-ml conical tubes containing 10% (v/v) ACD-buffer (85 mM trisodium citrate, 65 mM citric acid, 100 mM glucose) [231]. PRP was centrifugated at 800 × g for 10 min at RT, pelleted platelets were washed twice and finally resuspended in Tyrode´s

buffer (129 mM NaCl, 8.9 mM $NaHCO_3$, 0.8 mM KH_2PO_4, 0.8 mM $MgCl_2$, 5.6 mM glucose, 10 mM N-2-hydroxyethylpiperazine-N'-2-ethanesulfonic acid (HEPES) pH 7.4.

For the thrombin generation assay, PRP was prepared from freshly drawn blood (see above) and platelet count in PRP was adjusted with platelet poor plasma (centrifugation of PRP at 3000 × g, 10 min, RT) to 2×10^8/ml.

3.2.5 Isolation of human peripheral blood monocytes

Monocytes were obtained from leukocyte concentrates after dextran sedimentation and centrifugation on Nycoprep cushions. The mononuclear cells including lymphocytes and monocytes appear as a layer on Nycoprep cushion after centrifugation. The cells were washed three times with ice-cold PBS and resuspended in RPMI-1640 medium supplemented with 2 mM glutamine, 100 µg/ml streptomycin, 100 U/ml penicillin, and 10% FCS, and spread (2×10^7 /ml) in cell culture flasks at 37 °C and 6% CO_2. After 2 h, lymphocytes in suspension were removed, and adhered monocytes were gently detached and resuspended in medium (incl. 2% FCS).

3.2.6 Expression and purification of human recombinant 5-LO from E. coli

Human recombinant 5-LO protein was expressed in *E. coli* JM 109 cells, transfected with the plasmid pT3-5LO, and purification of 5-LO was performed via affinity chromatography as described [232]. Cells were grown overnight in LB medium supplemented with 100 µg/ml ampicillin, transferred to M9 minimal medium (48 mM Na_2HPO_4, 22 mM KH_2PO_4, 8.5 mM NaCl, 19 mM NH_4Cl, 6.3 mM NaOH, glycerol 2% and 100 µg/ml ampicillin, pH 7.4 casein 2 g/l) and expression of 5-LO was induced with 200 µM isopropyl-β-D-thiogalactopyranoside. Cells were harvested by centrifugation (7,700 × g, 15 min, 4 °C) lysed by incubation in 50 mM triethanolamine/HCl pH 8.0, 5 mM EDTA, soybean trypsin inhibitor (60 µg/ml), 1 mM phenylmethylsulfonylfluoride (PMSF), 1 mM dithiothreitol (DTT), and lysozyme (500 µg/ml), homogenized by sonification (3 × 15 s) (Bandelin, Sonoplus HD 200) on ice and centrifuged at 40,000 × g for 20 min at 4 °C (Sorvall RC 5B plus).The resulting 40,000 × g supernatant (S40) was immediately used for 5-LO activity assays or applied to an ATP-agarose column, and the column was eluted with 20 mM ATP in PBS plus 1 mM EDTA [233] to yield partially purified 5-LO, which was subsequently used for *in vitro* 5-LO activity assays.

3.2.7 Cell-free expression of human mPGES-1

Human mPGES-1 was obtained by the continuous-exchange cell-free expression (CECF) system according to [234]. Cell free expression is an elegant and versatile technique to produce functionally folded membrane proteins (MPs) in high amount avoiding serious problems (e.g.: toxicity due to overloading of the translocon machinery, inclusion bodies, mis-targeting and protein degradation) often emerged by over-expression of MPs in vivo. The CECF system comprises a reaction mixture (RM) that contains the *E. coli* S30 extract (derived from the A19 strain), T7 polymerase, tRNAs, pyruvate kinase and the template DNA for human mPGES-1 (cloned in the pBH4 vector derived from pET19b, Novagen, NJ 08027 USA). The RM is dialysed against the so called feeding mixture (FM) that supplies amino acids, energy equivalents acetyl phosphate and phosphoenolpyruvate as well as nucleotides. Reactions are usually incubated at 30 °C for up to 20 h. Protein synthesis take place in the RM and up to 1.5 mg of mPGES-1 per ml of RM can be obtained in the precipitate-forming cell-free expression (P-CF) mode as described [235]. This work was entirely performed by Sina Reckel (Goethe University of Frankfurt).

3.2.8 Stimulation of A549 cells and isolation of microsomes

Preparation of A549 cells was performed as described [142]. In brief, cells (2×10^6 in 20 ml medium) were plated in 175 cm^2 flasks and incubated for 16 h at 37 °C and 6% CO_2. Subsequently, the culture medium was replaced by fresh DMEM/High glucose (4.5 g/l) medium containing FCS (2%, v/v). In order to induce mPGES-1 expression, IL-1β (1 ng/ml) was added, and the cells were incubated for another 72 h. Thereafter, cells were detached with trypsin/EDTA, washed with PBS and frozen in liquid nitrogen. Ice-cold homogenization buffer (0.1 M potassium phosphate buffer pH 7.4, 1 mM PMSF, 60 µg/ml soybean trypsin inhibitor, 1 µg/ml leupeptin, 2.5 mM GSH and 250 mM sucrose) was added and after 15 min, cells were resuspended and sonicated on ice ($3 \times$ 20 s). The homogenate was subjected to differential centrifugation at 10,000 $\times$ g for 10 min and at 174,000 $\times$ g for 1 h at 4 °C. The pellet (microsomal fraction) was resuspended in 1 ml homogenization buffer and the protein concentration was determined by the Roti®-Nanoquant approach (see **3.2.35**).

3.2.9 Determination of release of [^{3}H]-labeled AA from intact platelets

Human PRP was labelled with 19.2 nM [^{3}H]AA (1 µCi/ml, specific activity 200 Ci/mmol) for 2 hours at 37 °C. Then, cells were washed twice with PBS pH 5.9 plus 1 mM $MgCl_2$, 11.5 mM $NaHCO_3$, 1 mg/ml glucose, and 1 mg/ml fatty acid-free BSA. Platelets were finally resuspended in PGC buffer (10^8/ml) and subsequently stimulated with thrombin (2 U/ml), β-BA or AKBA (30 µM, each) for 5 min at 37 °C and then put on ice for 10 min, followed by centrifugation (5,000 × g, 15 min). Aliquots (300 µl) of the supernatants were measured (Micro Beta Trilux, Perkin Elmer) to detect the amounts of [^{3}H]-labeled AA released into the medium. In order to ascertain that the radioactivity released is AA and not an AA metabolite, we directly analyzed the AA released from unlabelled platelets after separation by solid phase extraction, coupling to dimethoxyaniline hydrochloride (DMA-HCl) in presence of N-Ethyl-N'-(3-dimethylaminopropyl)carbodiimide (EDC) in methanol and the derivatized AA was analyzed by RP-HPLC at a wave length of 272 nm [236].

3.2.10 Determination of COX-1 product in intact human platelets

Freshly isolated platelets (10^8/ml in PG buffer) were supplemented with 1 mM $CaCl_2$. Since BAs act differentially on p12-LO (11-methylene-BAs stimulate, 11-keto-BAs inhibit) and thus, to avoid differential conversion of AA by p12-LO, the selective 12-LO inhibitor CDC (10 µM) [237], commonly used to block 12-LO activity in studies of platelet functions [10, 238], was included in all incubations to assure comparable AA levels for conversion by COX-1. COX-1 is the major enzyme in platelets converting AA into oxidized metabolites including 12-HHT [239, 240]. Washed platelets were pre-incubated with the indicated agents for 5 min at RT and COX-1 product formation was initiated by thrombin (2 U/ml), A23718 (2.5 µM), collagen (10 µg/ml) AA (5 µM). After further incubation for 5 min at 37 °C the reaction was stopped with 1 ml of ice-cold methanol and then, 30 µl HCl, 200 ng prostaglandin B_1 (PGB_1), internal standard) and 500 µl PBS were added. The COX-1 product (12-HHT) was extracted and then analyzed by HPLC as described [241, 242]. In detail, after centrifugation (800 × g, 10 min, RT) samples were applied to C-18 solid-phase extraction columns (100 mg; IST, Mid Glamorgan, UK), which have been preconditioned with methanol and water (1ml, each). The columns were washed with 1 ml water and 1 ml methanol 75% (v/v) and COX-1 products were eluted with 300 µl methanol and then diluted with 120 µl water. 100 µl diluted extract were analyzed by HPLC on a Nova-Pak® C18 column (5 × 100 mm, 4 µm particle size, Waters (Eschborn, Germany)) using 76% methanol aq. + 0.007% trifluoro acetic acid (v/v) as mobile phase at a flow rate of 1.2 ml/min and UV detection at 235/280 nm. The amount of 12-HHT was determined by peak area integration. COX-1 product formation is expressed as ng of 12-HHT per 10^8 cells.

3.2.11 Determination of COX-2 product formation in intact MM6 cells

The release of 6-keto-$PGF_{1\alpha}$ from LPS-stimulated MM6 cells expressing COX-2 was assessed by ELISA as described [241]. In brief, MM6 cells were differentiated with 50 nM calcitriol for 96 h, LPS (100 ng/ml) was added and after 6 h, cells were harvested and resuspended in PGC buffer (3×10^6 cells/ml). Cells were pre-incubated with the test compounds at the indicated concentrations for 15 min at 37 °C, and then stimulated with AA (30 µM) for another 15 min at 37 °C. The amount of 6-keto-$PGF_{1\alpha}$ released was determined by ELISA using a monoclonal antibody against 6-keto-$PGF_{1\alpha}$ according to the protocol described by Yamamoto *et al.*, 1987 [243]. The monoclonal antibody (0.2 µg in 200 µl) was coated to microtiter plates via a goat anti-mouse-IgG antibody. 6-keto $PGF_{1\alpha}$ (15 µg) was linked to bacterial β-galactosidase (0.5 mg) and the enzyme activity bound to the antibody was determined in an ELISA reader (SynergyHT, BioTEK, Germany) at OD550 nm (reference wavelength: 630 nm) using chlorophenol-red-β-D-galactopyranoside (Roche Diagnostic GmbH, Germany) as substrate.

3.2.12 Activity assays of isolated COX-1 and -2

Inhibition of the activities of isolated ovine COX-1 and human COX-2 was performed as described [244, 245]. Though the purified COX-1 is not of human origin, ovine COX-1 is generally used for inhibitor studies when examining the effectiveness of compounds on the activity of isolated COX-1 enzyme [245]. Briefly, purified COX-1 (ovine, 50 units) or COX-2 (human recombinant, 20 units) were diluted in 1 ml reaction mixture containing 100 mM Tris buffer pH 8, 5 mM GSH, 5 µM haemoglobin, 100 µM EDTA at 4 °C and pre-incubated with the test compounds for 5 min. Samples were pre-warmed for 60 s at 37 °C and AA (5 µM) was added to start the reaction for additional 5 min at 37 °C. In wash-out experiments COX-1 was incubated with or w/o 30 µM AKBA, 50 µM aspirin or 30 µM ibuprofen for 10 min at RT, each. Then, samples were splitted and one aliquot was diluted with assay buffer ten-fold, whereas the other one was not altered, and 5 µM AA was added to each aliquot to start the COX-1 reaction. COX product 12-HHT was extracted and then analyzed by HPLC as described for intact human platelets.

3.2.13 Determination of COX-1 product formation in whole blood

For assays in whole blood, freshly withdrawn blood from healthy adult donors was obtained by venipuncture and collected in monovettes containing 16 IE heparin/ml (Sarstedt, Nümbrecht, Germany). Aliquots of 2 ml were pre-incubated with the test compounds or with vehicle (DMSO) for 10 min at 37 °C, as indicated, and formation of COX-1 product formation was started by addition of A23187 (30 µM). The reaction was stopped on ice and the samples were centrifuged at 600 × g, 10 min, 4 °C (Thermofisher MicromaxRX, Fisher Scientific, Schwerte, Germany). Aliquots of the resulting plasma (500 µl) were then mixed with 2 ml of methanol and 200 ng PGB_1 were added as internal standard. The samples were placed at -20 °C for 2 h and centrifuged again (600 × g, 15 min, 4 °C). The supernatants were collected and diluted with 2.5 ml PBS and 75 µl HCl (1M). Formed 12-HHT was extracted and analyzed by HPLC as described for intact human platelets.

3.2.14 Determination of 5-LO product synthesis in human PMNL

For determination of cellular 5-LO product formation, 5×10^6 freshly isolated PMNL in 1 ml PGC buffer with or without bovine serum albumin (BSA) were pre-incubated with test compounds or with vehicle (DMSO) for 10 min at 37 °C, as indicated. 5-LO product formation was started by addition of A23187 (2.5 µM) with or without 20 µM AA. The reaction was stopped after 10 min with 1 ml of methanol and then 30 µl of 1 N HCl, 200 ng PGB_1 and 500 µl of PBS were added. Formed 5-LO metabolites were extracted and analyzed by HPLC in analogy to **3.2.10**. 5-LO product formation is expressed as ng of 5-LO products per 10^6 cells which includes LTB_4 and its all-trans isomers, 5(S),12(S)-di-hydroxy-6,10-trans-8,14-cis-eicosatetraenoic acid (5(S),12(S)-DiHETE), and 5-H(P)ETE. 5-HETE and 5-HPETE coelute as one major peak, integration of this peak represents both eicosanoids. Cys-LTs (LTC_4, D_4 and E_4) were not detected and oxidation products of LTB_4 were not determined.

3.2.15 Determination of 5-LO product synthesis in 40,000 × g supernatants of E. coli and of partially purified 5-LO

Aliquots of the S40 of *E. coli* lysates (corresponding to 4 ml *E. coli* culture) or 0.5 µg partially purified recombinant 5-LO, were diluted with ice-cold PBS containing 1 mM EDTA, and 1 mM ATP and PC as well as the test compounds (or DMSO as vehicle) were added, as indicated. After 10 min on ice, samples were pre-warmed for 30 s at 37 °C and AA (2 or 20 µM) was added together with or without 2 mM $CaCl_2$, as indicated. The reaction was stopped after 10 min at 37 °C by addition of 1 ml of ice-cold methanol and 200 ng PGB_1 were added. Formed 5-LO metabolites were extracted and analyzed by HPLC as described above.

3.2.16 Determination of 5-LO product synthesis in human whole blood

Freshly withdrawn venous blood was obtained as described in **3.2.13**. Aliquots of 2 ml (A23187) or 3 ml (LPS/fMLP) were pre-incubated with the test compounds or with vehicle (DMSO) for 10 min at 37 °C, as indicated. Formation of 5-LO products was started by addition of fMLP (1 µM) after 30 min priming with 1 µg/ml LPS, or by addition of A23187 (30 µM). The reaction was stopped on ice after 15 (fMLP) or 10 (A23187) min and the samples were centrifuged (600 × g, 10 min, 4 °C). Aliquots of the resulting plasma (500 µl) were then mixed with 2 ml of methanol and 200 ng PGB_1 were added as internal standard. The samples were placed at -20 °C for 2 h and centrifuged again (600 × g, 15 min, 4 °C). The supernatants were collected and diluted with 2.5 ml PBS and 75 µl HCl 1N. Formed 5-LO metabolites were extracted and analyzed by HPLC as described for intact PMNL.

3.2.17 Determination of PGE_2 synthase activity in microsomes of A549 cells

PGE_2 synthase activity was measured as described [142]. In brief, microsomal membranes of A549 cells were diluted in potassium phosphate buffer (0.1 M, pH 7.4) containing 2.5 mM GSH (100 µl total volume) and PGE_2 formation was initiated by addition of PGH_2 (20 µM, final concentration). After 1 min at 4 °C, the reaction was terminated with 100 µl of stop solution (40 mM $FeCl_2$, 80 mM citric acid and 10 µM of 11β-PGE_2), PGE_2 was separated by extraction using C-18 solid-phase extraction columns (100 mg; IST, Mid Glamorgan, UK), preconditioned with acetonitrile and water (1 ml, each). he columns were washed twice with water (400 µl) and PGE_2 was eluted with acetonitrile (200 µl), diluted with water (400 µl), and analyzed by RP-HPLC (30% acetonitrile aq. (v/v) + 0.007% TFA (v/v), Nova-Pak® C18 column, 5 × 100 mm, 4 µm particle size, flow rate 1 ml/min) with UV detection at 195 nm. 11β-PGE_2 was used as internal standard to quantify PGE_2 product formation by integration of the area under the peaks.

3.2.18 Determination of PGE_2 formation in intact A549 cells

A549 cells (2×10^6 cells) were plated in a 175 cm^2 flask and incubated for 16 h at 37 °C and 6% CO_2. Thereafter, medium was replaced by fresh DMEM high glucose (4.5 g/l) medium containing FCS (2%, v/v) and the cells were stimulated with IL-1β (1 ng/ml) for 72 h. Stimulation of A549 for 72 h with IL-1β results in co-expression of COX-2 and mPGES-1 [150], whereas COX-1 is essentially absent under such conditions [246]. After trypsination, the cells were washed twice with PBS. For determination of PGE_2, 2×10^6 cells resuspended in PBS (0.5 ml) containing $CaCl_2$ (1 mM) were pre-incubated with the indicated compounds at 37 °C for 10 min and PGE_2 formation was started by the addition of ionophore A23187 (2.5 µM), AA (1 µM)

and [^{3}H]AA (18.4 kBq). The use of exogenous A23187 and AA to induce PGE_2 formation excludes effects of BAs on receptor-coupled signal transduction and/or on endogenous substrate supply for COX-2. The reaction was stopped after 15 min at 37 °C and the samples were put on ice. After centrifugation (800 × g, 5 min, 4 °C), the supernatant was acidified to pH 3 by addition of 20 µl citric acid (2 M) and the internal standard 11β-PGE_2 (2 nmol) was added. Solid phase extraction and HPLC analysis were performed as described in **3.2.17**. The amount of 11β-PGE_2 was quantified by integration of the area under the eluted peaks. For quantification of radiolabeled PGE_2, fractions (0.5 ml) were collected and mixed with Ultima GoldTM XR (2 ml) for liquid scintillation counting in a LKB Wallac 1209 Rackbeta Liquid Scintillation Counter.

3.2.19 Determination of PGE_2 and 6-keto-$PGF_{1\alpha}$ in whole blood

Determination of PGE_2 formation in whole blood was assayed according to [247]. Peripheral blood from healthy adult volunteers was obtained as described in **3.2.13**. Aliquots of whole blood (0.8 ml) were mixed with the thromboxane synthase inhibitor CV4151 (1 µM) [248] and aspirin (50 µM). A total volume of 1 ml was adjusted with sample buffer (10 mM potassium phosphate buffer pH 7.4, 3 mM KCl, 140 mM NaCl and 6 mM D-glucose). After pre-incubation with the indicated compounds for 10 min at RT, the samples were stimulated with LPS (10 µg/ml) for 5 h at 37 °C. The reaction was stopped on ice and the samples were centrifuged (2300 × g, 10 min, 4 °C). On aliquot of the supernatant was used to analyze the formation of 6-keto-$PGF_{1\alpha}$ by ELISA. The other aliquot was acidified by addition of citric acid (30 µl, 2 M) and after another centrifugation step (2300 × g, 10 min, 4 °C), solid phase extraction and HPLC analysis of PGE_2 were performed as described **(3.2.17)**. The PGE_2 peak (3 ml), identified by co-elution with authentic standard, was collected and acetonitrile was removed under a nitrogen stream. The pH was adjusted to 7.2 by addition of 10 × PBS buffer pH 7.2 (230 µl), before PGE_2 was quantified using a PGE_2 High Sensitivity EIA Kit (Assay Designs, Ann Arbor, USA) according to the manufacturer's protocol.

3.2.20 Carrageenan-induced paw edema

Animal care complied with Italian protocols (Ministerial Decree 116192) as well as with the European Economic Community regulations (Official Journal of E.C. L 358/1 12/18/1986). Male adult CD1 mice (25-35 g, Harlan, Milan, Italy) were divided into groups (n = 10 for each group) and lightly anaesthetized with enflurane 4% mixed with O_2, 0.5 l/min, and N_2O, 0.5/l min. Each group of animals received subplantar administration of saline (0.05 ml) or λ-carrageenan 1%

type IV (w/v) (0.05 ml) in saline. The paw was marked in order to immerge it always at the same extent in the measurement chamber. The volume was measured by using a hydropletismometer, specially modified for small volumes (Ugo Basile, Milan, Italy) immediately before subplantar injection and 2, 4 and 6 h thereafter [249]. The assessment of paw volume was performed always in double blind and by the same operator. In the treated group of animals, β-BA (0.25 and 1 mg/kg) or indomethacin (5 mg/kg) was given intraperitoneal (i.p.), 30 min before carrageenan. The vehicle-treated group of mice received (DMSO 2%, i.p.) instead of test compounds. The increase in paw volume was calculated by subtracting the initial paw volume (basal) to the paw volume measured at each time point. Data represent the mean ± S.E. of 10 mice. Experiments were conducted in collaboration with the laboratory of Dr. L. Sautebin (University of Naples Federico II, Italy).

3.2.21 Carrageenan-induced pleurisy

Animal care complied with Italian protocols (Ministerial Decree 116192) as well as with the European Economic Community regulations (Official Journal of E.C. L 358/1 12/18/1986). Male Wistar Han rats (200-220 g, Harlan, Milan, Italy) were anaesthetized with enflurane 4% mixed with O_2, 0.5 l/min, N_2O, 0.5 l/min, and submitted to a skin incision at the level of the left sixth intercostal space. The underlying muscle was dissected, and saline (0.2 ml) or λ-carrageenan type IV 1% (w/v) (0.2 ml) was injected into the pleural cavity. The skin incision was closed with a suture, and the animals were allowed to recover. At 4 h after the injection of λ-carrageenan, the animals were killed by inhalation of CO_2. The chest was carefully opened, and the pleural cavity was rinsed with 2 ml saline solution containing heparin (5 U/ml). The exudate and washing solution were removed by aspiration, and the total volume was measured. Any exudate that was contaminated with blood was discarded. The amount of exudate was calculated by subtracting the volume injected (2 ml) from the total volume recovered. Leukocytes in the exudate were resuspended in PBS and counted with an optical light microscope in a Burker's chamber after vital trypan blue staining. In the treated group of animals, AKBA and β-BA (1 mg/kg, each) was given i.p. 30 min before carrageenan. Indomethacin (5 mg/kg) were used as reference compound and vehicle-treated group of rats received DMSO (4% (v/v), i.p.) 30 min before carrageenan.The amount of PGE_2, 6-keto-$PGF_{1\alpha}$ and LTB_4 in the supernatant of centrifuged exudate ($800 \times g$ for 10 min) was assayed by radioimmunoassay and ELISA, respectively (Assay Designs, Inc., Ann Arbor, USA), according to manufacturer's protocol. The results are expressed as ng per rat and represent the mean ± S.E. of 10 rats. Experiments were conducted in collaboration with the laboratory of Dr. L. Sautebin (University of Naples Federico II, Italy).

3.2.22 Immobilization of BAs and protein pull-down assays

For immobilization of BAs, β-BA and KBA were linked to EAH Sepharose 4B beads, via the C3-OH group using glutaric acid as a linker as described before [11] yielding Glutaroyl-(K)BA-Sepharose ((K)BA-Seph) (**Figure 3.1**). Preparation of immobilized BAs was performed by Dr. N. Kather (University Saarbrücken).

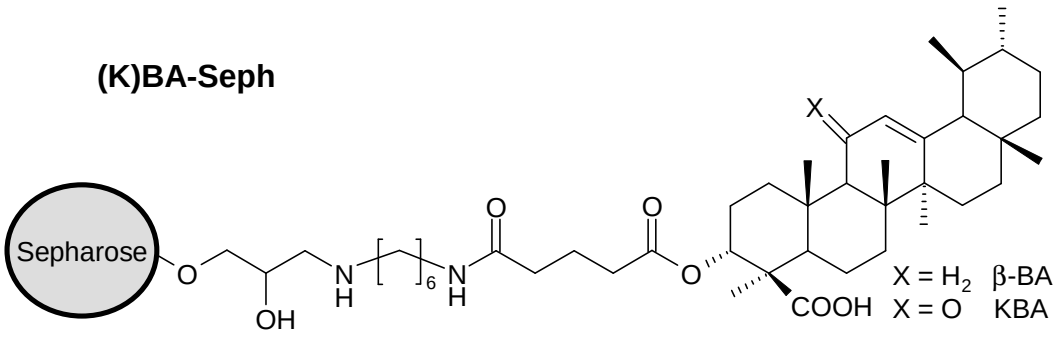

Figure 3.1: Chemical structure of immobilized BAs

For protein pull-down experiments, 1×10^7 A549 cells, 1×10^9 human platelets or 3×10^7 MM6 cells were lysed in 375 µl (A549 cells) or 1 ml (platelets and MM6 cells) lysis buffer (50 mM HEPES pH 7.4, 200 mM NaCl, 1 mM EDTA, 1% (v/v) Triton X-100, 2 mM PMSF, 10 µg/ml leupeptin, 120 µg/ml soybean trypsin inhibitor). After sonification ($3 \times$ 8 s) on ice and centrifugation (12,000 × g, 10 min, 4 °C) 125 µl (500 µl for human platelets and MM6 cells) of the sepharose slurries (50%, v/v) were added to the lysates and incubated at 4 °C over night under continuous rotation.

For pull-down experiments using *in vitro*-translated mPGES-1, the enzyme was resuspended in 50 mM potassium phosphate buffer pH 7.4, 1 mM GSH, 10% glycerol and 2% (w/v) LysoFos12 choline (Anatrace, Maumee, OH, USA) for 2 h at 30 °C. Then insoluble parts were removed by centrifugation (10,000 × g 10 min, 10 °C) and finally, 200 ng of the purified enzyme was diluted into 500 µl lysis buffer containing 1000-fold excess of *E. coli* (BL21 strain) protein [250] and 100 µl of the sepharose slurries (50%, v/v) were added.

For pull-down of purified COX-1/2, 10 units of the purified enzyme were diluted into 500 µl of lysis buffer containing 0.1 µg/ml BSA (as blocking agent), and 200 µl of sepharose slurry (50%, v/v) was added. After incubation over night the sepharose beads were spun down and intensively washed ($3 \times$) with 10 volumes of binding buffer (HEPES pH 7.4, 200 mM NaCl, 1 mM EDTA) and precipitated proteins were finally separated and denatured by addition of sodium SDS sample loading buffer (SDS-b; 20 mM Tris-HCl, pH 8, 2 mM EDTA, 5% (m/v) SDS, 10% (v/v) β-mercaptoethanol). After boiling (95°C, 6 min), beads were removed by centrifugation (10,000 × g, 10 min, RT) and the proteins in the supernatant were separated by SDS-polyacrylamide gel electrophoresis (SDS-PAGE) (see **3.2.31**) and visualized by silver or

Coomassie staining (**3.2.32** and **3.2.33**, respectively) or detected by WB analyses (**3.2.34**). Ponceau S staining of the membranes after blotting assured comparable unspecific protein-binding by Seph, KBA-Seph and b-BA-Seph, respectively.

3.2.23 In-gel digestion and nanoflow liquid chromatography tandem MS (nano-LC-ESI-MS/MS)

Proteins of interest were in-gel digested overnight using porcine trypsin (sequencing grade, Modified; Promega, Mannheim, Germany) at 37 °C and reversed-phase nano-LC-MS/MS was performed as described [11, 251]. Finally proteins were identified by correlating the data from the MS/MS spectra with the NCBI nr-protein sequence database (version 20060511, taxonomy Homo sapiens) applying the search engine MASCOT (Matrix Science Ltd. London, UK). This work was done in collaboration with the Proteom Center Tübingen (Dr. A. Nordheim).

3.2.24 Surface plasmon resonance experiments

All experiments were carried out on a BIAcore® X device (GE Healthcare Freiburg, Germany). *In vitro*-translated mPGES-1 (100 µg/ml) in 10 mM Na-acetate pH 6.0 was coupled to a carboxymethylated dextran surface (CM-5 chip, GE Healthcare) using standard amine coupling chemistry according to the manufacturer's directions. There are two flow cells on each chip, whereas flow cell 1 wasn't altered and functioned as reference, mPGES-1 (236 fmol/mm^2) was immobilized to flow cell 2 corresponding to 4700 resonance units (RU). Equilibration of the baseline was completed by passing a continuous flow of assay buffer (10 mM HEPES, 150 mM NaCl, 0.01% surfactant P20, and 1% DMSO, pH 7.4) through the chip for 2 h. During the SPR experiments the stock solution of test compounds (dissolved in DMSO) was diluted into assay buffer. All measurements were performed at 25 °C and a flow rate of 30 µl/min.

After recording association, the liquid phase was replaced by assay buffer and the dissociation was monitored. The binding profiles were obtained after subtracting the response signal of the untreated reference cell 1 and sensograms were processed by using automatic correction for non-specific bulk refractive index effects using BIAEVALUATION Version 3.1 software (GE Healthcare). All experiments were carried out in duplicates.

Analysis of binding data:

To obtain dissociation constants from the equilibrium binding data two different fitting models were adopted. First, the change in the equilibrium amount of compound bound as a function of the concentration of compound was fit to the equation for a simple 1:1 binding model: $R = (R_{max}*[cmpd]/(K_D + [cmpd])$; where R is the response, R_{max} is the maximum response and K_D is the dissociation constant. In our case a good fit was obtained by this model. A Scatchard analysis was also used to estimate K_D. A global analysis using the BIAEVALUATION software version 3.1 was used to determine the kinetic data. The integrated rate equation describing a 1:1 Langmuir interaction was fit simultaneously to the entire concentration range for ox-KBA. This fit yielded the association rate Ka, the dissociation rate Kd and the dissociation constant K_D [252, 253]. The goodness of the fit was determined by the χ^2 values, as well as the magnitude and distribution of the residuals.

3.2.25 Automated docking

Automated molecular docking of BAs into X-ray structures of COX-1 and COX-2 was performed using GOLD 3.1.1, which relies on a genetic algorithm for structure optimization [254]. Crystal structure of COX-1, PDB-code 1Q4G at 2.0 Å resolution, with bound inhibitor 2-(1,1'-biphenyl-4-yl)propanoic acid (BFL), a defluorinated flurbiprofen analog [255] was used. For COX-2, the PDB entry 6COX at 2.8 Å resolution, complexed with the selective inhibitor SC-558 [256] was selected. Hydrogens were added to the proteins, and energy minimized using the AMBER99 force field, within the software MOE 2006.08 (Chemical Computing Group, Montreal, Canada). For the co-crystallized inhibitors hydrogen atoms were added, and energy minimization was performed using the MMFF94x force field [257]. Starting conformations for the 3D structures of the four BAs were calculated with MOE using the MMFF94x force field. GOLD parameter settings for the genetic algorithm were: number of operations = 10,000, population size = 100, selection pressure = 1.1, number of islands = 1, niche size = 2, migrate = 0, mutate = 100, crossover = 100. A 10 Å radius around the bound inhibitor in the active site defined the binding pocket. The Chemscore function [258] was used for scoring the predicted binding poses. Greater positive score values indicate more favorable protein-ligand complexes; negative values indicate unfavorable binding modes (non-binding). Each docking run was repeated ten times. The same method was used for re-docking of the co-crystallized inhibitors. Root mean square deviation (RMSD) values between the PDB X-ray structures and the docking solutions were computed, and a mean value with standard deviation was calculated. PyMOL was used for visualization of docking poses [259].This work was entirely performed by Dr. Lutz Franke and Bettina Hofman (University of Frankfurt).

3.2.26 Albumin-binding of BAs

PG buffer (2.5 ml), supplemented with BSA (0, 1 or 10 mg/ml, as indicated) was incubated with 50 µM AKBA for 10 min at 37 °C. Separation of AKBA and albumin was carried out by gel filtration using a Sephadex® G-25 (PD-10) column (GE Healthcare, Freiburg, Germany). In detail, the Sephadex® G-25 column was equilibrated with PG buffer and the sample (2.5 ml) was applied. 500 µl aliquots of the eluate were collected and immediately analysed for AKBA by HPLC, and for BSA using Roti®-nanoquant (**3.2.35)** according to the instructions of the manufacturer (Carl Roth, Karlsruhe, Germany). Quantification of AKBA by RP-HPLC was performed on a Nova-Pak® C18 column (5 × 100 mm, 4 µm particle size, Waters (Eschborn, Germany)) using 85% methanol aq. + 0.01% TFA (v/v) as mobile phase at a flow rate of 1.2 ml/min and UV detection at 250 nm. Calibration was based on the external standard method, with the peak area as assay parameter. The concentration of AKBA (without BSA) versus elution volume was analysed by a non-linear fit (Gaussian distribution) providing μ, δ and the area under the curve (AUC) using the GraphPad Prism 4 (GraphPad software Inc., San Diego, CA, USA) program. Based on this evaluation the amount of unbound AKBA was determined by the AUC ($\mu \pm 3\delta$) for incubation with 1 or 10 mg/ml BSA.

3.2.27 Measurement of intracellular Ca^{2+} levels

Washed human platelets (6×10^8/ml PG buffer) were incubated with 2 µM Fura-2/AM (1-[2-(5-carboxyoxazol-2-yl)-6-aminobenzofuran-5-oxy]-2-(2'-amino-5'-methyl-phenoxy) ethane-N,N,N',N'-tetraacetic acid) for 30 min at 37 °C. After washing platelets (10^8/ml in PG buffer) were pre-incubated with the indicated agents for 15 min at RT. Then, the samples were transferred into a thermally controlled (37 °C) fluorimeter cuvette in a spectrofluorometer (Aminco-Bowman series 2, Thermo Spectronic, Rochester, NY) with continuous stirring. Two min prior stimulation with 0.5 U/ml thrombin, 8 µg/ml collagen or 1 µM U-46619, 1 mM $CaCl_2$ was added. The fluorescence emission at 510 nm was measured after excitation at 340 and 380 nm, respectively, and $[Ca^{2+}]_i$ was calculated according to Grynkiewicz et al. [260]. F_{max} (maximal fluorescence) was obtained by lysing the cells with 1% Triton-X 100 and F_{min} by chelating Ca^{2+} with 10 mM EDTA.

3.2.28 Platelet aggregation (turbidimetric)

Aggregation of washed human platelets was determined using a turbidimetric light-transmittance device (two channel Chrono-Log aggregometer, Haverton, PA). Washed human platelets were prepared as described in **3.2.4** and adjusted to 2×10^8/ml. The instrument was calibrated with a platelet suspension for basal (0%) light transmission and with Tyrode`s buffer alone for 100% light transmission. Aliquots of 0.5 ml platelets were incubated with the indicated BAs for 10 min at RT. For aggregation, the response to 0.5 U/ml thrombin, 0.6 µg/ml collagen or 1 µM U-46619 is given as % of the maximal light transmission A_{max}. $CaCl_2$ (1 mM) was added right before the start of the measurement. Aggregation was recorded under continuous stirring (1000 rpm) at 37 °C for 5 min.

3.2.29 Measurement of thrombin generation

Thrombin generation was assessed by using a fluorometric assay, based on the cleavage of a thrombin-specific fluorogenic substrate, Z-Gly-Gly-Arg-AMC (Bachem, Bubendorf, Switzerland) resulting from stimulation of recalcified PRP [261]. 80 µl of PRP untreated or pre-incubated as indicated and 20 µl of buffer containing the thrombin generation trigger (2 µg/ml collagen, 5 µM U-46619, BAs or vehicle (DMSO), as indicated) were added to each well of a 96-well microtiter plate. The reaction was started by adding 20 µl of substrate solution (20 mM Hepes, 150 mM NaCl, BSA 60 mg/ml, 0.1 M $CaCl_2$ and 5 mM fluorogenic substrate) leading to the final concentration as follows: substrate: 833 µM; $CaCl_2$: 16.7 mM and DMSO: 0.41 %. The fluorometer Fluoroskan Ascent, type 374 with dispenser (ThermoFisher Scientific, Germany) was used with excitation wavelength of 390 nm, emission wavelength of 460 nm, and a measurement integration time per well of 20 ms. All experiments were standardized by using Thrombin Calibrator (Thrombinoscope BV, Maastricht, Netherlands) according to the manufacturer`s protocol which allow to calculate the molar concentration of thrombin regardless of substrate consumption, inner filter effects or donor-to-donor variability in the color of plasma. The first derivative of the fluorescence–time curve reflects the course of thrombin activity in the sample. The parameter of interest in the samples using recalcified PRP was the velocity index. The velocity index reflects the rate of thrombin generation between lag phase and peak thrombin concentration (max. (= peak) thrombin formation/peak time-lag time) in nM/min. All experiments were performed in triplicates.

3.2.30 Determination of tyrosine phosphorylation and activation of Src family kinases and PLCγ2 in human platelets

Human platelets were obtained as described (**3.2.4)** and adjusted to 5×10^8/ml in PG buffer. Platelets were pre-incubated with AKBA, PP2 (or its inactive analogue PP3) or vehicle (DMSO) for 10 min at RT. Samples were pre-warmed for 30 s at 37 °C and subsequently stimulated with collagen (10 µg/ml) or β-BA (30 µM). After 3 min the reaction was terminated by adding a half-volume of 3× SDS-b. Samples were sonificated (3×10 s) and finally subjected to SDS-PAGE followed by WB using specific antibodies (**3.2.31** and **3.2.34**).

3.2.31 SDS-PAGE

Cell suspensions or given sample preparations were incubated as specified and the reaction was stopped by the addition of ice-cold $2 \times$ SDS-polyacrylamide gel electrophoresis (SDS-PAGE) sample loading buffer (SDS-b; 20 mM Tris/HCl, pH 8, 2mM EDTA, 5% SDS (w/v), 10% (v/v) β-mercaptoethanol), vortexed, sonificated (3×15 s) if required and heated for 6 min at 95 °C. The protein samples (18 µl) were mixed with 4 µl of glycerol/0.1% bromophenolblue (1:1, v/v) and analyzed by SDS-PAGE using a Mini Protean system (Bio-Rad, Hercules, CA, USA) according to Laemmli [262]. Depending on the molecular weight of the proteins to be analyzed, the polyacrylamid (PAA) concentration was adjusted to: 8% (p-Tyr screening, p-PLCγ2), 10% (pull-down experiments using platelets lysates as protein source, isolated COX1/2 and p-Src family kinases) or 14% (pull-down experiments using A549 lysates as protein source and *in vitro*-translated mPGES-1 experiments). Molecular weight of the proteins was estimated by comparison with either prestained or non-stained broad range molecular weight markers (peqGOLD IV and peqGOLD II, respectively; PEQLAB Biotchenology, Erlangen Germany).

3.2.32 Coomassie staining

Washed (in MQ water) gels from SDS-PAGE were fixed and stained 6 - 12 h on a shaking table at RT in colloidal staining solution (0.08% Coomassie Brilliant Blue G250 (w/v), 1.6% ortho-phosphoric acid (v/v), 8% ammonium sulfate (w/v), 20% methanol (v/v)) and destained in MQ until background was clear [263]. Proteins of interest were excised and applied to MS-analytics (**3.2.23**).

3.2.33 Silver staining

After SDS-PAGE, proteins in the gels were fixed in 5% acetic acid and 10% methanol (v/v, 4 × for 30 min), washed in MQ water and sensitized 2 min in freshly prepared 0.02% $Na_2S_2O_3$ (w/v) solution. After washing in MQ water and incubation in 0.1%, "silver solution" ($AgNO_3$, w/v) for 30 min the gel was developed several minutes under slow shaking in 2.5% Na_2CO_3; 0.04% formaline and fixed in 1% acetic acid (w/v) [264]. Proteins of interest were excised and applied to MS-analytics (**3.2.23**)

3.2.34 Western Blot

After electroblot (tank blotting method) of gels from SDS-PAGE to nitrocellulose membrane (Amersham Pharmacia, Little Chalfont, UK), membranes were blocked with 5% (w/v) non-fat dry milk or BSA blocking buffer (50 mM Tris/HCl, pH 7.4, and 100 mM NaCl (Tris-buffered saline (TBS)) plus 0.1% Tween 20 (TBS-Tween)) for 1 h at RT. Correct loading of the gel and transfer of proteins to the nitrocellulose membrane was confirmed by Ponceau S staining unless stated otherwise. Membranes were washed (TBS-Tween) and then incubated with the respective primary antibody (AB) overnight at 4 °C (**Table 3.1**).

Table 3.1: Primary antibodies used.

Primary antibody	Isotype	Dilution	Company
Actin	goat IgG	1: 1000	Santa Cruz Biotechnology
COX-1	mouse IgG2b	1:200	Cayman Chemical
COX-2	rabbit IgG	1:1000	Biomol
mPGES-1	mouse IgG	1:200	Cayman Chemical
Phospho-Src family (Tyr416)	rabbit IgG	1:500	Cell Signaling
Phospho-Tyr (PY20)	mouse IgG2b	1:2500	Santa Cruz Biotechnology
Phospho-PLCγ2 (Tyr759)	rabbit IgG	1:1000	Cell Signaling

Antibodies were diluted in TBS Tween, 0.05% NaN_3 (v/v), 5% milk or BSA as indicated. The membranes were washed and incubated with 1:1000 dilution of secondary AB (alkaline peroxidase-conjugated IgGs) for 3 h at RT. After washing (4 × with TBS-Tween and TBS), proteins were visualized with nitro blue tetrazolium and 5-bromo-4-chloro-3-indolylphosphate in

detection buffer (100 mM Tris/HCl, pH 9.5; 100 mM NaCl, 5 mM $MgCl_2$) All steps regarding the incubation of the membrane were performed under gentle agitation.

3.2.35 Determination of protein concentration

The Roti®-Nanoquant approach based on a modification of the Bradford protein quantification method [265, 266] was used for determination of protein concentration. Standard (BSA) and protein of interest was diluted in appropriate buffer and pipetted in triplicates, 50 µl per well in a 96-well plate. After addition of Roti®-Nanoquant (1×) assay reagent (200 µl) the plate was agitated for 5 min and measured in a microplate reader (Victor^3 plate reader, PerkinElmer, Rodgau-Juegesheim, Germany) at 590 nm and 450 nm. The quotient $OD_{590/450}$ was plotted against the amount of standard.

3.2.36 Statistics

Data are expressed as mean ± S.E.; IC_{50} and EC_{50} values, obtained from measurements at 4 - 5 different concentrations of the compounds, were calculated by GraphPad Prism 4 (GraphPad Software Inc., San Diego, CA) and data were fitted using the sigmoidal-concentration response equation (variable slope) or are approximations determined by graphical analysis (linear interpolation between the points between 50% activity). Statistical evaluation of the data was performed by one-way ANOVAs for independent or correlated samples followed by Tukey HSD post-hoc tests (GraphPad Software Inc.). Where appropriate, Student´s t test for paired and correlated samples was applied. A *P* value of < 0.05 (*); < 0.01 (**) and < 0.001 (***) was considered significant.

All experiments using DMSO, ethanol or methanol as solvent never exceed 1% (v/v) final solvent concentration unless stated otherwise.

4 RESULTS

4.1 Interaction of boswellic acids with cyclooxygenases

4.1.1 BAs suppress COX-1 product formation in washed human platelets

Previous experiments revealed that various BAs induce release of AA in human platelets but further transformation to 12-H(P)ETE was only caused by 11-methylene-BAs [8]. Accordingly, the effects of 11-methylene-BA (i.e. β-BA) and 11-keto-BA (i.e. AKBA) on 12-HHT formation in platelets from endogenous AA (**Table 4.1**) were determined. Both, β-BA and AKBA (30 µM, each) caused AA release comparable to thrombin (2 U/ml). Accordingly, β-BA as well as thrombin induced formation of 12-HHT, but AKBA was hardly effective (**Table 4.1**), despite its ability to release AA as substrate for COX-1. This work was done in collaboration with Dr. Daniel Pöckel (University of Tübingen, Germany).

Table 4.1 Induction of AA release and 12-HHT formation in washed human platelets.
For determination of AA release, platelets (10^8/ml PGC buffer) were incubated with the indicated agents for 5 min at 37 °C, DMSO was used as vehicle. [^{3}H]AA released into the medium was measured as described. Data are given as counts per minute (cpm), mean ± S.E., n = 5. For determination of 12-HHT formation, platelets (10^8/ml PGC buffer) were incubated with the indicated agents for 5 min at 37 °C and 12-HHT formation was determined. Data are given as mean ± S.E., n = 4.

Compound	AA release (cpm)	12-HHT formation (ng per 10^8 cells)
Vehicle	445 ± 173	3.5 ± 1.3
Thrombin (2 U/ml)	1255 ± 180	165.4 ± 39.4
β-BA (30 µM)	921 ± 101	141.2 ± 5.1
AKBA (30 µM)	1045 ± 117	5.4 ± 1.9

In order to determine if BAs (in particular AKBA) may inhibit agonist-induced COX-1 product formation, human washed platelets were pre-incubated with BAs and stimulated with thrombin, collagen, and Ca^{2+}-ionophore A23187 (circumventing receptor signaling). AKBA and KBA concentration-dependently inhibited COX-1 product synthesis in platelets stimulated with A23187 (**Figure 4.1A**) or thrombin (**Figure 4.1B**).

For AKBA, the IC_{50} values were determined at approx. 6 µM (stimulation with A23187) and 17 µM (stimulation with thrombin) and for KBA at approx. 14 and 55 µM, respectively. Also collagen-induced COX-1 product formation was significantly reduced by AKBA (IC_{50} = 10 µM), whereas for KBA only modest inhibition at comparably high concentration became apparent (**Figure 4.1C**). In contrast, the 11-methylene-BAs are less potent COX-1 inhibitors with IC_{50} values >100 µM, and for thrombin- and collagen-activated platelets, 11-methylene-BAs even slightly enhanced 12-HHT formation (**Figure 4.1B** and **C**). The structural BA analogue α-amyrin, lacking the C4-carboxylic moiety (100 µM) gave no significant inhibition (88.4 ± 4.6 % of control), whereas the reference drugs aspirin (100 µM) and ibuprofen (30 µM) efficiently blocked thrombin-induced 12-HTT formation (3.1 ± 0.5% and 5.9 ± 1.8% of control, respectively). To confirm that BAs inhibit COX-1 and to exclude suppressive effects of BAs on agonist-induced AA supply the effects of BAs on 12-HHT formation in platelets that received exogenous added AA (5 µM) were assessed As shown in **Figure 4.1D**, a concentration-dependent inhibition of 12-HHT formation was observed for all BAs with AKBA being most potent (IC_{50} value approx. 23 µM), whereas the IC_{50} values for other BAs were > 50 µM. The negative control α-amyrin was not active up to 100 µM (**Figure 4.1D**), and aspirin (100 µM) or ibuprofen (30 µM) inhibited 12-HTT formation as expected (18 ± 9% and 23.8 ± 6.4% of control, respectively).

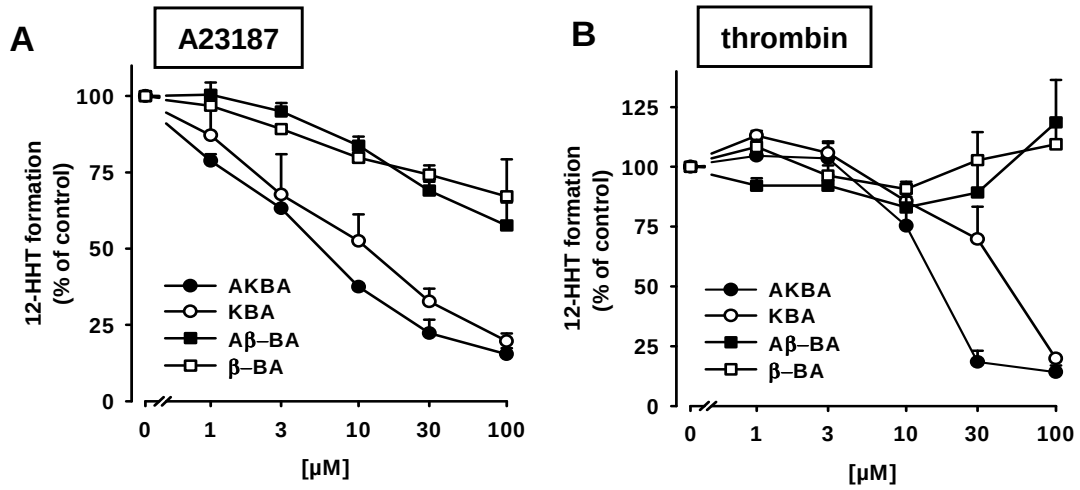

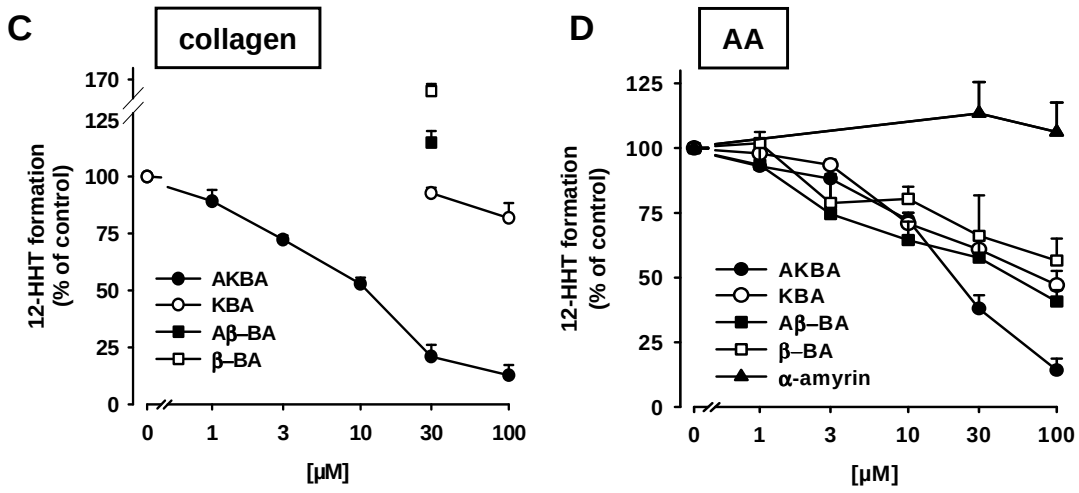

Figure 4.1: Inhibition of COX-1 activity by BAs in intact human platelets.
Washed human platelets (10^8/ml PGC buffer) were incubated with the indicated concentrations of the BAs or α-amyrin. After 5 min at RT, (**A**) 2.5 µM A23187, (**B**) 2 U/ml thrombin, (**C**) 10 µg/ml collagen or (**D**) 5 µM AA was added to induce COX-1 product formation. After additional 5 min at 37 °C the reaction was terminated and 12-HHT was determined by HPLC. Data are given as mean + S.E., n = 4-6. 12-HHT formation in the absence of test compounds (100%, control) was 104.6 ± 8.9 (A23187), 165.4 ± 39.4 (thrombin), 102.8 ± 11.3 (collagen) and 186.4 ± 17.6 (AA) ng per 10^8 platelets.

4.1.2 BAs suppress the activity of isolated COX-1

To determine if BAs directly interfere with COX-1 activity, isolated ovine COX-1 was incubated with 5 µM AA in the presence of GSH, leading to generation of 12-HHT as the major COX-1 product [244]. As shown in **Figure 4.2A** all BAs reduced the activity of COX-1. The IC_{50} value for AKBA was determined at approx. 32 µM being almost equipotent with ibuprofen (IC_{50} = 25 µM, data not shown), and α-amyrin (up to 100 µM) failed to suppress 12-HHT synthesis. To investigate if AKBA blocks COX-1 in a reversible manner, wash-out experiments were performed. As shown in **Figure 4.2B**, dilution of COX-1 incubations with 50 µM aspirin to a final concentration of 5 µM caused no change in the magnitude of COX-1 inhibition, but dilution of incubations containing AKBA or ibuprofen resulted in a significant loss of inhibition. To determine whether COX-1 inhibition by AKBA is affected by the AA substrate concentration, assays were performed at increasing amounts of AA in the absence or the presence of 30 µM AKBA or 20 µM ibuprofen. Potent inhibition of COX-1 was obvious for AKBA and ibuprofen at low (3 or 5 µM) substrate concentrations but modest inhibition was observed at high (60 µM) amounts of AA (**Figure 4.2C**).

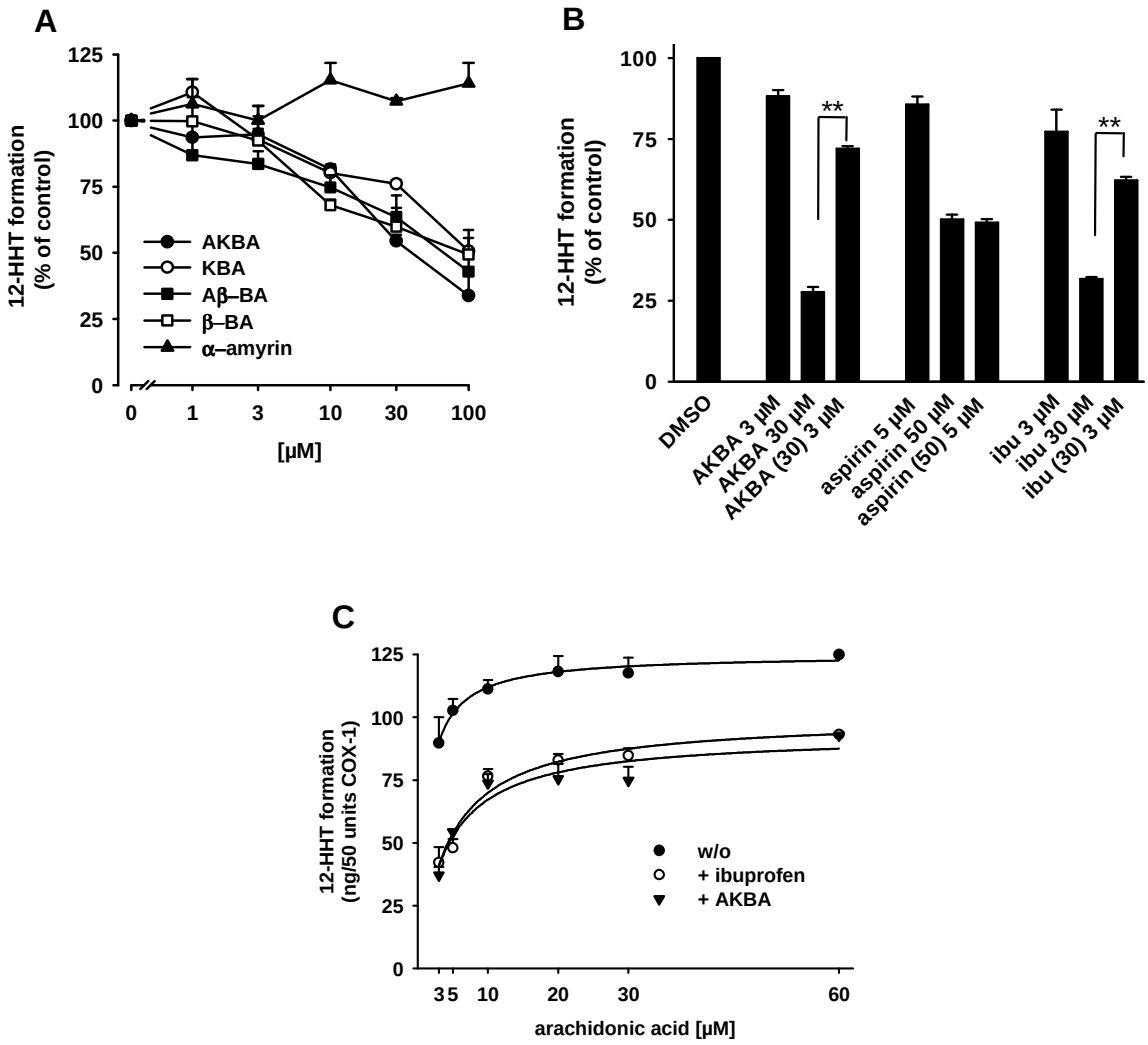

Figure 4.2: Inhibition of COX-1 activity by BAs in cell-free assays.
(**A**) Concentration-response studies. Isolated COX-1 (50 units) was diluted in 1 ml reaction mixture and pre-incubated with BAs or α-amyrin for 5 min at 4 °C, as specified. Samples were then pre-warmed for 60 s at 37 °C and 5 µM AA was added to start the reaction. After 5 min at 37 °C, 12-HHT was analyzed as described. COX-1 product formation in the absence of test compounds was (100% control) was 3.46 ± 0.73 ng/U COX-1. (**B**) Reversibility of COX-1 inhibition. Isolated COX-1 (50 units) was incubated with or without 30 µM AKBA, 50 µM aspirin, 30 µM ibuprofen, or vehicle (DMSO) for 5 min at RT, each. One aliquot of the samples was diluted with assay buffer ten-fold whereas the other one was not altered, and 5 µM AA was added to start the COX-1 reaction. For comparison, COX-1 was pre-incubated with 3 µM AKBA, 5 µM aspirin or 3 µM ibuprofen and then 5 µM AA was added (no dilution). All samples were incubated for 5 min at 37 °C and formed 12-HHT was analyzed. ** $P <$ 0.01, one-way ANOVA and Tukey HSD post hoc tests. (**C**) Effects of variation of the AA concentration. Isolated COX-1 (50 units) in 1 ml reaction mixture was pre-incubated with 30 µM AKBA or 20 µM ibuprofen and the indicated concentrations of AA were added. All data are given as mean + S.E., n = 4-5.

4.1.3 COX-1 binds to immobilized BAs

In order to assess the binding of COX-1 protein-binding strategy using immobilized BAs was applied. Fishing experiments revealed a protein with an apparent mass of 72 kDa in samples of β-BA-Seph and KBA-Seph, but not in controls where sepharose beads without ligand (Seph) were utilized (**Figure 4.3A**). In-gel trypsin digestion and subsequent nano-LC-ESI-MS/MS analysis (data not shown) identified this protein as human COX-1, confirmed by WB using specific AB against COX-1 (**Figure 4.3B**). To exclude an indirect precipitation of COX-1 via any possible linker molecule present in platelet lysates (that could actually be the binding partner of BAs), isolated ovine COX-1 (50 ng) was incubated with Seph, KBA-Seph, and β-BA-Seph in the presence of BSA (0.1 mg/ml, as blocking agent). Again, KBA-Seph, and β-BA-Seph precipitated COX-1 but not Seph without ligand (**Figure 4.3C**).

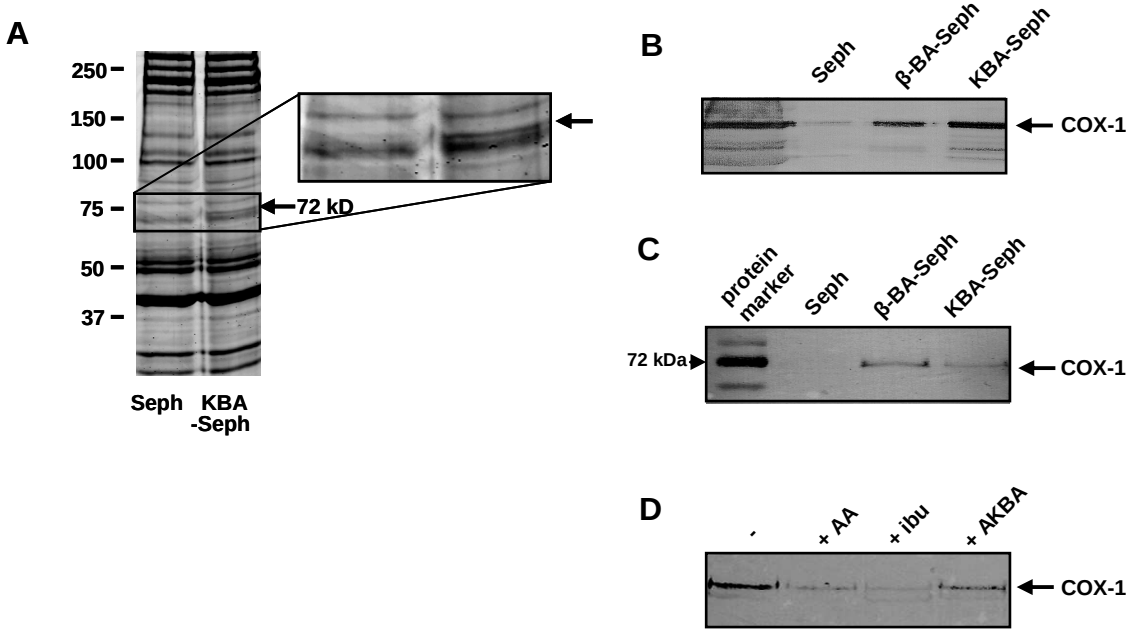

Figure 4.3: Pull-down of COX-1 by immobilized BAs.
Supernatants of platelet lysates were incubated over night at 4 °C with either β-BA-Seph, KBA-Seph or with crude Seph, as indicated. Precipitates were intensively washed, solubilized by addition of SDS-b and separated by SDS-PAGE. (**A**) Proteins were visualized by silver-staining, bands of interest at 72 kDa were excised, in-gel digested and analyzed by LC-ESI-MS/MS (data not shown). (**B**) Proteins were visualized by WB using specific antibodies against COX-1. An aliquot of platelet supernatant was used as a positive control. (**C**) Isolated COX-1 (50 ng) was incubated with β-BA-Seph, KBA-Seph, or Seph, in the presence of BSA (0.1 mg/ml). (**D**) Isolated COX-1 (50 ng) was incubated as above in the presence of AA (50 µM), ibuprofen (ibu, 50 µM) or AKBA (100 µM), as indicated. COX-1 was visualized by WB. Similar results were obtained in three independent experiments.

Using the pull-down strategy described above, the interaction between COX-1 and KBA-Seph was further characterized. Co-incubation with AA (50 µM) or ibuprofen (50 µM) strongly reduced the amounts of COX-1 that bound to KBA-Seph (**Figure 4.3D**). Furthermore, AKBA (100 µM) competed with KBA-Seph for binding to COX-1.

4.1.4 BAs moderately interfere with COX-2

Next, the effects of BAs on COX-2 were determined. Therefore, LPS-stimulated MM6 cells that had been differentiated with calcitriol were used as a cellular model [241]. 6-keto-$PGF_{1\alpha}$ was analyzed as COX-2-derived product after incubation of MM6 cells with 30 µM AA. As shown in **Figure 4.4A**, BAs caused only marginal inhibition of COX-2 product synthesis in MM6 cells (IC_{50} > 100 µM), whereas celecoxib (10 µM) or diclofenac (10 nM), used as positive controls) clearly suppressed the formation of 6-keto-$PGF_{1\alpha}$. To assess direct inhibition of COX-2 in cell-free assays, isolated human recombinant COX-2 was incubated with AA in the presence of BAs. All BAs, suppressed COX-2 product synthesis (**Figure 4.4B**), although the potencies (IC_{50} > 100 µM) were modest as compared to celecoxib (IC_{50} < 5 µM). Note that also α-amyrin (100 µM) slightly affected COX-2 product synthesis (82.2 ± 1.6 % of control). Incubation of isolated COX-2 with BA- or KBA-Seph yielded only traces of COX-2 protein (**Figure 4.4C**) and attempts to precipitate COX-2 from lysates of LPS-stimulated MM6 cells (in analogy to the pull-down experiments for COX-1) failed **(Figure 4.4D)**.

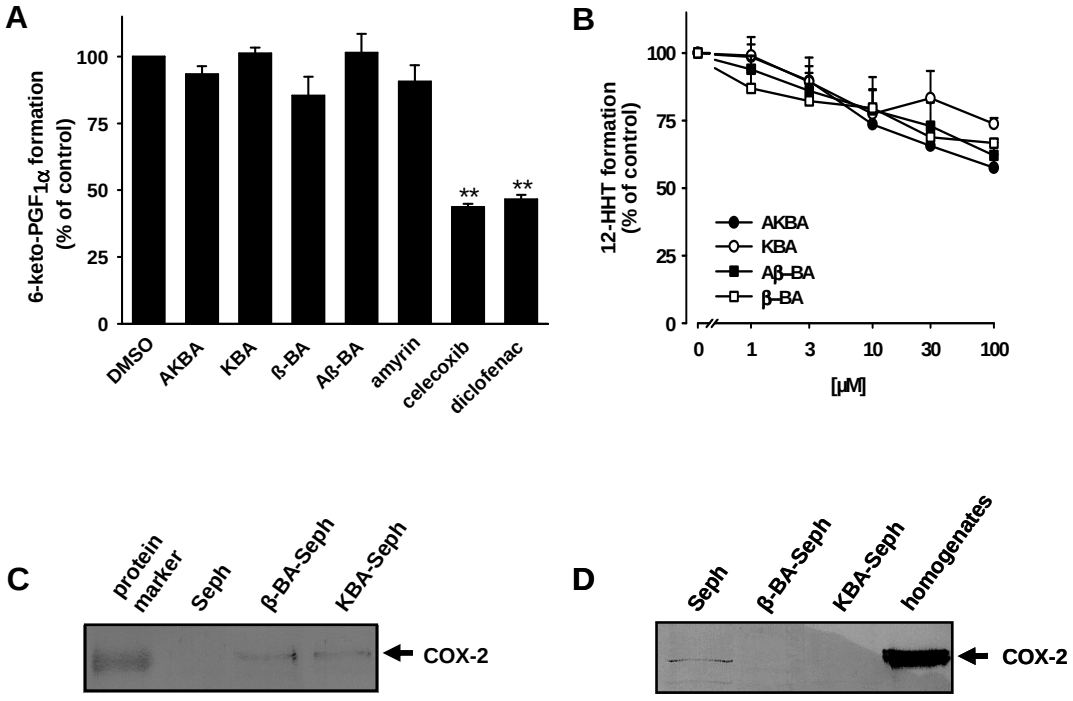

Figure 4.4: Interference of BAs with COX-2.
(**A**) Inhibition of COX-2 in intact MM6 cells. Cells (3×10^6 /ml PGC) were first pre-incubated with BAs (100 µM, each), celecoxib (10 µM), diclofenac (10 nM), or vehicle (DMSO) and then AA (30 µM) was added to start the COX-2 product formation. After 15 min at 37 °C the formed amounts of 6-keto-$PGF_{1\alpha}$ were determined by ELISA. Results are given as mean + S.E., n = 3. Formation of 6-keto $PGF_{1\alpha}$ in the presence of DMSO (100%, control) was 2.1 ± 0.2 ng per 10^6 MM6 cells. One-way ANOVA and Tukey HSD post hoc tests were performed; ** $P < 0.01$ vs vehicle control (DMSO) (**B**) Inhibition of COX-2 in cell-free assays. Isolated human recombinant COX-2 (20 units) was used and experiments were performed in analogy to isolated COX-1. Results are given as mean + S.E., n = 4. (**C**) Isolated COX-2 (82 ng) was incubated with β-BA-Seph, KBA-Seph, and Seph, in the presence of BSA (0.1 mg/ml). (**D**) Supernatants of MM6 lysates were incubated over night at 4 °C with either β-BA-Seph, KBA-Seph or with crude Seph, as indicated. Precipitates were treated as described and COX-2 was visualized by WB analysis. Similar results were obtained in three independent experiments.

4.1.5 Docking of BAs into X-ray structures of COX enzymes

Automated molecular docking of the BAs was performed to find potential binding modes for each BA within the active sites of the COX enzymes. As control, the known co-crystallized inhibitors BFL (COX-1) and SC-558 (COX-2) were successfully re-docked. Regarding COX-1, the RMSD for the inhibitor BFL was 0.34 ± 0.02. The acquired binding mode was identical to the X-ray structure, yielding an average Chemscore of 37.3 ± 0.9. Docking of AKBA into the same docking box resulted in an average score of 14.5 ± 2.0. Aβ-BA achieved a Chemscore of 18.5 ± 2.0, KBA 10.9 ± 1.3 and β-BA 15.9 ± 1.1. All four BAs showed the same orientation in the binding pocket (**Figure 4.5A** and **B**). For COX-2, the RMSD for the inhibitor SC-558 was 0.49 ± 0.04. The acquired binding mode was identical to the X-ray structure and yielded a Chemscore of 30.5 ± 1.0. Docking of BAs into this docking box resulted in comparably low docking scores. Thus, the average docking score of AKBA was 2.0 ± 5.0, Aβ-BA achieved a Chemscore of 6.6 ± 4.5, KBA 8.6 ± 1.9, and β-BA 8.7 ± 2.4 (**Figure 4.5C**).

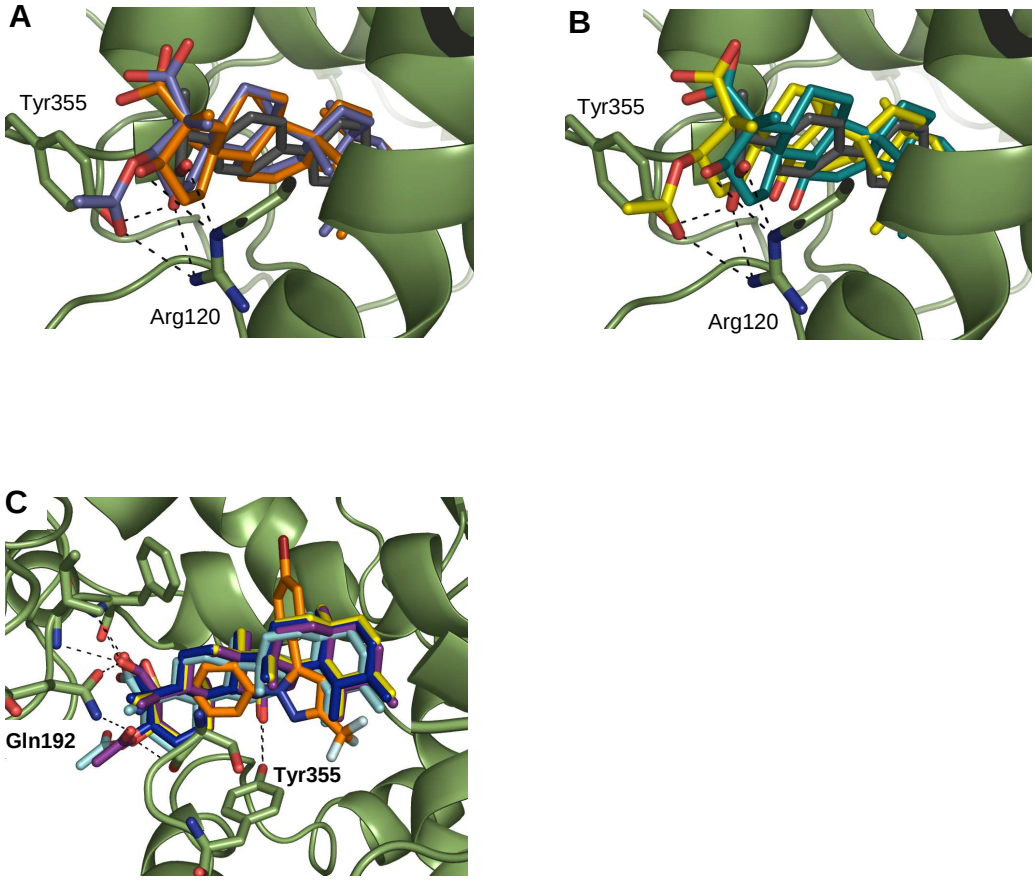

Figure 4.5: Automated molecular docking of BAs into X-ray structures of COX-1 and COX-2. .
(**A**, **B**) Scheme of the active site of COX-1 (1Q4G) with the co-crystallized inhibitor BFL displayed in grey. Possible hydrogen bonds of the BAs formed with Arg120 and Tyr355 are indicated. (**A**) β-BA (orange) and Aβ-BA (lila) are shown. (B) KBA (green) and AKBA (yellow) are shown in the same orientation as BFL (grey). (**C**) Scheme of the active site of COX-2 (6COX) with co-crystallized inhibitor SC-558, displayed in orange. Potential hydrogen bonds from Gln192 to the carboxyl- and acetyl-groups are highlighted, as well as possible interactions of the keto-groups with Tyr355. β-BA: blue, Aβ-BA: light blue, KBA: yellow, AKBA: purple. This work was entirely performed by Dr. Lutz Franke and Bettina Hofman (University of Frankfurt, Germany).

4.1.6 Effects of BAs on COX-1 product formation in whole blood

Finally, BAs (50 µM, each) were analyzed for their ability to suppress COX-1 product formation in whole blood which is regarded to adequately reflect the efficacy *in vivo*. Human whole blood was pre-incubated with the test compounds (10 min) and stimulated with A23187 (30 µM). As shown in **Figure 4.6**, despite the potent inhibition of COX-1 activity in cell-free assays or in intact platelets, none of the BAs (50 µM) tested suppressed 12-HHT formation in human whole blood. Control inhibitors aspirin (30 µM) and indomethacin (20 µM) efficiently blocked COX-1 activity in this whole blood assay, as expected.

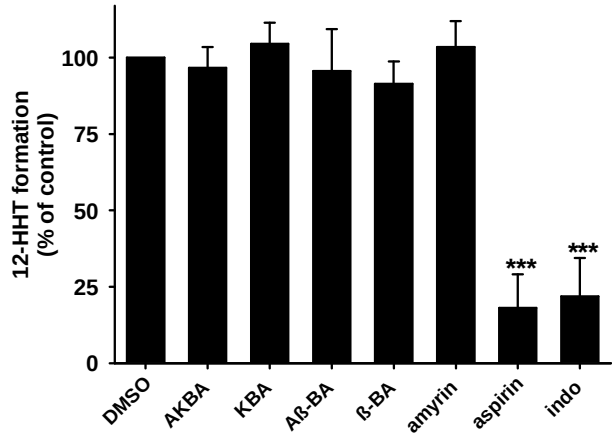

Figure 4.6: Inhibition of COX-1 product formation in human whole blood.
Freshly withdrawn blood was pre-incubated with BAs, α-amyrin (50 µM, each), aspirin (30 µM), indomethacin (indo, 20µM) or vehicle (DMSO) at 37 °C, and the reaction was started by addition of A23187 (30 µM). COX-1 product (12-HHT) synthesis in the absence of test compounds (100%, control) was 74.35 ± 7.8 ng/ml blood. Data are given as mean + S.E.; n = 3, duplicates. One-way ANOVA and Tukey HSD post hoc tests were performed; ***$P < 0.001$ vs vehicle control (DMSO).

Together, these results demonstrate that BAs directly interfere with COX-1 and preferably AKBA, concentration-dependently suppress cellular and cell-free COX-1 activity in a reversible and substrate-dependent manner. In contrast, BAs hardly inhibit COX-2 activity and are not able to reduce COX-1 product formation in human whole blood.

4.2 Interference of boswellic acids with 5-lipoxygenase

4.2.1 Inhibition of 5-LO activity by BAs in cell-free assays and influence of assay parameters on the potency

The efficacy of 5-LO inhibitors largely depends on the assay conditions (for review see [267, 268]). Previous studies demonstrated that partially purified 5-LO from human PMNL is inhibited by AKBA with an IC_{50} value of 16 µM [54]. Other BAs were not tested. Therefore, the potency of natural occurring BAs to inhibit partially purified human recombinant 5-LO from *E. coli* in a well-established and defined cell-free assay using 20 µM AA as substrate and 1 mM Ca^{2+} as supplement [269] was analyzed. The major β-configurated BAs AKBA, KBA, β-BA, and Aβ-BA inhibited 5-LO product synthesis in a concentration-dependent manner, with IC_{50} values of 2.9, 6.3, 23.9, and 30 µM, respectively (**Figure 4.7**).

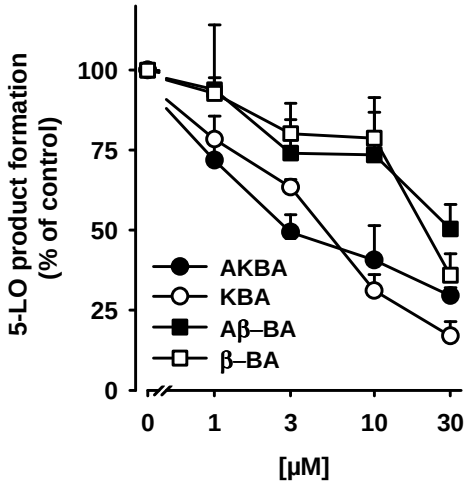

Figure 4.7: Inhibition of human 5-LO by BAs.
Partially purified, human recombinant 5-LO was pre-incubated with the indicated concentrations of BAs or vehicle (DMSO) in the presence of 1 mM Ca^{2+} and 1 mM ATP. 5-LO product formation was started by addition of 20 µM AA and analyzed by HPLC. Values are given as mean + S.E.; n = 3-4

Of interest, also the α-boswellic acid (α-BA) inhibited 5-LO activity with an IC_{50} = 15.3 µM, whereas the pentacyclic triterpenes α-amyrin (lacking the essential C4-carboxylic moiety) failed in this respect (IC_{50} >> 30 µM) (**Table 4.2**).

Table 4.2: Efficacy of various BAs for inhibition of 5-LO in different test systems.
IC_{50} values (µM) of BAs were determined regarding 5-LO activity of human purified 5-LO enzyme, crude 5-LO in supernatants of E. coli and in isolated human PMNL stimulated with either 2.5 µM A23187 with or without 20 µM AA in the presence of Ca^{2+} (1 mM). The synthetic 5-LO inhibitor BWA4C was used as control.

Compound	5-LO purified enzyme	*E. coli* supernatant	PMNL (A23187)	PMNL (A23187 + AA)
AKBA	2.9	23.5	3.2	3.3
KBA	6.3	27.1	8.8	2.8
Aβ-BA	>30	>30	>30	>30
β-BA	23.9	>30	>30	28.1
α-BA	15.3	18.5	23.1	16
α-amyrin	>>30	>>30	>>30	>>30
BWA4C	0.1	0.15	0.03	0.05

Subsequent studies under selected assay conditions were carried out with the most efficient derivatives, i.e. AKBA and KBA. As observed before [269], removal of Ca^{2+} from the standard activity assay increased 5-LO activity under these incubations conditions about two-fold, but the efficacies of KBA and AKBA were not markedly changed (**Figure 4.8A**). The efficacy of AKBA at higher concentrations (10 and 30 µM) was slightly increased in the absence of Ca^{2+}. The presence of 25 µg/ml PC in the standard activity assay, often included as stimulatory factor in 5-LO activity assays [189, 270], impaired the 5-LO inhibitory potential of AKBA (IC_{50} = 19.8 µM), whereas the potency of KBA was essentially unaffected (**Figure 4.8B**).

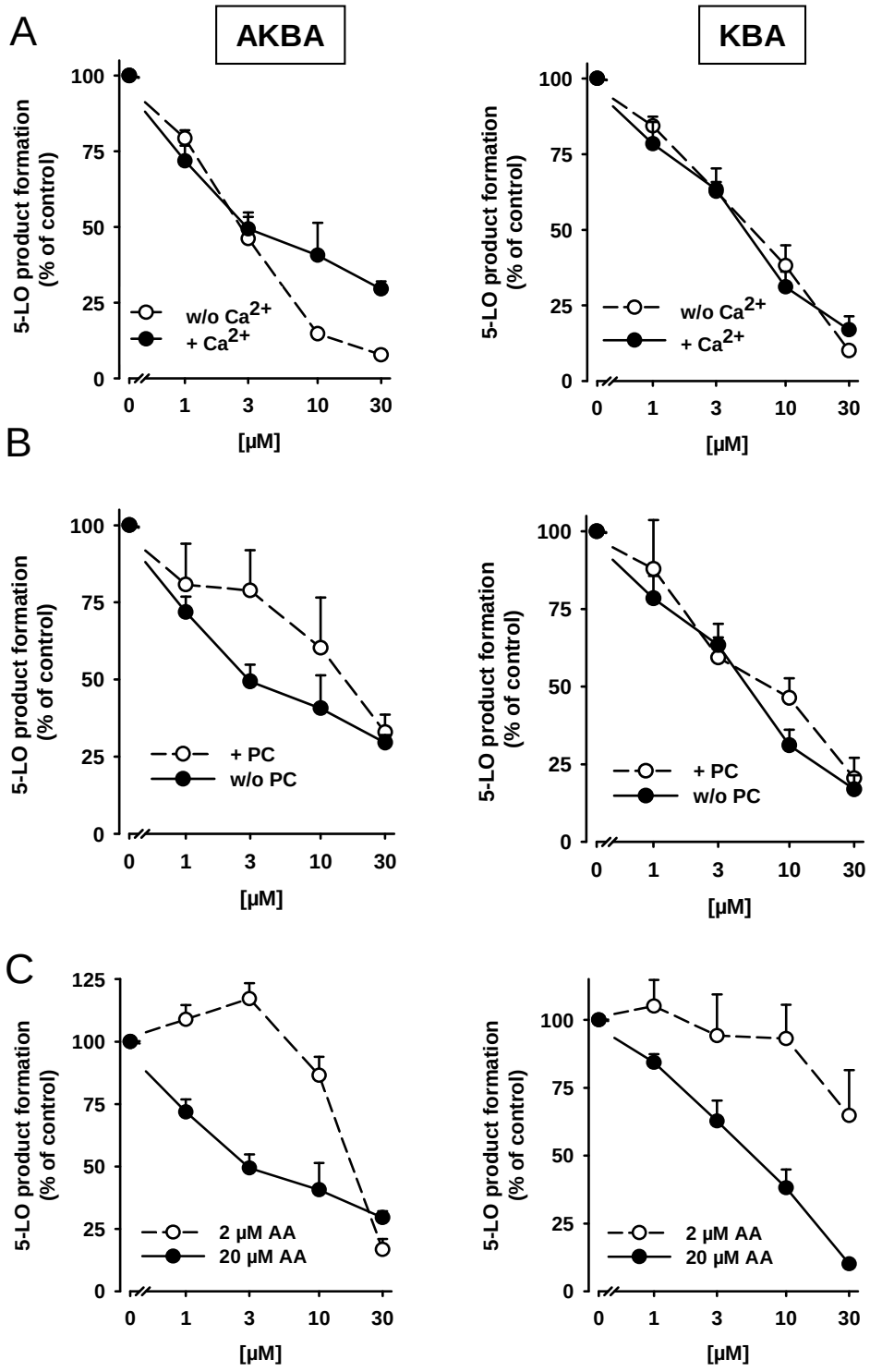

Figure 4.8: Modulation of inhibition of human 5-LO by BAs in cell-free assays.
(**A**) Effect of Ca^{2+}. Partially purified, human recombinant 5-LO was pre-incubated in 1 ml PBS containing 1 mM EDTA and 1 mM ATP with the indicated concentrations of AKBA (left panel) or KBA (right panel) or vehicle (DMSO) at 4 °C. After 10 min, samples were pre-warmed at 37 °C for 30 s, 2 mM $CaCl_2$ (as indicated) and 20 µM AA were added and after another 10 min, 5-LO product formation was determined. (**B**) Effect of PC. Partially purified 5-LO was pre-incubated as in the standard assay together with or w/o 25 µg/ml PC. (**C**) Inhibition of 5-LO by boswellic acids at 2 and 20 µM AA. Partially purified 5-LO was pre-incubated with the test compounds (see (**A**)). In the presence of Ca^{2+} (1 mM) 5-LO product formation was initiated by AA (2 or 20 µM, as indicated). Values are given as mean + S.E.; n = 3-4.

Of interest, switching from 20 to 2 µM AA as 5-LO substrate in the standard activity assay significantly reduced the potency of both 11-keto-BAs, and the IC_{50} values were determined at 21.5 µM for AKBA and > 30 µM for KBA (**Figure 4.8C**). A weak loss of potency was observed also for BWA4C, a well-recognized iron ligand-type 5-LO inhibitor (**Table 4.3**).

Table 4.3: Influence of assay parameters on the potencies of AKBA and KBA to inhibit 5-LO.
IC_{50} values (µM) for AKBA and KBA assessing the activity of partially purified 5-LO in the presence or absence of 1 mM free Ca^{2+}. PC (25 µg/ml) and AA (2 or 20 µM) were added as indicated. The synthetic 5-LO inhibitor BWA4C was used as control.

Compound	AA (20 µM)	AA (20 µM) + Ca^{2+}	AA (2 µM) + Ca^{2+}	AA (20 µM) + Ca^{2+} + PC
AKBA	2.8	2.9	11.5	19.8
KBA	7.6	6.3	>30	11.4
BWA4C	0.14	0.1	0.24	0.11

Finally, when 40,000 ×*g* supernatants of *E. coli* lysates were used as source of crude 5-LO enzyme in the standard activity assay (**Figure 4.9**), the potency of all four β-configurated BAs was strongly impaired. Note that α-BA hardly lost its potency and was the most potent derivative with IC_{50} = 18.5 µM (**Table 4.2**).

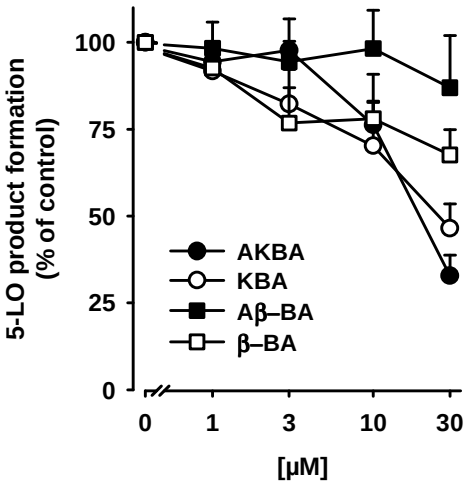

Figure 4.9: Effects of BAs on crude 5-LO in supernatants from E. coli lysates.
Supernatants (40,000 × g) from *E. coli* lysates in PBS containing 1 mM EDTA, 1 mM PMSF, and 1 mM ATP were pre-incubated with the test compounds at 4 °C. After 10 min samples were pre-warmed at 37 °C for 30 s, 2 mM $CaCl_2$ and 20 µM AA were added and after 10 min 5-LO product formation was determined. Values are given as mean + S.E.; n = 3-4.

4.2.2 Inhibition of 5-LO activity by BAs in cell-based assays using isolated human PMNL

PMNL stimulated with A23187 are the classical test system for screening and evaluation of LT synthesis inhibitors. AKBA and KBA potently inhibited 5-LO product synthesis in human isolated PMNL challenged by A23187 in a concentration-dependent manner with IC_{50} = 3.2 and 8.8 µM, respectively (**Figure 4.10**), and also the frankincense extract H15® blocked 5-LO product synthesis by 78 ± 9% at a concentration of 30 µg/ml. Aβ-BA, β-BA, and α-amyrin were hardly active (IC_{50} >> 50 µM), but α-BA suppressed 5-LO product synthesis with an IC_{50} = 23.1 µM). Upon stimulation of PMNL with A23187 plus exogenous AA (20 µM), estimating FLAP interference, the efficacy of AKBA was not altered, whereas the potency of KBA increased (IC_{50} = 2.8) and also α-BA was more active under these conditions (IC_{50} = 16 µM) (**Table 4.2**).

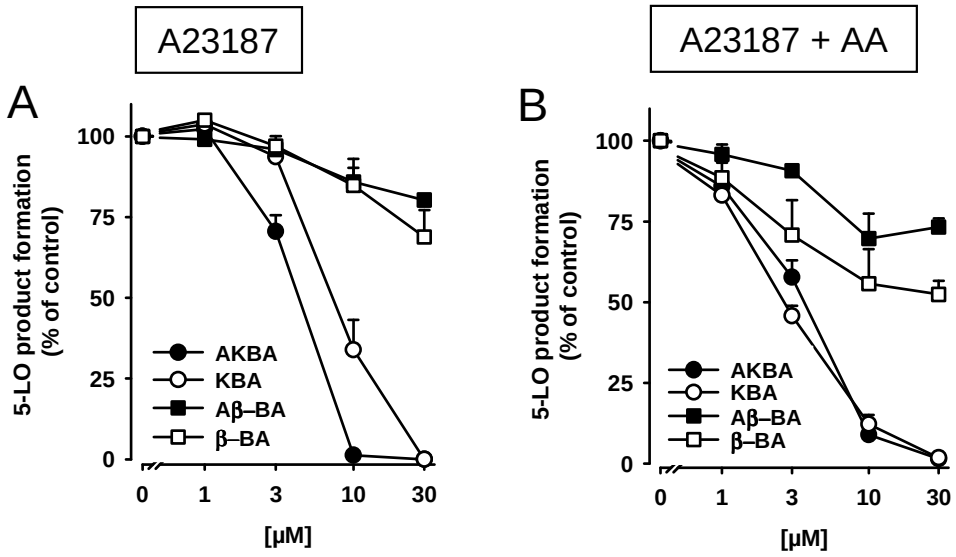

Figure 4.10: Inhibition of 5-LO product formation in intact human PMNL.
Isolated PMNL (5×10^6/ml PGC) were pre-incubated with the test compounds or vehicle (DMSO) at the indicated concentrations. After 10 min at 37 °C, cells were stimulated with 2.5 µM A23187 (**A**) or with 2.5 µM A23187 plus 20 µM AA (**B**) and 5-LO products were extracted and determined by HPLC. 5-LO product synthesis in the absence of test compounds (100 %, control) was 68.1 ± 6 (A23187) and 276.8 ± 40 (A23187 + AA) ng per 10^6 PMNL. Data are given as mean + S.E.; n = 3.

4.2.3 Inhibition of 5-LO activity by BAs in human whole blood

The ability of a given compound to suppress LT formation in the whole blood assay is assumed to reflect its efficacy *in vivo*. Human whole blood was pre-incubated with the test compounds and stimulated either with A23187 or primed with LPS and then challenged with fMLP. Stimulation of blood with fMLP following LPS-priming is considered a physiologically relevant stimulus, thus, reflecting pathophysiological conditions *in viv*o. As shown in **Figure 4.11**, despite the potent inhibition of 5-LO activity in cell-free assays or in intact PMNL, neither the BAs (50 µM) nor the frankincense extract (30 µg/ml) suppressed 5-LO product formation. The control inhibitor BWA4C efficiently inhibited 5-LO activity in the whole blood assay, as expected.

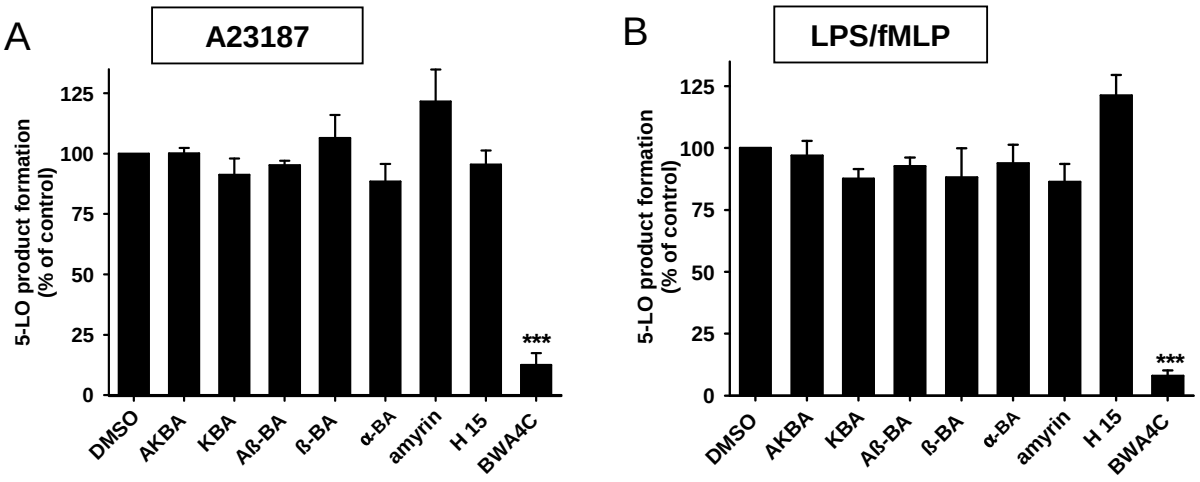

Figure 4.11: **Inhibition of 5-LO product formation in human whole blood.**
Blood was pre-incubated with BAs (50 µM, each), H15® extract (30 µg/ml), BWA4C (3 µM) or vehicle (DMSO), and formation of 5-LO products was started by addition of (**A**) A23187 (30 µM; 10 min, 37 °C) or by (**B**) fMLP (1 µM; 15 min, 37 °C) after 30 min priming with LPS (1 µg/ml). The formation of 5-LO products were determined as described. 5-LO product synthesis in the absence of test compounds (100%, control) was 196.9 ± 46 (A23187) and 34.3 ± 0.5 (LPS and fMLP) ng/ml blood. Data are means + S.E.; n = 3-4 (fMLP and LPS), duplicates; n = 3 (A23187). One way ANOVA + Tukey HSD post-hoc were performed; ****P* < 0.001 vs vehicle (DMSO) control.

4.2.4 Inhibition of 5-LO activity by BAs in human isolated PMNL is abolished by albumin

Since AKBA and KBA are inactive in whole blood while being efficient in isolated PMNL, and because BAs represent lipophilic acids, it appeared reasonable to speculate that plasma protein (i.e. albumin)-binding of BAs is responsible for the lack of efficacy in whole blood. Thus, the albumin-binding ability of AKBA using a gel filtration method was investigated. As shown in **Figure 4.12**, AKBA (50 µM) extensively bound to 10 mg/ml BSA and to a minor extent when 1 mg/ml BSA was present. The unbound free AKBA was 0% and 30.9% for 10 and 1 mg/ml albumin, respectively.

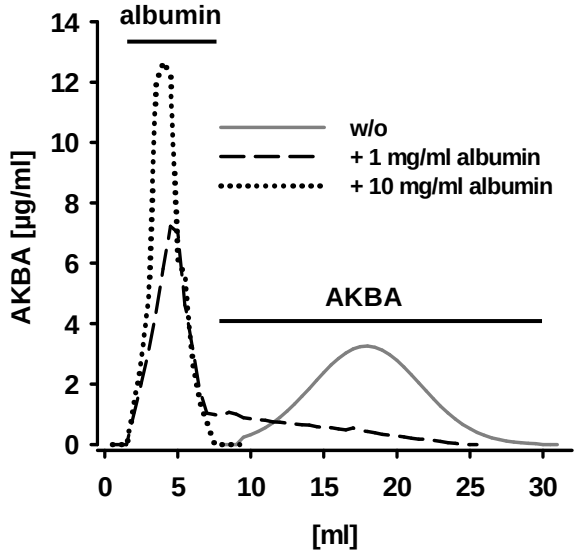

Figure 4.12: **Binding of AKBA to albumin.**
BSA (0, 1 or 10 mg/ml, as indicated) was incubated with 50 µM AKBA for 10 min at 37 °C. Separation of AKBA and albumin was carried out by gel filtration using a PD-10 column and AKBA was quantified by HPLC analysis. The concentration of AKBA (without BSA) vs elution volume was analyzed. Based on this evaluation the amount of unbound AKBA was determined by the AUC ($\mu \pm 3\delta$) for incubation with 1 or 10 mg/ml albumin. Results shown are representative for at least 3 independent determinations.

Next, the effects of BSA on inhibition of 5-LO product synthesis by AKBA and KBA in isolated PMNL was analyzed. This work was done in cooperation with Dr. Carlo Pergola (University Tübingen, Germany). The presence of 1 mg/ml BSA attenuated the potency of AKBA and KBA about 2- to 7-fold in PMNL challenged by A23187 without (**Figure 4.13**) and with 20 µM exogenous AA (**Figure 4.13**). When 10 mg/ml BSA was included, neither KBA nor AKBA significantly inhibited 5-LO product formation up to 30 µM. Similarly, also the suppressive effect of H15® extract (30 µg/ml) was completely reversed by 10 mg/ml BSA (not shown).

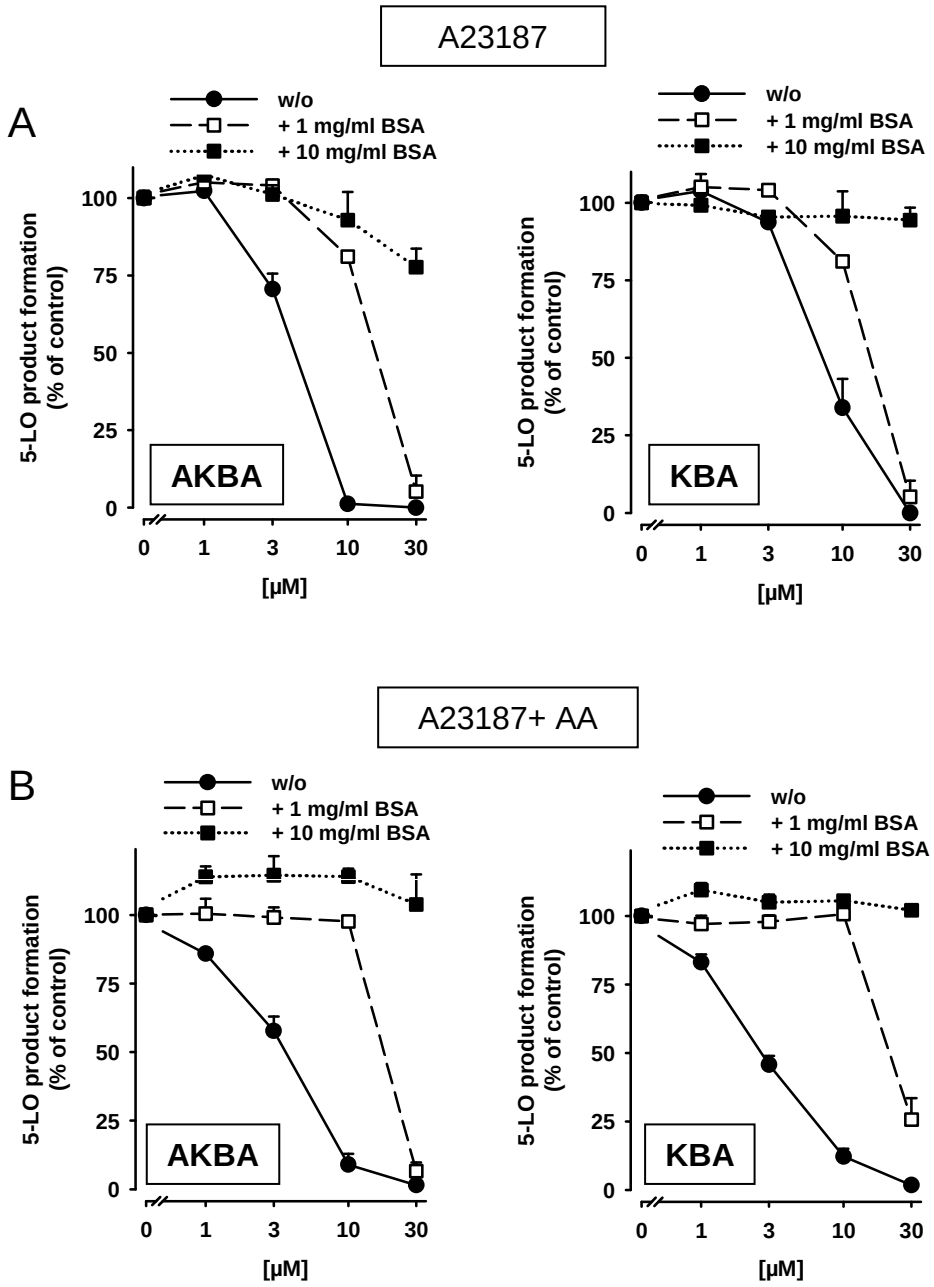

Figure 4.13: Influence of BSA on the efficacy of BAs to inhibit 5-LO product formation in human PMNL. Freshly isolated PMNL (5×10^6/ml PGC) were supplemented with or w/o 1 or 10 mg/ml BSA. AKBA (left panel) or KBA (right panel), or vehicle (DMSO) were added at the indicated concentrations. After 10 min at 37 °C, cells were stimulated with 2.5 µM A23187 (**A**) or with 2.5 µM A23187 plus 20 µM AA (**B**) and 5-LO product formation was determined. 5-LO product synthesis in the absence of test compounds (100%, control) was 68.1 ± 6 (A23187), 40.8 ± 3 (A23187 + 1 mg/ml BSA), 22.2 ± 4 (A23187 + 10 mg/ml BSA), 276.8 ± 40 (A23187 + AA), 78.3 ± 7 (A23187 + AA + 1 mg/ml BSA), and 32.3 ± 6 (A23187 + AA + 10 mg/ml BSA) ng per 10^6 PMNL. Values are given as mean + S.E., n = 3, duplicates.

4.2.5 LTB_4 levels in human subjects treated with frankincense extracts

In a phase 1 clinical trial the safety, tolerability and pharmacokinetics of a single oral dose application of *B. serrata* resin extract (PS0201Bo) in healthy male volunteers (n = 12) was investigated. Two capsules of PS0201Bo, each containing 400 mg of native *B. serrata* resin extract (total 800 mg PS0201Bo), were administered to healthy volunteers. Then, blood was collected as indicated in **Figure 4.14**, plasma was prepared, and LTB_4 was analyzed by ELISA. The plasma levels of LTB_4 were not impaired within 24 h of frankincense administration, instead a weak but statistically not significant increase was observed 2 to 8 h after intake of the extracts, correlating with the plasma concentrations of AKBA and KBA that peaked after approx. 3 h, and half maximal concentrations of KBA were determined after 6-8 h (not shown). These experiments were carried out at Frankfurt University Hospital under the supervision of Dr. Carsten Skarke.

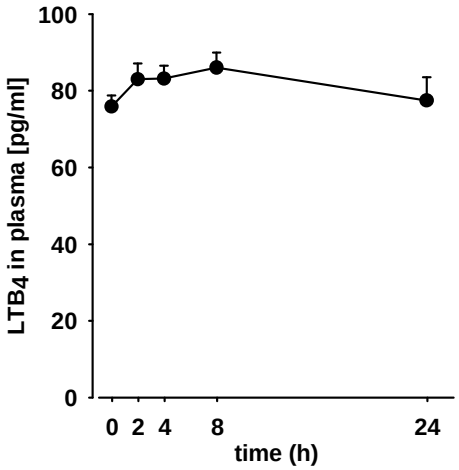

Figure 4.14: Effects of single dose orally administered frankincense preparation on LTB_4 plasma levels. Healthy male volunteers received two capsules containing frankincense extract (PS 0201Bo) as single dose (800 mg) application. Venous blood was taken at the indicated time points, plasma was prepared and LTB_4 in the plasma was determined by ELISA. Data are shown as mean + S.E., n = 12 volunteers.

Taken together, both α- and β-configurated BAs (preferentially 11-keto-BAs) act as direct 5-LO inhibitors in cell-free and cellular-based experiments, but the potencies strongly depend on the defined assay conditions. Furthermore, none of the BAs tested is able to prevent 5-LO product synthesis in whole blood assays and also single dose oral administration of frankincense extracts to healthy human volunteers causes no reduction of plasma LTB_4 levels.

4.3 Interference of boswellic acids with the inducible microsomal prostaglandin E_2 synthase-1

4.3.1 Identification of mPGES-1 as a BA-binding protein by pull-down experiments and surface plasmon resonance spectroscopy

The target fishing approach using immobilized BAs was used in order to investigate whether or not BAs interact with mPGES-1. Lysates of Il-1β-treated A549 cells, expressing mPGES-1 and COX-2 [142], were incubated with the respective resins and precipitates were analyzed by WB using specific antibody against mPGES-1 and COX-2. As shown in **Figure 4.15A,** substantial amounts of mPGES-1 bound to BA-Seph beads but not to Seph beads without ligand. In contrast, attempts to identify COX-2 in the BA-Seph beads precipitates by WB failed. Furthermore, *in vitro*-translated mPGES-1 (200 ng purified protein) in the presence of 1000-fold excess of *E. coli* protein was precipitated by both KBA-Seph and β-BA-Seph, but not by Seph without ligand (**Figure 4.15B**).

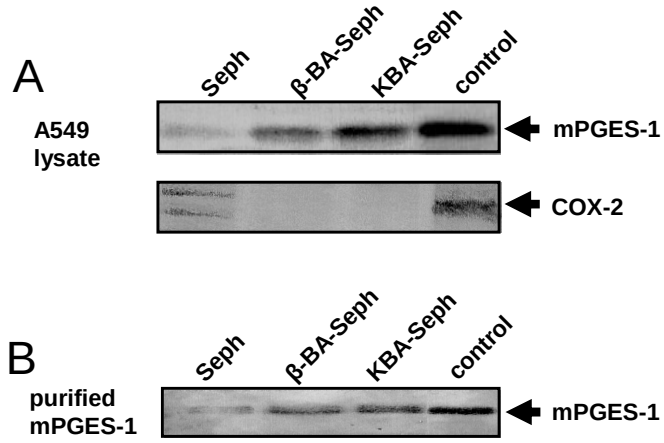

Figure 4.15: BAs selectively bind mPGES-1.
(**A**) Supernatants of A549 cell lysates were incubated over night at 4 °C with either β-BA-Seph, KBA-Seph, or with crude Seph, as indicated. Precipitated proteins were visualized by WB using specific antibodies against mPGES-1 or COX-2. An aliquot of the supernatant was used as positive control. (**B**) Purified mPGES-1 (200 ng) was incubated with β-BA-Seph, KBA-Seph or with Seph in the presence of 1000-fold excess of E. coli protein. Similar results were obtained in three additional experiments.

To confirm the direct interaction of BAs with mPGES-1, SPR spectroscopy studies were carried out. SPR spectroscopy is a label-free optical detection method which allows to analyze the binding of soluble analyte to immobilized biomolecules (ligands) in real-time [261, 271]. The progress of interaction, binding of analyte (association), and dissociation of analyte from the immobilized ligand is monitored as a sensogram, expressing changes in binding responses as resonance units (RU). Unfortunately, no consistent binding patterns were obtained by using naturally occurring BAs as analyte (data not shown). Neither the addition of BSA as a carrier protein nor variation of commercial assay buffers (± detergent) or changes in temperature improved the quality of the recorded sensograms. Hence, the more hydrophilic synthetic derivate

3-*O*-oxaloyl-KBA (ox-KBA) was used. Indeed, more valuable and reproducible sensograms were obtained, which indicate specific reversible binding to mPGES-1 (**Figure 4.16A**) whereas α-amyrin (negative control) up to 30 µM failed in this respect (**Figure 4.16A**). In order to determine equilibrium binding constants, ox-KBA at different concentrations were sequentially injected over the two surfaces and the equilibrium response (R_{eq}) was calculated, and fitting the data to the 1:1 binding model (Eqn. 1) and Scatchard plot yielded K_D values = 13 and 5.2 µM, respectively (**Figure 4.16B**). Kinetic data were estimated using BIAEVALUATION 3.1 software, a general analysis in which the association and dissociation phases are fitted simultaneously [261]. The fit and the distribution of the residuals are presented in **Figure 4.16C**. Assuming the simple relationship $k_a/k_d = K_D$ for ox-KBA, a K_D-value of 23 µM was calculated that essentially matches the K_D obtained from the equilibrium binding data.

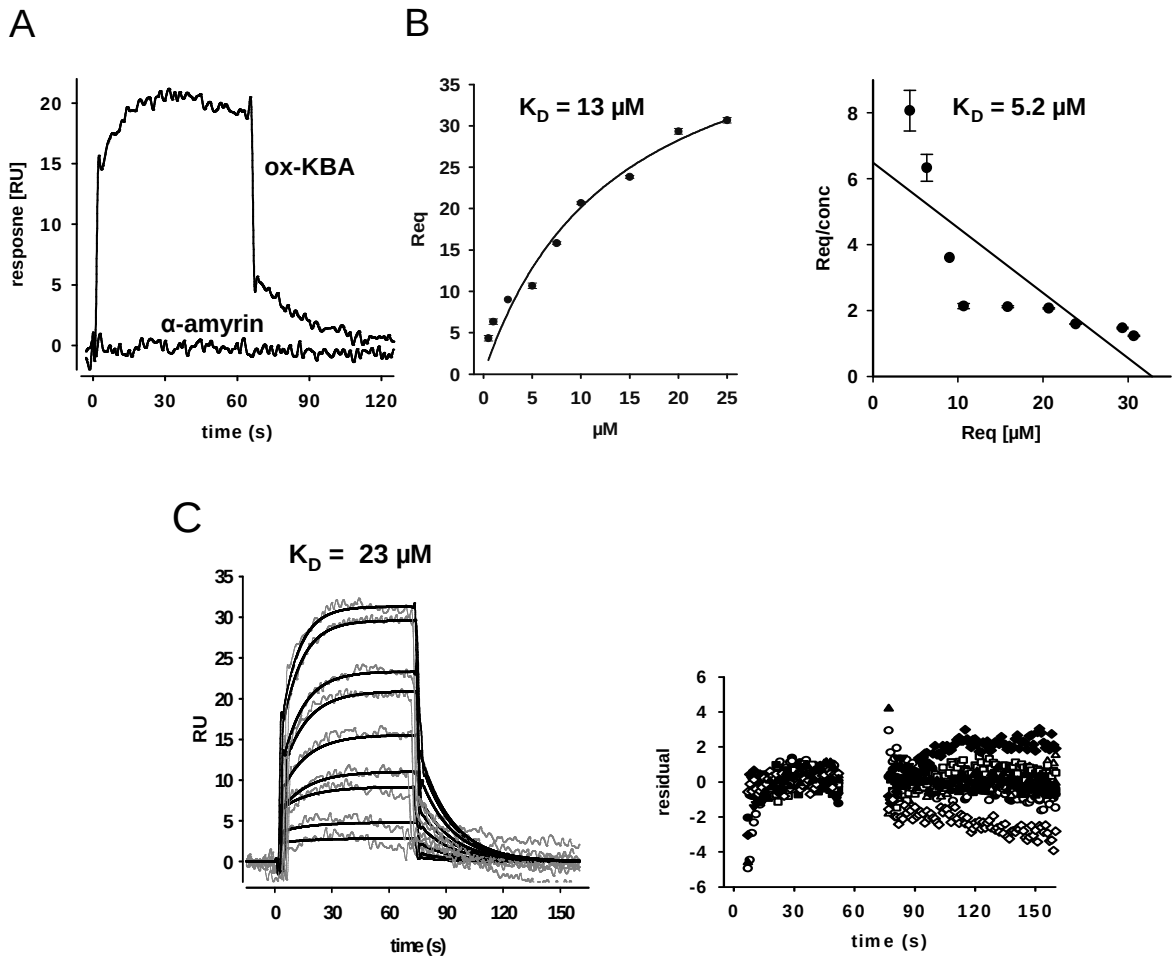

Figure 4.16: Analysis of the binding of BAs to mPGES-1 by SPR spectroscopy.
In vitro translated mPGES-1 (ligand) and ox-KBA (analyte) were used. Specific binding profiles were obtained after subtracting the signal (response units, RU) from the untreated control cell. (**A**) The binding of ox-KBA (10 µM) and amyrin (30 µM) to mPGES-1. (**B**) Binding curves for ox-KBA. The equilibrium responses for ox-KBA at different concentrations were plotted vs. the concentration of the compound. The nonlinear fit to Eqn (1) and a Scatchard plot yield the dissociation constant K_D. (**C**) Kinetic analysis of ox-KBA-binding to mPGES-1. Representative sensograms for the injection of 0.5 µM up to 25 µM ox-KBA are shown. A general analysis was applied to fit the data to a 1:1 binding model (solid lines), and the quality of the fit is displayed by the plots of the residuals.

4.3.2 BAs inhibit the catalytic activity of mPGES-1 in a cell-free assay

Next, it was investigated whether the direct interference of BAs with mPGES-1 affects the catalytic activity of the enzyme. Isolated microsomes of IL-1β treated A549 cells (source of mPGES-1) were pre-incubated with BAs and PGE_2 formation was induced by addition of 20 µM PGH_2. The mPGES-1 inhibitor MK-886 was used as reference drug and concentration-dependently blocked PGE_2 formation with an IC_{50} = 2 µM (not shown) in agreement with the literature [272]. All BAs concentration-dependently suppressed PGE_2 formation with IC_{50} values of 3, 5 and 10 µM for AKBA, β-BA and KBA, respectively, comparable to MK-886. As observed for other mPGES-1 inhibitors in previous studies [169], about 20% activity still remained even at high concentrations of BAs (100 µM, **Figure 4.17A**) or of MK-886 (30 µM, not shown). The synthetic derivative ox-KBA also suppressed PGE_2 formation (IC_{50} = 5 µM). Aβ-BA was somewhat less potent and failed to suppress PGE_2 formation by more than 50% up to 100 µM. Furthermore, the pentacyclic triterpene α-amyrin (lacking the 4-COOH-group) was entirely inactive up to 100 µM (not shown). To assess whether inhibition of mPGES-1 by BAs occurs in a reversible fashion, wash-out experiments were performed. Microsomal preparations of A549 cells were pre-incubated with AKBA or β-BA at 1 and 10 µM for 15 min. MK-886 at 0.3 and 3 µM served as a control for a reversible mPGEs-1 inhibitor [169]. Whereas BAs at 1 µM or MK-886 at 0.3 µM caused only minor inhibition of mPGES-1, incubations with MK-886 at 3 µM or with BAs at 10 µM efficiently blocked PGE_2 formation (**Figure 4.17B**). Upon 10-fold dilution of the latter samples, a significant loss of potency was obvious. In order to determine if mPGEs-1 inhibition by BAs depends on the substrate concentration the concentration of PGH_2 was varied from 20 µM to 1 µM in the assay. The efficacy of AKBA was not affected by variation of the substrate concentration (**Figure 4.17C**). Of interest, for β-BA a slight loss of potency was evident at lower PGH_2 concentrations.

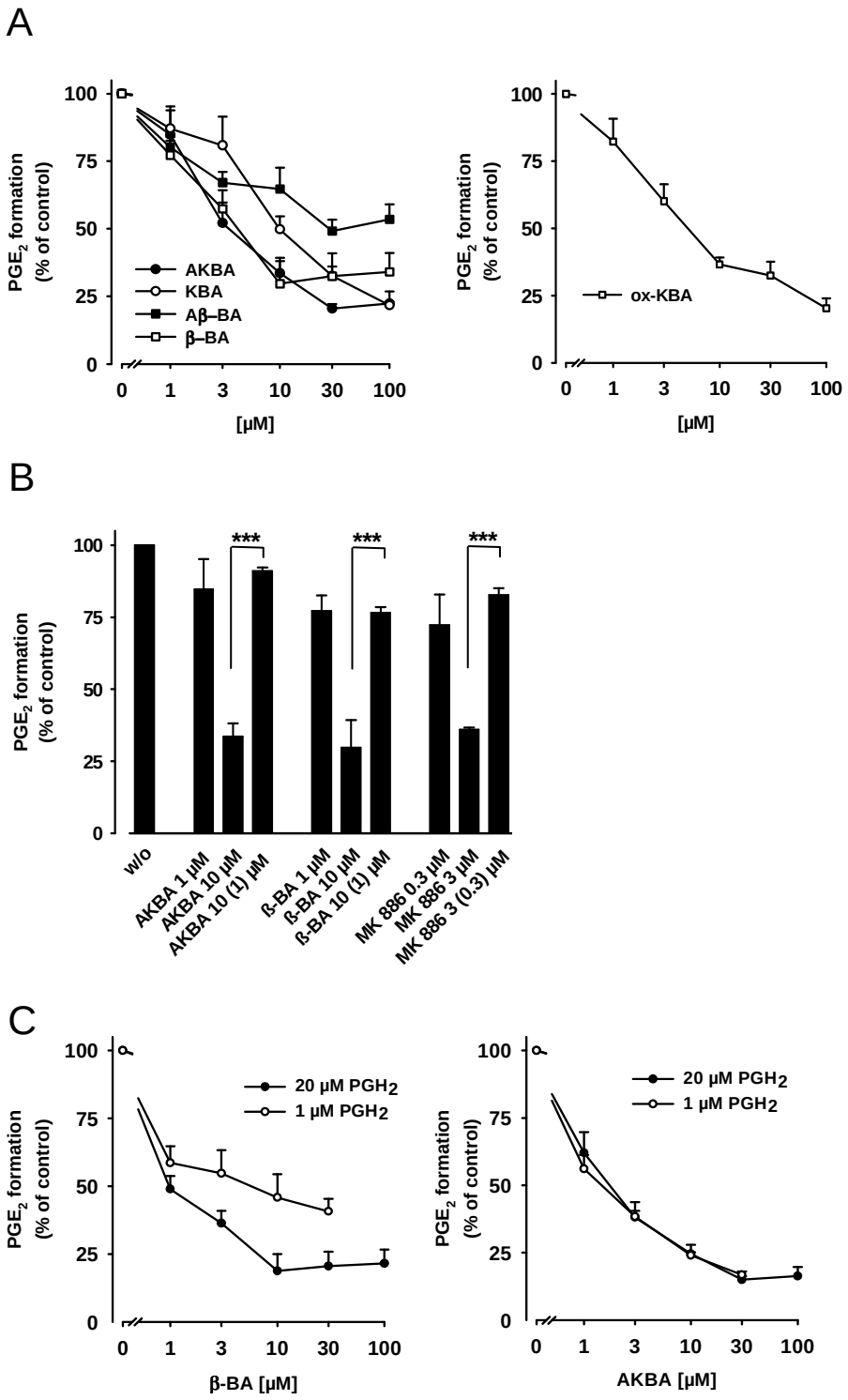

Figure 4.17: Effects of BAs on the activity of mPGES-1 in cell-free assays.
(**A**) Concentration-response analysis of BAs. Microsomal preparations of IL-1β-stimulated A549 cells were pre-incubated with BAs or vehicle (DMSO)and PGE_2 formation was induced by the addition of 20 µM PGH_2. (**B**) Reversibility of mPGES-1 inhibition by AKBA, β-BA and MK-886 using wash out experiments. One way ANOVA + Tukey HSD post-hoc tests were performed;***$P < 0.001$. The 100% value corresponds to 944 ± 118 pmol PGE_2. (**C**) The efficacy of AKBA and β-BA for mPGES-1 inhibition was compared at 1 and 20 µM PGH_2 as substrate. PGE_2 was quantified for 1 µM PGH_2 by use of a PGE_2 High Sensitivity EIA Kit. PGE_2 production at 10 µM MK-886 was set 0% of vehicle (DMSO) control in order to compare both data sets. Data are given as mean + S.E., n = 3-4.

4.3.3 Effect of BAs on PGE_2 synthesis in intact cells

The capacity of BAs to inhibit PGE_2 formation also in intact cells was determined. Since COX-2 activity in cell-free or cellular experiments was not significantly inhibited by BAs stimulation of IL-1β-pretreated A549 cells with 2.5 µM A23187 plus 1 µM AA and ^{3}[H]AA (18.4 kBq) were used as model to selectively assess modulation of COX-2-derived PGH_2 transformation to PGE_2 via mPGES-1 by BAs. Again AKBA, β-BA and KBA suppressed PGE_2 synthesis in concentration-dependent manner (IC_{50} = 20µM) whereas Aβ-BA and α-amyrin were hardly effective (**Figure 4.18**). Nevertheless, suppression of PGE_2 formation by BAs was not complete, and also MK-886 (30 µM) caused only 47% inhibition under these assay conditions. On the other hand, the COX-1/2 inhibitor indomethacin (20 µM) and the COX-2 selective celecoxib (5 µM), almost completely suppressed PGE_2 formation as expected.

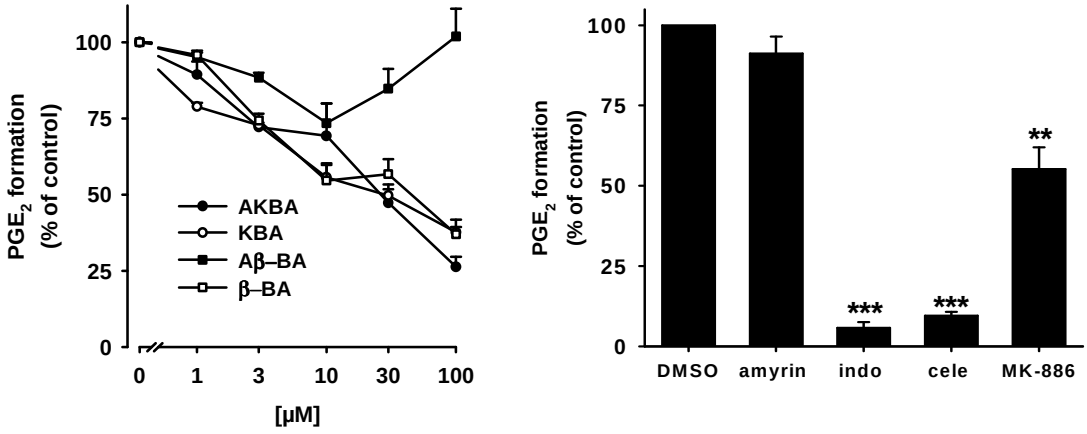

Figure 4.18: Effects of BAs on PGE_2 formation in intact A549 cells.
IL-1β-stimulated A549 cells (6×10^6/ml) were pre-incubated with BAs, α-amyrin (30 µM), indomethacin (indo, 20 µM), celecoxib (cele, 5 µM), MK-886 (30 µM) or vehicle (DMSO) for 10 min, and then 2.5 µM A23187 plus 1 µM AA and [^{3}H]AA (18.4 kBq) were added. After 15 min at 37 °C, formed [^{3}H]PGE_2 was analyzed by RP-HPLC and liquid scintillation counting as described in the method section. Data are given as mean + S.E., n = 3-5. One way ANOVA + Tukey HSD post-hoc tests were performed;**$P < 0.01$ ***$P < 0.001$ vs vehicle (DMSO) control.

4.3.4 Effects of BAs on the formation of PGE_2 and 6-keto-$PGF_{1\alpha}$ in human whole blood

In order to estimate the efficacy of BAs to interfere with (COX-2/mPGES-1-derived) PGE_2 formation *in vivo*, human whole blood assays were performed. Aliquots of human heparinized blood were pre-incubated with BAs, prior stimulation with LPS (10 µg/ml). As shown in **Figure 4.19A**, β-BA significantly reduced PGE_2 synthesis (46.2% inhibition) at 10 µM comparable to MK-886 at 30 µM (45.4% inhibition) whereas the other BAs and the negative control α-amyrin failed in this respect. Concentration-response experiments revealed an IC_{50} value of 20 µM for β-BA (**Figure 4.19B**), but even at high concentrations (100 µM) about 40% PGE_2 still remained. In contrast, formation of 6-keto-$PGF_{1\alpha}$ was not affected by β-BA and also not by AKBA (10 µM, each) (**Figure 4.19C**). Indomethacin (50 µM) and celecoxib (20 µM) efficiently inhibited PGE_2 and 6-keto-$PGF_{1\alpha}$ synthesis as expected.

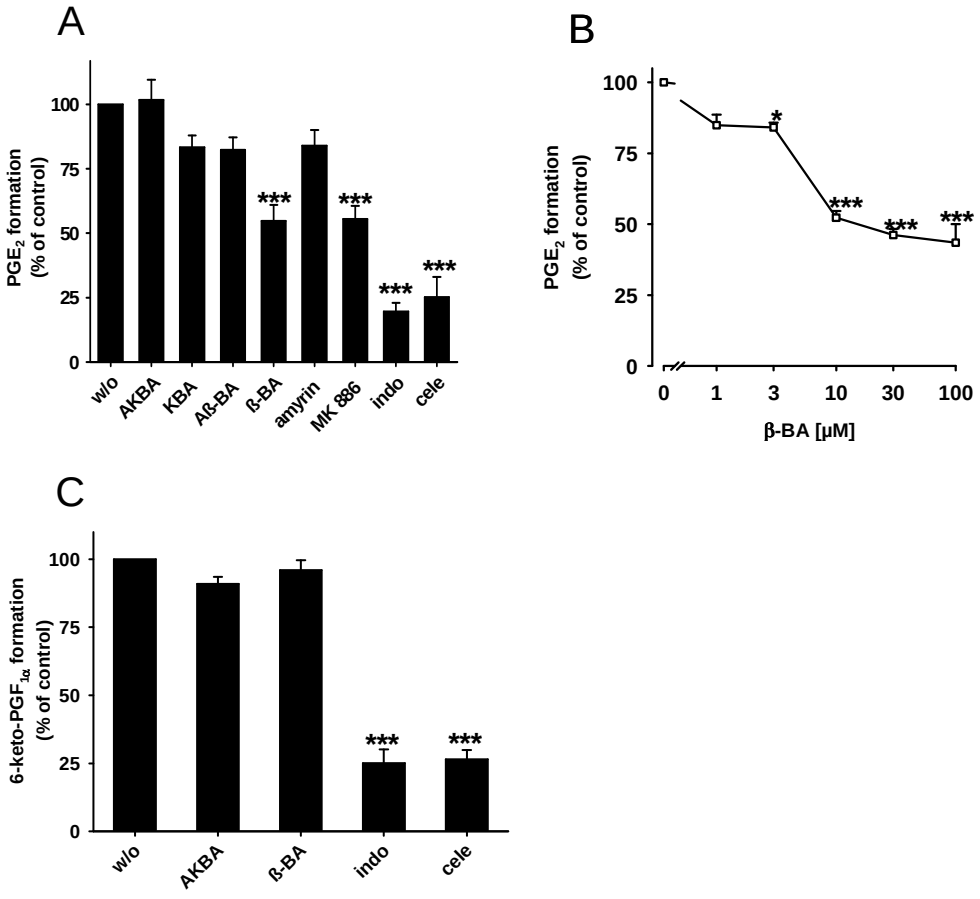

Figure 4.19: Effects of BAs on PGE_2 and 6-keto-$PGF_{1\alpha}$ biosynthesis in human whole blood.
Heparinized human whole blood was pre-incubated with (**A**) BAs and amyrin (10 µM, each) or vehicle (DMSO) for 10 min at RT and then, PGE_2 formation was induced by addition of 10 µg/ml LPS. After 5 h at 37 °C, PGE_2 was extracted from plasma, separated by RP-HPLC and quantified by ELISA as described. MK-886 (30 µM), indomethacin (indo, 50 µM), and celecoxib (cele, 20 µM) were used as controls. (**B**) Concentration-response of β-BA. (**C**) Assessment of 6-keto-$PGF_{1\alpha}$ formation. 6-keto-$PGF_{1\alpha}$ was directly determined in blood plasma derived from samples from above incubated with 10 µM β-BA or AKBA, respectively, by ELISA. The 100% values correspond to 221.81 ± 19.69 pg/ml PGE_2 and 382.5 ± 22.25 pg/ml 6-keto-$PGF_{1\alpha}$, respectively. Data are given as mean + S.E., n = 4-5. One way ANOVA + Tukey HSD post-hoc tests were performed; $^*P < 0.05$; $^{***}P < 0.001$ vs vehicle (DMSO) control.

Notably, expression pattern of COX-2 and mPGES-1 were not essentially altered by β-BA in isolated monocytes (major source of mPGES-1) during a 5 h incubation phase (**Figure 4.20**) used to induce PGE_2 formation in whole blood.

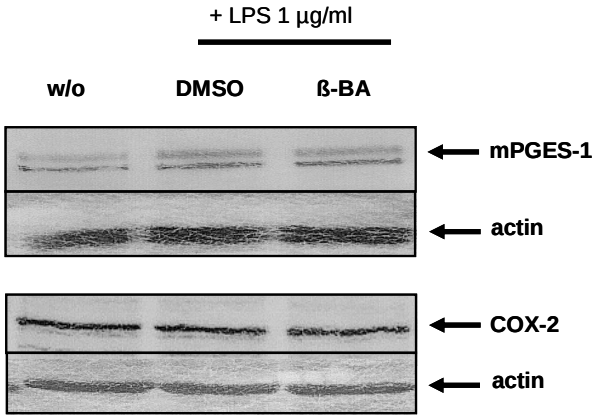

Figure 4.20: Expression of mPGES-1 and COX-2 in monocytes.
Human monocytes (5×10^6/exp. in RPMI 1640 medium containing 2% FCS, P/S and 2 mM glutamine) were pre-incubated with β-BA or vehicle (DMSO) for 10 min at RT prior stimulation with LPS (1 µg/ml) for 5 h at 37 °C or left untreated. After washing (3× PBS), cells were lysed (2× SDS-b.) and samples were subjected to SDS-PAGE and WB using specific antibodies against mPGES-1 and COX-2. Results shown are representative of two independent experiments.

4.3.5 Effects of β-BA on carrageenan-induced mouse paw edema and rat pleurisy

The carrageenan-induced paw edema is considered as suitable model to assess a pathophysiological role of mPGES-1 in inflammation *in vivo* [273]. In mice treated (i.p.) with β-BA (0.25 mg/kg) the response to carrageenan at 4 h was already reduced by almost 20% and pretreatment with 1 mg/kg β-BA, respectively resulted in 50% suppression. Indomethacin (5 mg/kg) caused 56% inhibition of the carrageenan response (**Table 4.4**). The animal experiments were carried out at University of Naples by Drs Antonietta Rossi and Lidia Sautebin.

Table 4.4: Effects of β-BA on carrageenan-induced mouse paw edema.
Percentages of inhibition caused by the treatments of 0.25, 1 mg/kg β-BA and 5mg/kg indomethacin or vehicle DMSO 2%); n = 10 mice. One-way ANOVA and Tukey post hoc test were performed; ***$P < 0.001$ vs vehicle (DMSO).

Treatment	mg/kg	Inhibition (%)
β-BA	0.25	19.58 ± 9.2
β-BA	1	49.48 ± 8.2***
indomethacin	5	56.70 ± 9.3***

Injection of carrageenan into the pleural cavity of rats elicited, at 4 h, an acute inflammatory response characterized by the accumulation of fluid that contained large numbers of inflammatory cells (**Table 4.5**). As observed in the paw edema model, β-BA (1 mg/kg i.p., 30 min prior to carrageenan) significantly inhibited the inflammatory response, as demonstrated by the significant attenuation of exudate formation (75%) and cell infiltration (64%). Moreover, PGE_2 level in the exudate were reduced by almost 50%, whereas the amounts of 6-keto-$PGF_{1\alpha}$ and LTB_4 in the exudate were not significantly altered. Indomethacin (5 mg/kg) reduced exudate formation and cell infiltration as well (77 and 65% respectively) without significant higher potency than β-BA (**Table 4.5**) but reduced almost completely PGE_2. Of interest, pretreatment of AKBA (1 mg/kg i.p., 30 min prior to carrageenan) caused no significant decrease in exudate formation, cell-infiltration or PGE_2 levels in this model.

Table 4.5: Effect of β-BA on carrageenan-induced pleurisy in rats.
Thirty min before intrapleural injection of carrageenan, rats (n=10 for each experimental group) were treated i.p. with 1 mg/kg β-BA, 5 mg/kg indomethacin, 1 mg/kg AKBA or vehicle (DMSO 4%). Exudate volume, PGE_2, 6-keto-$PGF_{1\alpha}$ and LTB_4 levels as well as inflammatory cell accumulation in pleural cavity were assessed 4 h after carrageenan injection. Data are expressed as mean ± S.E., n = 10. ANOVA + Tukey HSD post-hoc tests were performed, $^{**}P < 0.01$; $^{***}P < 0.01$ vs vehicle (DMSO 4%), n.d. = not determined.

Treatment	Exudate volume (ml)	Inflammatory cells × 10^6	PGE_2 (ng/rat)	6-keto-$PGF_{1\alpha}$ (ng/rat)	LTB_4 (ng/rat)
Vehicle	0.52 ± 0.03	49 ± 1.38	1.67 ± 0.11	5.46 ± 0.65	0.67 ± 0.16
β-BA (1 mg/kg)	0.13 ± 0.04***	17.80 ± 4.20***	0.82 ± 0.19**	3.46 ± 0.87	0.33 ± 0.1
AKBA (1 mg/kg)	0.42 ± 0.06	42.6 ± 2.75	1.30 ± 0.15	n.d.	n.d.
Indomethacin (5 mg/kg)	0.12 ± 0.03***	17.15 ± 3.25***	0.17 ± 0.03***	0.033 ± 0.01***	n.d.

Together, this data show that BAs bind to mPGES-1, interfere with the catalytic activity of mPGES-1 and in particular β-BA selectively inhibits PGE_2 biosynthesis (without affecting 6-keto-$PGF_{1\alpha}$ formation) in human whole blood and in rat pleural exudates, accompanied by potent anti-inflammatory effectiveness.

4.4 Boswellic acids differentially modulate platelet physiology

4.4.1 Modulation of agonist-evoked Ca^{2+} mobilization in washed human platelets by BAs.

Previous studies showed that 11-methylene-BAs (i.e. β-BA and Aβ-BA) induced a rapid and pronounced elevation of $[Ca^{2+}]_i$ in human washed platelets at concentrations ≥ 3 µM, comparable to thrombin (0.5 U/ml, optimized concentration), whereas 11-keto-BAs (i.e. AKBA or KBA) were hardly effective [64]. This study investigated, whether BAs may have detrimental actions on agonist-evoked mobilization of Ca^{2+}. Concentration-response studies in Fura-2-loaded washed human platelets revealed consistent effective concentrations of platelet agonists for Ca^{2+} mobilization as follows: 0.5 U/ml thrombin, 8 µg/ml collagen, and 1 µM U-46619 (data not shown). These concentrations were used for subsequent analysis of BA effects on $[Ca^{2+}]_i$ mobilization. In agreement with previous studies [64], at a concentration of 10 µM, AKBA and KBA caused only a slight and delayed (and transient) elevation of $[Ca^{2+}]_i$, whereas β-BA and Aβ-BA (10 µM, each) led to substantial Ca^{2+} mobilization (**Figure 4.21A**). Of interest, pre-incubation of platelets for 15 min with AKBA (10 µM) reduced the subsequent Ca^{2+} mobilization induced by U-46619 and collagen, but not so when thrombin was used as agonist (**Figure 4.21B**).

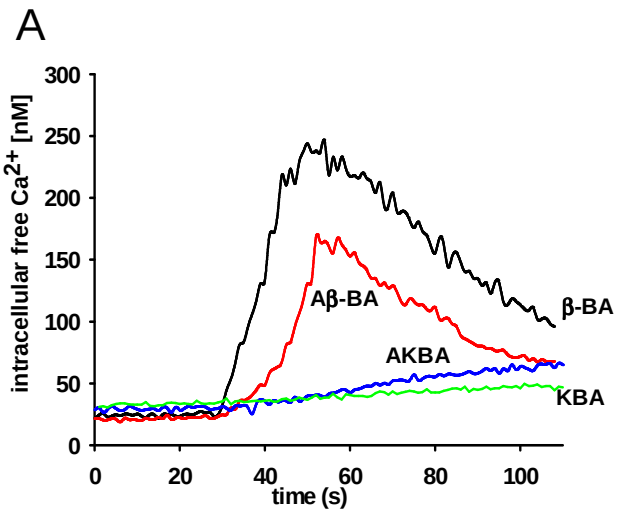

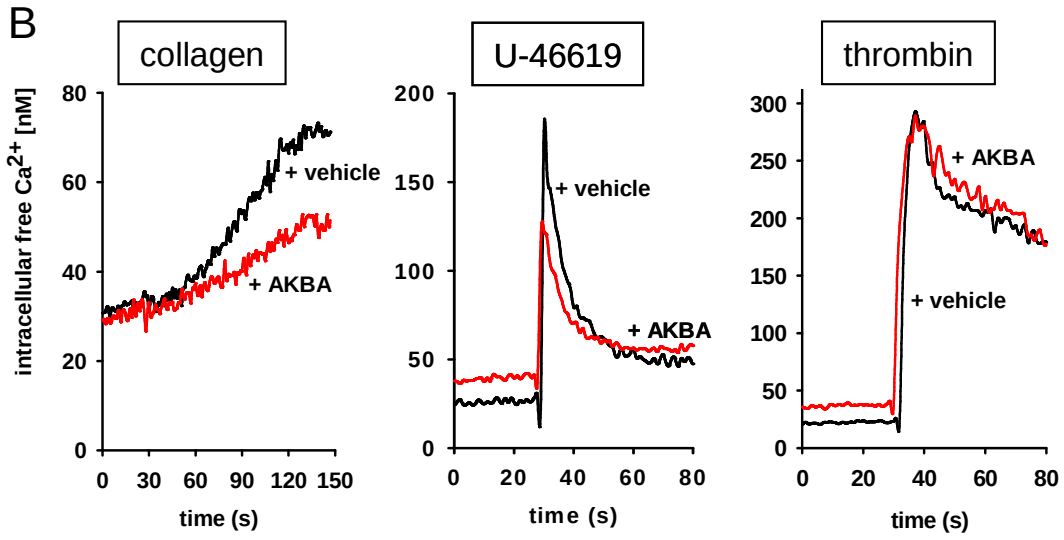

Figure 4.21: Differential effects of BAs on $[Ca^{2+}]_i$ in human washed platelets.
To Fura-2 loaded platelets (10^8/ml PG buffer), $CaCl_2$ (1 mM) was added 2 min prior determination of $[Ca^{2+}]$i. (**A**) BAs (10 µM, each) were added after 30 s. (**B**) Fura-2 loaded platelets were pre-incubated with 10 µM AKBA or with vehicle (DMSO) as indicated. After 15 min CaCl2 (1 mM) was added, the measurement of $[Ca^{2+}]$i was started and after additional 30 s, 0.5 U/ml thrombin, 8 µg/ml collagen, or 1 µM U-46619 were added. Curves are representative for at least 4 independent experiments.

Next, the efficacy of all four BAs (10 µM, each) to prevent agonist-induced Ca^{2+} mobilization was compared. As shown in Figure 4.22, for platelets stimulated with collagen or U-46619, AKBA was most efficient, followed by β-BA and Aβ-BA (the latter was somewhat less potent) whereas KBA even enhanced Ca^{2+} mobilization. Notably, all BAs essentially failed to prevent Ca^{2+} mobilization induced by thrombin**.**

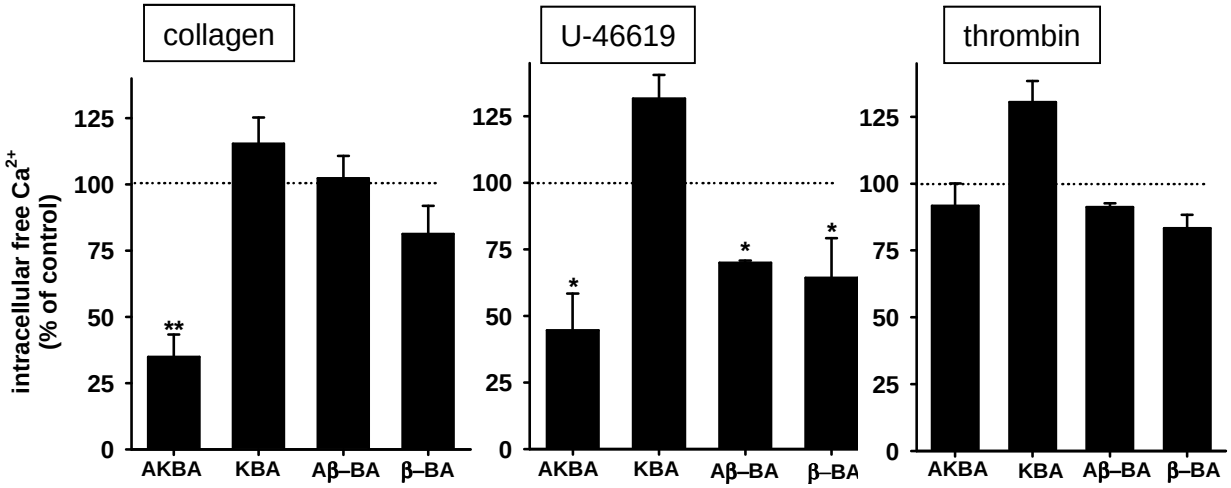

Figure 4.22: BAs selectively suppress agonist-induced Ca^{2+} mobilization in human washed platelets.
Fura-2 loaded platelets (10^8/ml PG buffer) were pre-incubated with the indicated BAs (10 µM, each) or with vehicle (DMSO, negative control) for 15 min at RT as indicated. $CaCl_2$ (1mM) was added 2 min prior the measurement of $[Ca^{2+}]_i$ was started and 0.5 U/ml thrombin, 8 µg/ml collagen, or 1 µM U-46619 were added after 30 s. The maximal increase in $[Ca^{2+}]_i$ determined within 100 s of measurement is expressed as percentage of control (DMSO). Values are given as mean + S.E., n = 4-6. One-way ANOVAs followed by Tukey HSD tests were applied to data related to unstimulated controls (DMSO);*$P < 0.05$ **$P < 0.01$.

Concentration-response studies for the most potent BA analogues revealed IC_{50} values for AKBA and β-BA at 6 and 23 µM for collagen-induced Ca^{2+} mobilization, respectively, and at 8 and 18 µM for U-46619-induced Ca^{2+} mobilization, respectively (**Figure 4.23**). When thrombin was used as agonist, the IC_{50} values for AKBA and β-BA were > 30 µM. Pre-treatment of platelets with AKBA (10 µM) also partially prevented the elevation of $[Ca^{2+}]_i$ induced by β-BA (43% ± 6.5) similar as observed for collagen or U-46619.

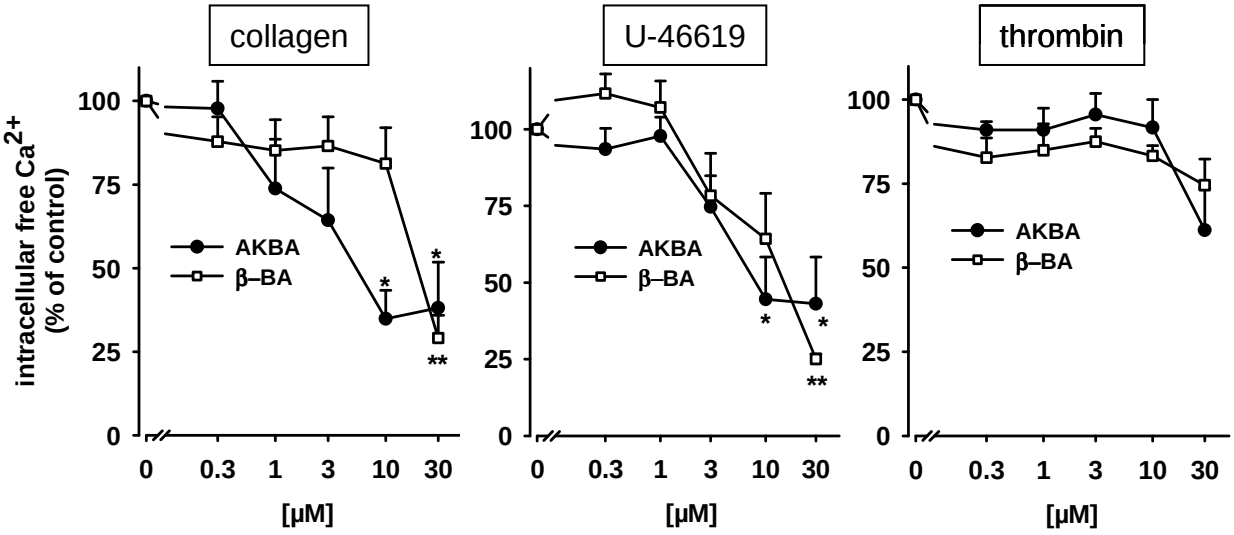

Figure 4.23: Concentration-response curves for AKBA and β-BA.
Fura-2 loaded platelets (10^8/ml PG buffer), were pre-incubated with the indicated concentrations of AKBA or β-BA and after 15 min $CaCl_2$ (1mM) was added and the measurement of $[Ca^{2+}]_i$ was started. After 30 s, 0.5 U/ml thrombin, 8 µg/ml collagen, or 1 µM U-46619 were added and the maximal increase in $[Ca^{2+}]_i$ was determined within 100 s, expressed as percentage of control (DMSO). Values are given as mean + S.E., n = 4-5. One way ANOVA followed by Tukey HSD tests were applied to data related to unstimulated controls;*$P < 0.05$ or **$P < 0.01$.

Since β-BA (≥ 3 µM), and to a minor degree also AKBA (≥ 10 µM), caused a transient elevation of $[Ca^{2+}]_i$ returning to baseline after about 5 to 7 min, it appeared possible that such an unspecific increase in $[Ca^{2+}]_i$ leading to desensitized platelets could be the reason for the subsequent failure in Ca^{2+} mobilization upon addition of other agonists. Accordingly, U-46619 which causes a transient Ca^{2+} mobilization similar as observed for 11-methylene-BAs, was first added to platelets and after 15 min, platelets were stimulated with either collagen or thrombin. In contrast to 11-methylene-BAs, preincubation with U-46619 do not substantially suppress elevation of $[Ca^{2+}]_i$ evoked by either collagen or thrombin, although a slight and significant reduction of the signals were detectable (**Figure 4.24**).

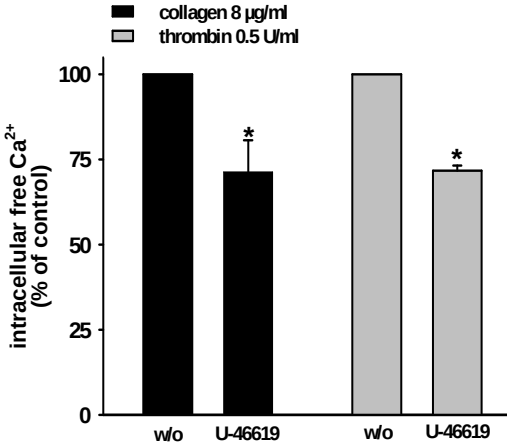

Figure 4.24: Effect of U-46619 on collagen- and thrombin-induced $[Ca^{2+}]_i$ mobilization.
Fura-2 loaded platelets (10^8/ml PG buffer) were pre-incubated with 1 µM U-46619 or vehicle (DMSO) for 15 min at RT. $CaCl_2$ was added and after 30 s platelets were stimulated with either 0.5 U/ml thrombin or 8 µg/ml collagen. The maximal increase in $[Ca^{2+}]_i$ was determined within 100 s, expressed as percentage of control (DMSO). Values are given as mean + S.E., n = 3. Directed t-tests for correlated samples were applied to data related to unaltered control,*$P < 0.05$.

4.4.2 Suppression of agonist-evoked platelet aggregation by 11-keto-BAs

Rapid and pronounced elevation of $[Ca^{2+}]_i$ in platelets is a determinant for platelet aggregation in response to various stimuli [204, 205]. Since AKBA potently prevented the elevation of Ca^{2+} in platelets stimulated by collagen and U-46619 at rather low effective concentrations ($\geq$ 3 µM) it seemed reasonable that BAs could inhibit aggregation induced by these agonists. First, the capacity of selected agonists and BAs themselves were analyzed for their ability to induce aggregation of washed platelets. As shown in **Figure 4.25A**, collagen, thrombin, and U-46619 caused marked aggregation of platelets within seconds or few minutes. Differential effects for the BAs were observed: whereas both 11-methylene-BAs at 30 µM efficiently induced platelet aggregation, the 11-keto-BAs AKBA as well as KBA (30 µM, each) failed in this respect (**Figure 4.25B**).

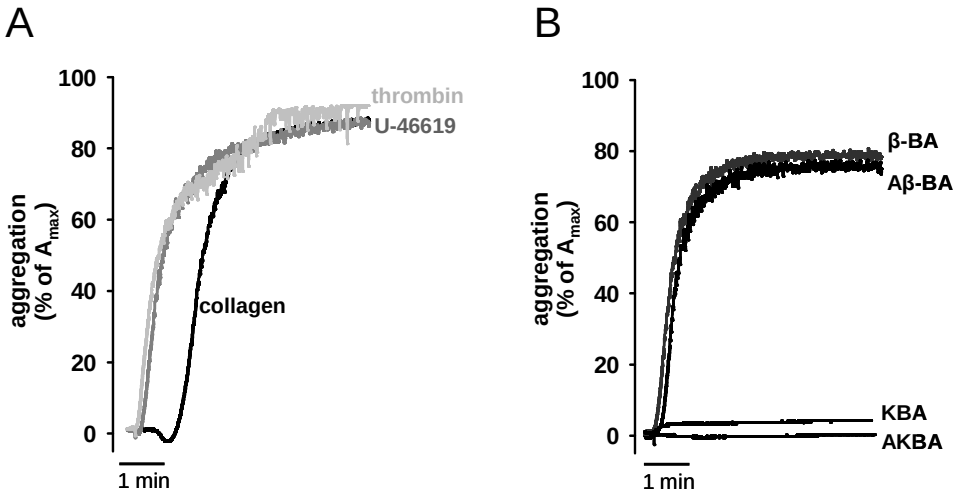

Figure 4.25: Platelet aggregation induced by different agonists and by BAs.
(**A**) Human washed platelets (2×10^8/ml) were resuspended in Tyrode´s buffer. Platelet aggregation was recorded for 5 min using a turbidimetric light-transmittance device. $CaCl_2$ (1 mM) was added right before the start of the measurement. Cells were stimulated with 0.5 U/ml thrombin, 1 µM U-46619 or 0.6 µg/ml collagen. (**B**) Aggregation of platelets was determined under the same conditions as described above using AKBA, KBA, Aβ-BA or β-BA (30 µM, each) as agonists. The aggregation response is given as percentage of the maximal light transmission A_{max}. Curves are representative for at least 5 independent determinations.

Next, platelets were pre-incubated with BAs (3 µM or 30 µM, each) for 15 min and subsequently stimulated with collagen, thrombin, and U46619 and aggregation was analyzed. Among the four BAs, only AKBA (3 µM) efficiently prevented collagen-induced aggregation (**Figure 4.26A)**. In contrast, thrombin-evoked aggregation was not prevented by AKBA (up to 30 µM) or any other BA (not shown). Of interest, for U-46619-induced aggregation AKBA (30 µM) was only moderate and KBA (30 µM) hardly efficient (**Figure 4.26A**).

Detailed concentration-response studies showed that AKBA prevented platelet aggregation induced by collagen with an IC_{50} value ≤ 1 µM, whereas for U-46619 the IC_{50} value was approximated at 25 µM (**Figure 4.26B**). Despite the robust inhibition of collagen-induced aggregation by AKBA, only a moderate effect was measured with KBA (IC_{50} = 23 µM) and thrombin-evoked aggregation was not impaired.

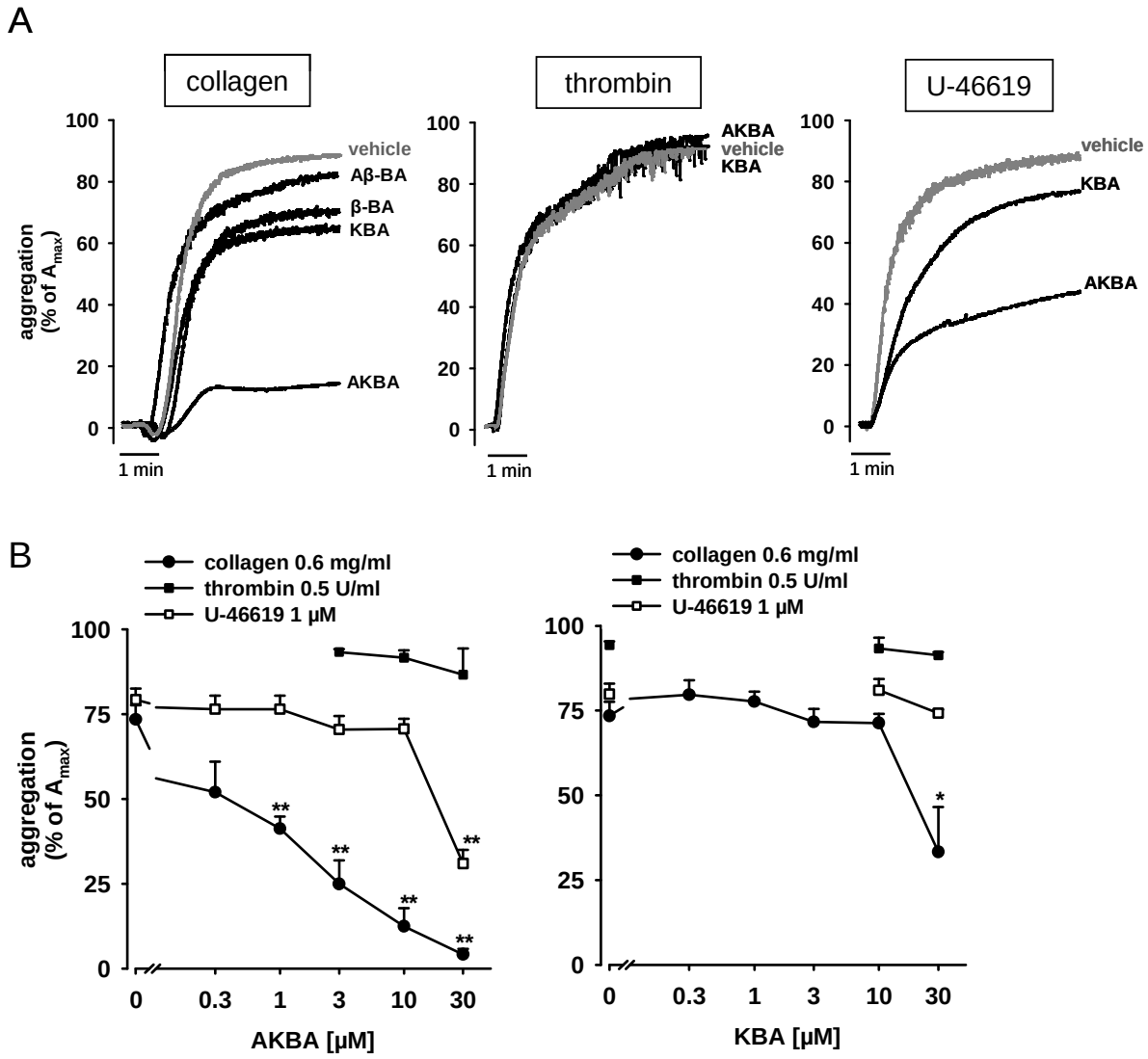

Figure 4.26: AKBA selectively and potently prevents collagen-induced platelet aggregation.
(**A**) Human washed platelets (2×10^8/ml in Tyrode´s buffer) were pre-incubated with AKBA and KBA (3 µM, each) prior activation by collagen. Platelets treated with thrombin or U-46619 were pre-incubated with AKBA and KBA (30 µM, each). After 15 min at RT $CaCl_2$ (1 mM) was added, cells were stimulated with 0.6 µg/ml collagen, 0.5 U/ml thrombin or 1 µM U46619 and aggregation was recorded. Curves are representative for at least 4-5 independent determinations. (**B**) Concentration-response curves for AKBA and KBA. Cells were pre-incubated with the indicated concentrations of AKBA and KBA or vehicle (DMSO) for 15 min at RT and aggregation was elicited in response to the agonists as indicated. The aggregation response is displayed as percentage of the maximal light transmission A_{max}. Values are given as mean + S.E., n = 3. ANOVAs followed by Tukey HSD tests were applied to data related to untreated controls; $*P < 0.05$ $**P < 0.01$.

Activation of platelets with collagen, via the GPVI receptor, involves phosphorylation of several non-receptor tyrosine including Src family kinases (Src, Fyn, Lyn Hck and Yes), Syk, Fak and Jak family kinases and finally leads to the activation of PLCγ2 [221]. To determine the effect of AKBA in the collagen signaling pathway, human platelets were pre-incubated with AKBA for 10 min at RT prior activation by collagen. As shown in **Figure 4.27A** pretreatment with AKBA resulted in a marked reduction of collagen-induced tyrosine phosphorylation of a protein with an approx. molecular mass of 150 kDa comparable to the effect of the selective Src family kinase inhibitor PP2 [274]. Accordingly, experiments to elucidate a direct effect of AKBA on the collagen-related activation of PLCγ2 (phosphorylation at Tyr759) [222] and the upstream Src family kinases (phosphorylation at Tyr416) [275] were performed. Preincubation with PP2 essentially decreased phosphorylation of PLCγ2 and Src family tyrosine kinases, whereas the effect obtained by AKBA was moderate. (**Figure 4.27B**).

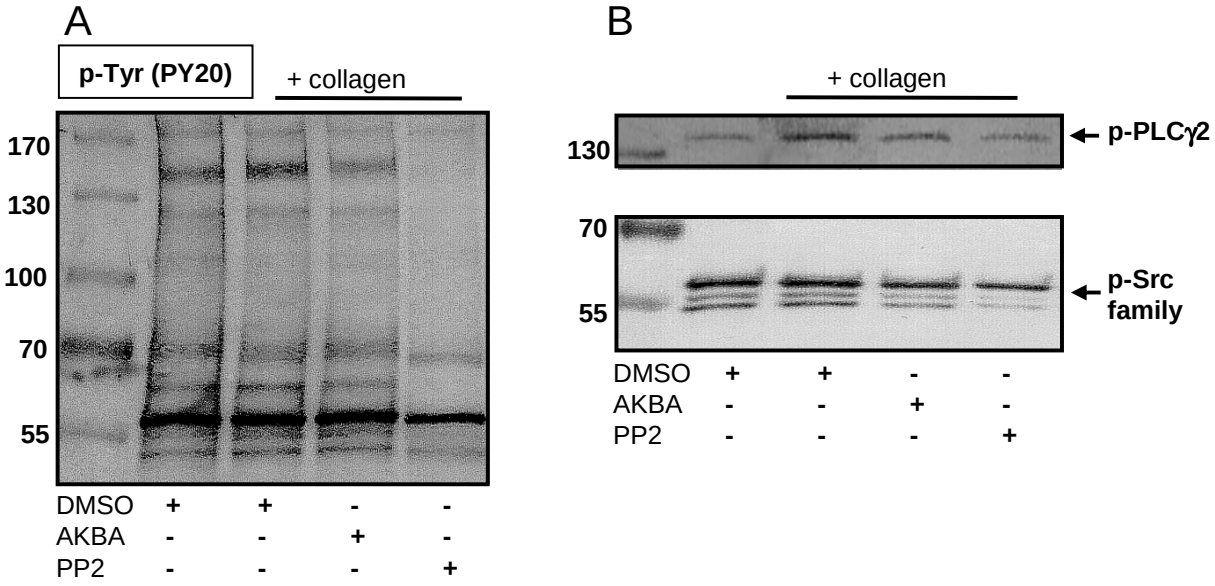

Figure 4.27: Effect of AKBA on collagen-induced protein tyrosine phosphorylation.
(**A**) Washed human platelets (5×10^8/ml in Tyrodes buffer) were pre-incubated with AKBA (30 µM), PP2 (3 µM) or vehicle (DMSO) for 10 min at RT. Then, platelets were supplemented with $CaCl_2$ (1mM) and treated with or w/o collagen (10 µg/ml) at 37 °C for 3 min. WB analysis on whole platelet lysates were performed using a monoclonal anti-phosphotyrosine antibody (PY20). (**B**) Samples were treated as described above except detection by WB analysis, which was performed utilizing phospho-specific antibodies against the Tyr759 phosphorylated PLCγ2 or Tyr416 phosphorylated Src family kinases.

4.4.3 Platelet aggregation induced by 11-methylene-BAs is Src family kinase and PLC dependent.

As already shown in **4.4.2** β-BA and Aβ-BA (30 µM, each) provoke aggregation of human washed platelets. Concentration-response studies revealed EC_{50} values ≤ 10 µM for both 11-methylene-BAs (**Figure 4.28**).

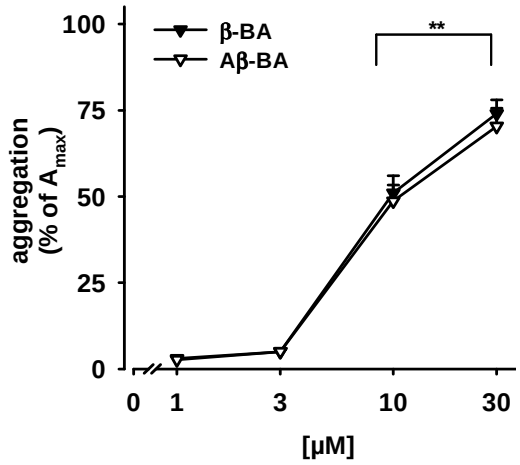

Figure 4.28: Concentration-response studies for Aβ-BA and β-BA.
Aggregation of platelets was determined under the same conditions as described above. The aggregation response is given as percentage of the maximal light transmission A_{max} and data are given as mean + S.E., n = 4. ANOVAs followed by Tukey HSD tests were applied to data related to untreated controls; $^{**}P < 0.01$.

Previously a partial involvement of Src family kinases and PLC was described for elevation of $[Ca^{2+}]_i$ by 11-methylen BAs [64]. To examine the involvement of PLC and Src family kinases in BA-induced platelet aggregation, U-73122 as an inhibitor of PLC-dependent processes [276] and the selective Src family kinase inhibitors PP2 (and its inactive analogue PP3) and SU6656 [277] were used (**Figure 4.29**).

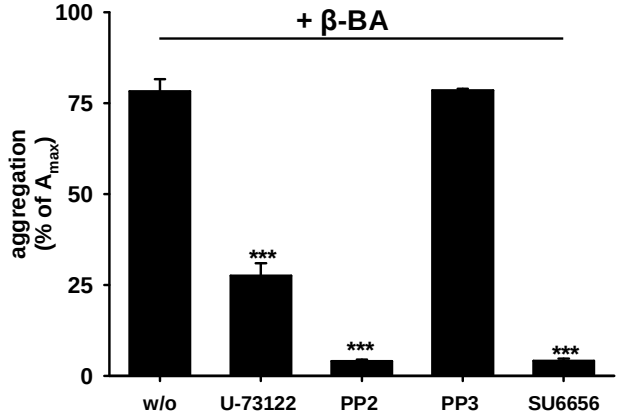

Figure 4.29: Modulation of β-BA-induced platelet aggregation by PLC-and Src family kinases inhibitors.
Platelets (2×10^8/ml) were pre-incubated with U-73122, PP2 (and its inactive analogue PP3), SU6656 or vehicle (DMSO) for 15 min at RT. $CaCl_2$ (1 mM) was added and cells were stimulated with 30 µM β-BA. The aggregation response is displayed as percentage of the maximal light transmission A_{max}. Values are given as mean + S.E., n = 3. ANOVAs followed by Tukey HSD tests were applied to data related to untreated controls, $^{***}P < 0.001$.

Preincubation with U-73122 (3 µM) strongly suppressed β-BA-induced platelet aggregation comparable to experiments using thrombin or collagen as stimuli (not shown). SU5565 (5 µM) almost completely abolished aggregation response initiated by β-BA being equipotent with PP2 (3µM), whereas its inactive analogue PP3 (3µM) was not active.

Upon platelets stimulation multiple proteins become phosphorylated at tyrosine residues [278]. Treatment of platelets by β-BA (30 µM) induced marked protein tyrosine phosphorylation (**Figure 4.30A**) being equipotent with collagen (10 mg/ml) and both phosphorylation pattern were essentially reduced by preincubation with PP2. Hence, the capacity of β-BA to evoke PP2-sensitive phosphorylation processes such as activation of Src family kinases and downstream PLCγ2 was investigated (**Figure 4.30B**). Both Src family kinases and PLCγ2 were slightly phosphorylated in response to β-BA and a weak suppression by PP2 preincubation was observed. The substantial tyrosine phosphorylation evoked by β-BA of proteins with approx. molecular weights of 120 and 60 kDa (**Figure 4.30B**) remains to be elucidated.

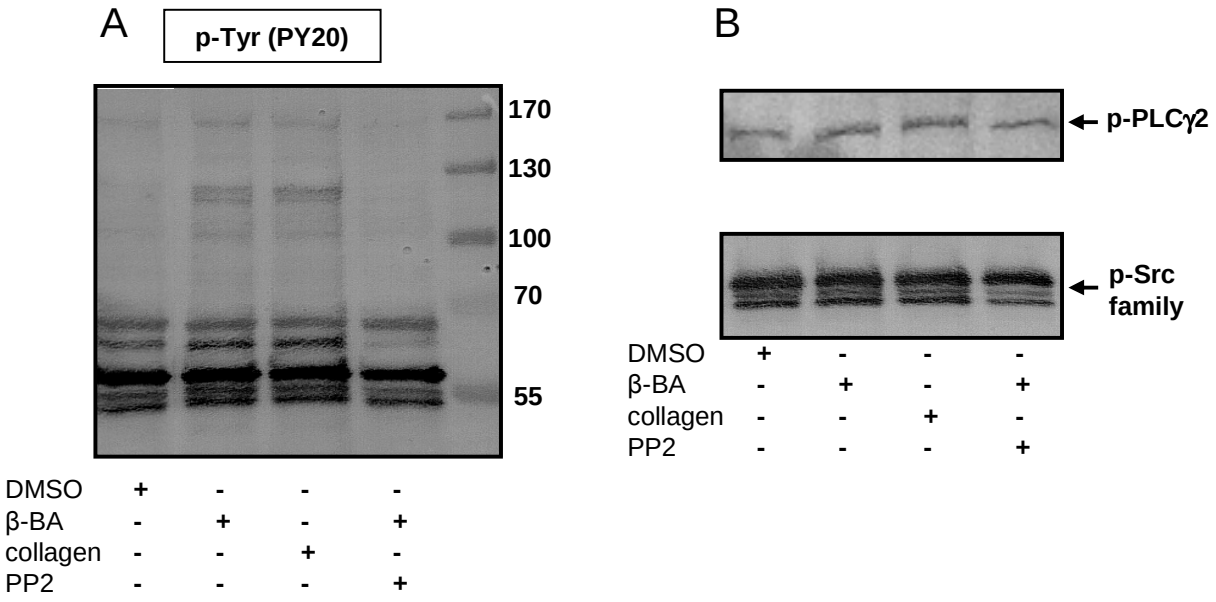

Figure 4.30: β-BA induces tyrosine phosphorylation in washed human platelets.
(**A**) Washed human platelets (5 x 10^8/ml in Tyrodes buffer) were supplemented with $CaCl_2$ (1mM) and activated by β-BA, collagen (10 µg/ml) or vehicle (DMSO) at 37 °C for 3 min, as indicated. PP2 preincubation at RT was 10 min prior stimulation with the respective activators. WB analysis on whole platelet lysates were performed using a monoclonal anti-phosphotyrosine antibody (PY20). (**B**) Samples were treated as described above except detection by WB, which was performed utilizing phospho-specific antibodies against Tyr759 phosphorylated PLCγ2 or Tyr416 phosphorylated Src family kinases.

4.4.4 BAs differentially modulate thrombin generation

Besides aggregation, formation of thrombin is considered an essential functional platelet response [202]. Recalcified PRP supplemented with β-BA, Aβ-BA, AKBA, KBA or vehicle (DMSO/HEPES) was analyzed for generation of thrombin, and as shown in **Figure 4.31A**, both 11-methylene-BAs (i.e. β-BA, Aβ-BA) significantly evoked thrombin formation. In contrast, the effectiveness of AKBA and KBA up to 30 µM was only moderate compared to 11-methylene-BAs and thrombin generation was in the range of vehicle (DMSO/HEPES) response. Further concentration-response studies revealed an effective concentration of 3 µM for both 11-methylene-BAs to induce thrombin generation (**Figure 4.31B and C**).

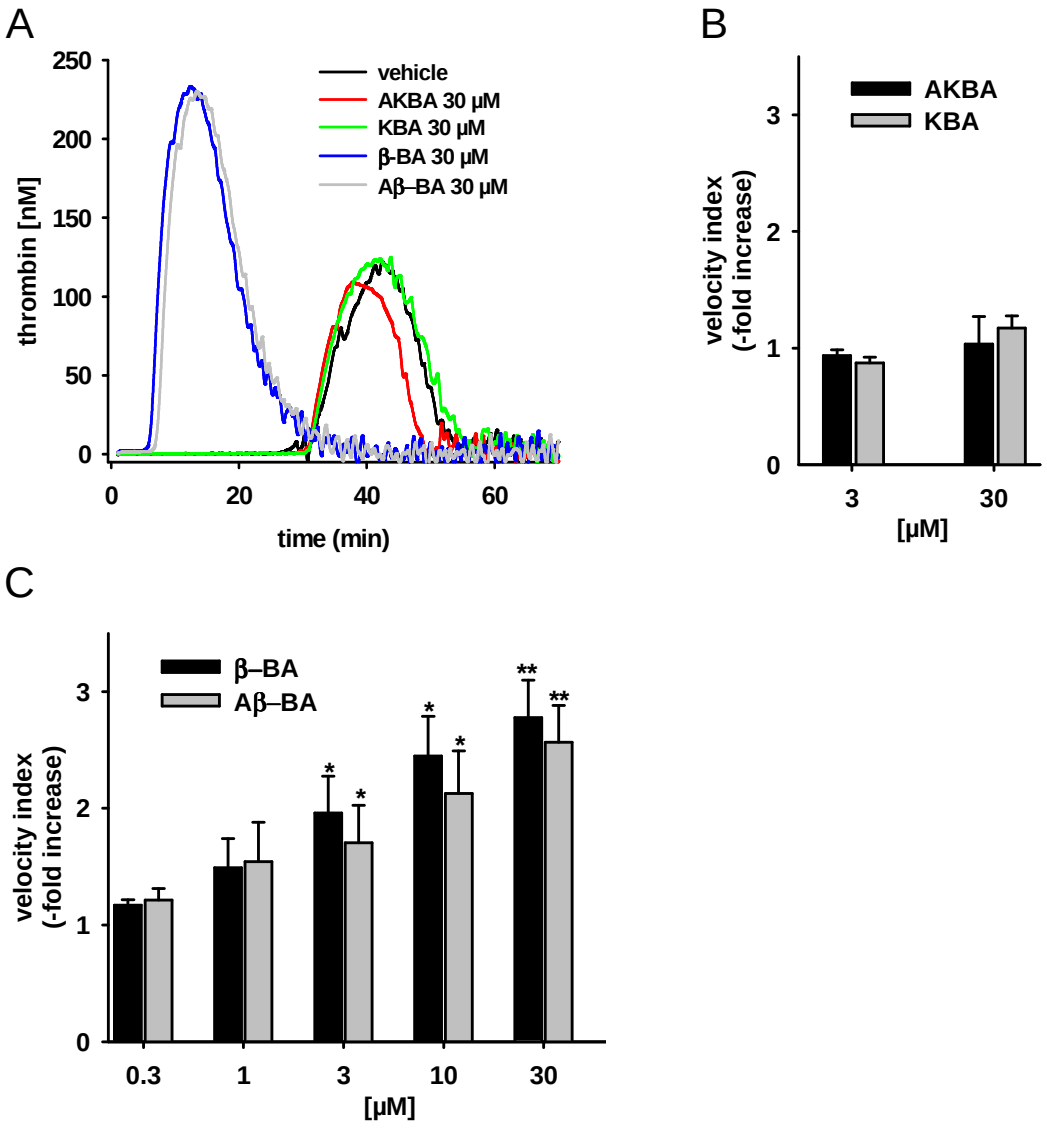

Figure 4.31: Effects of BAs on thrombin generation.
Thrombin generation was assessed in recalcified PRP. (**A**) Representative original traces of thrombin generation (given as [nM] thrombin). PRP and buffer containing BAs or vehicle (DMSO/HEPES) were tested for their ability to induce thrombin generation. (**B**, **C**) Concentration-response studies of BAs. Data are expressed as mean velocity index (increase over unstimulated cells) + S.E., n= 4. One way ANOVA and Tukey HSD were performed, **P* < 0.05 or ***P* < 0.01.

To determine if BAs may exert detrimental effects on agonist-induced thrombin generation, recalcified PRP was pre-incubated with the indicated BAs for 15 min at RT and thrombin generation was initiated by collagen (2 µg/ml) or U-46619 (5 µM). Both agonists led to a substantial formation of thrombin (**Figure 4.32A**) as described in literature [279]. However, thrombin generation evoked by collagen or U-46619 remained unaffected by preincubation with AKBA or KBA (**Figure 4.32B**). In contrast, preincubation with β-BA or Aβ-BA substantially potentiated generation of thrombin induced by collagen or U-46619.

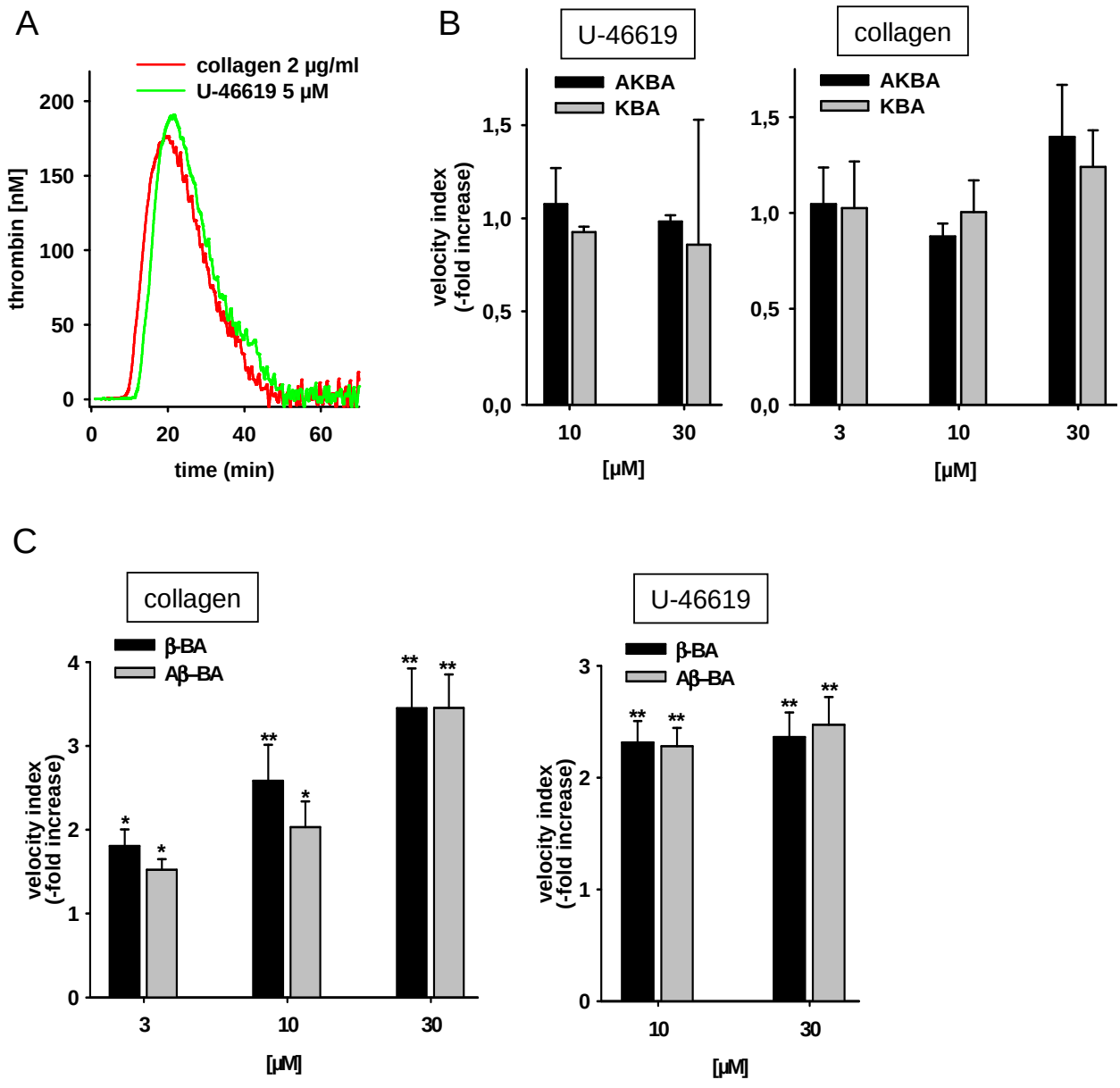

Figure 4.32: Effects of BAs on agonist-induced thrombin generation.
(**A**) Recalcified PRP was treated with collagen (2 µg/ml) or U-46619 (5 µM) to induce thrombin generation (representative original curves) PRP was pre-incubated with AKBA, KBA (**B**); BA, Aβ-BA (**C**) or vehicle (DMSO/HEPES) as indicated and thrombin generation (given as velocity index) was elicited by collagen (2 µg/ml) or U-46619 (5 µM). Data are expressed as mean + S.E., n= 3. One way ANOVA and Tukey HSD were applied to data related to unstimulated controls, **P* < 0.05 or ***P* < 0.01.

4.4.5 Effects of *B. serrata* extracts on Ca^{2+} mobilization, platelet aggregation and thrombin generation.

Extracts of *B. serrata* contain both 11-keto-BAs and 11-methylene-BAs. In the H15® extract, AKBA and KBA are sparsely present (approx. 3.7% and 6.1%), whereas the contents of β-BA and Aβ-BA (approx. 18.1% and 10.5%) are much higher [15]. In contrast, the extract VBSE (Pharmasan GmbH, Freiburg, Germany) is prepared based on a special manufacturing technique where 11-keto-BAs are enriched over 11-methylene-BAs. Due to the opposing effects of isolated 11-keto-BAs and 11-methylene-BAs, the overall effects of the two *B. serrata* extracts on Ca^{2+}mobilization, platelet aggregation and thrombin generation were assessed. In analogy to the results observed with isolated 11-methylene-BAs, the H15® extract rapidly (approx. 25 s after exposure) and significantly evoked release of $[Ca^{2+}]_i$ in washed human platelets at concentrations ≥ 3 µg/ml (**Figure 4.33**), whereas the VBSE extract caused only weak and rather slow (70-85 s after exposure) Ca^{2+}mobilization at significantly higher concentrations (≥ 30 µg/ml).

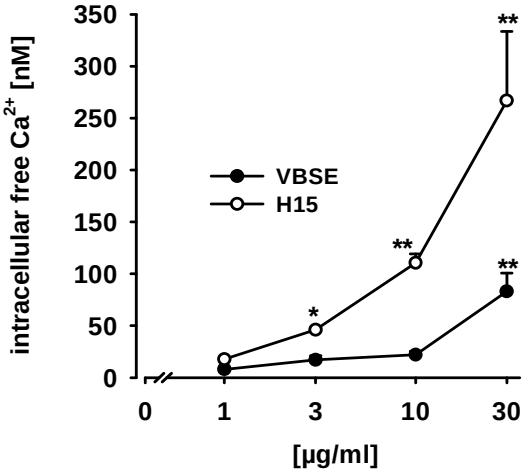

Figure 4.33: Effects of *B. serrata* extracts on $[Ca^{2+}]_i$ mobilization in human washed platelets.
To Fura-2 loaded platelets (10^8/ml PG buffer), $CaCl_2$ (1 mM) was added 2 min prior determination of $[Ca^{2+}]_i$ and H15® and VBSE extracts as indicated were added 30 s after the measurement was started. Data are expressed as mean + S.E., n= 4. One way ANOVA and Tukey HSD were applied to data related to unstimulated controls, **P* < 0.05 or ***P* < 0.01.

To assess if the extracts may exhibit inhibitory effects on agonist-induced intracellular Ca^{2+}mobilization, as observed for isolated BAs (see **4.4.1)**, Fura-2 loaded platelets were pre-incubated with H15® and VBSE extracts or vehicle for 15 min at RT and Ca^{2+}mobilization was initiated by collagen (8 µg/ml). Interestingly neither H15® extract nor VBSE extract up to 10 µg/ml altered the effect of collagen significantly, whereas both extracts at 30 µg/ml slightly enhanced $[Ca^{2+}]_i$ mobilization elicited by collagen (**Figure 4.34**).

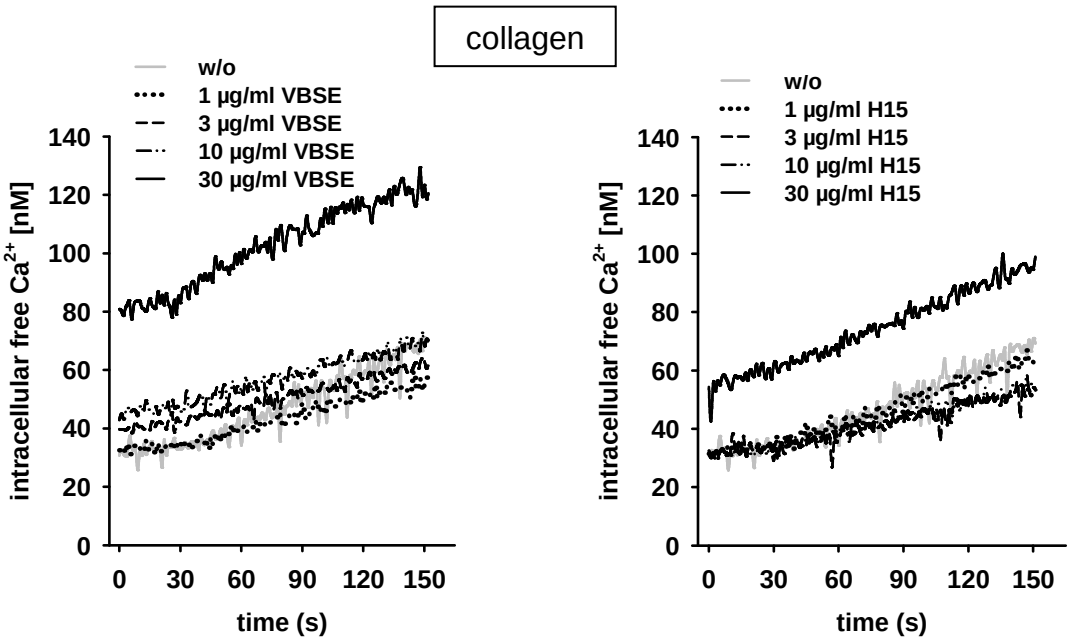

Figure 4.34: Effects of *B. serrata* extracts on collagen-induced $[Ca^{2+}]_i$ mobilization in human platelets. Fura-2 loaded platelets (10^8/ml PG buffer) were pre-incubated with VBSE extract (left panel) or H15® extract (right panel) for 15 min at RT. $CaCl_2$ (1 mM) was added 2 min prior determination of $[Ca^{2+}]_i$ and collagen (8 µg/ml) were added 30 s after the measurement was started. Curves are representative for at least 3 independent experiments.

Next, the capacity of the extracts to evoke platelet aggregation was assessed. In agreement with the results obtained by isolated BAs (see **Figure 4.28**), the H15® extract rapidly and potently induced aggregation of washed human platelets with effective concentrations ≥ 10 µg/ml, comparable to 11-methylene-BAs. In contrast, the VBSE extract (up to 30 µg/ml) caused no aggregation (**Figure 4.35A**). Pre-treatment of platelets with H15® (up to 10 µg/ml) failed to inhibit aggregation induced by collagen but on the other hand, the VBSE potently suppressed the collagen-induced response (IC_{50} = 10 µg/ml). Again, in spite of the prominent prevention of collagen-induced aggregation by VBSE, only moderate inhibition at higher concentration of VBSE (30 µg/ml) was detectable for U-46619-evoked aggregation, and no effect was observed when thrombin was used as agonist (**Figure 4.35B**).

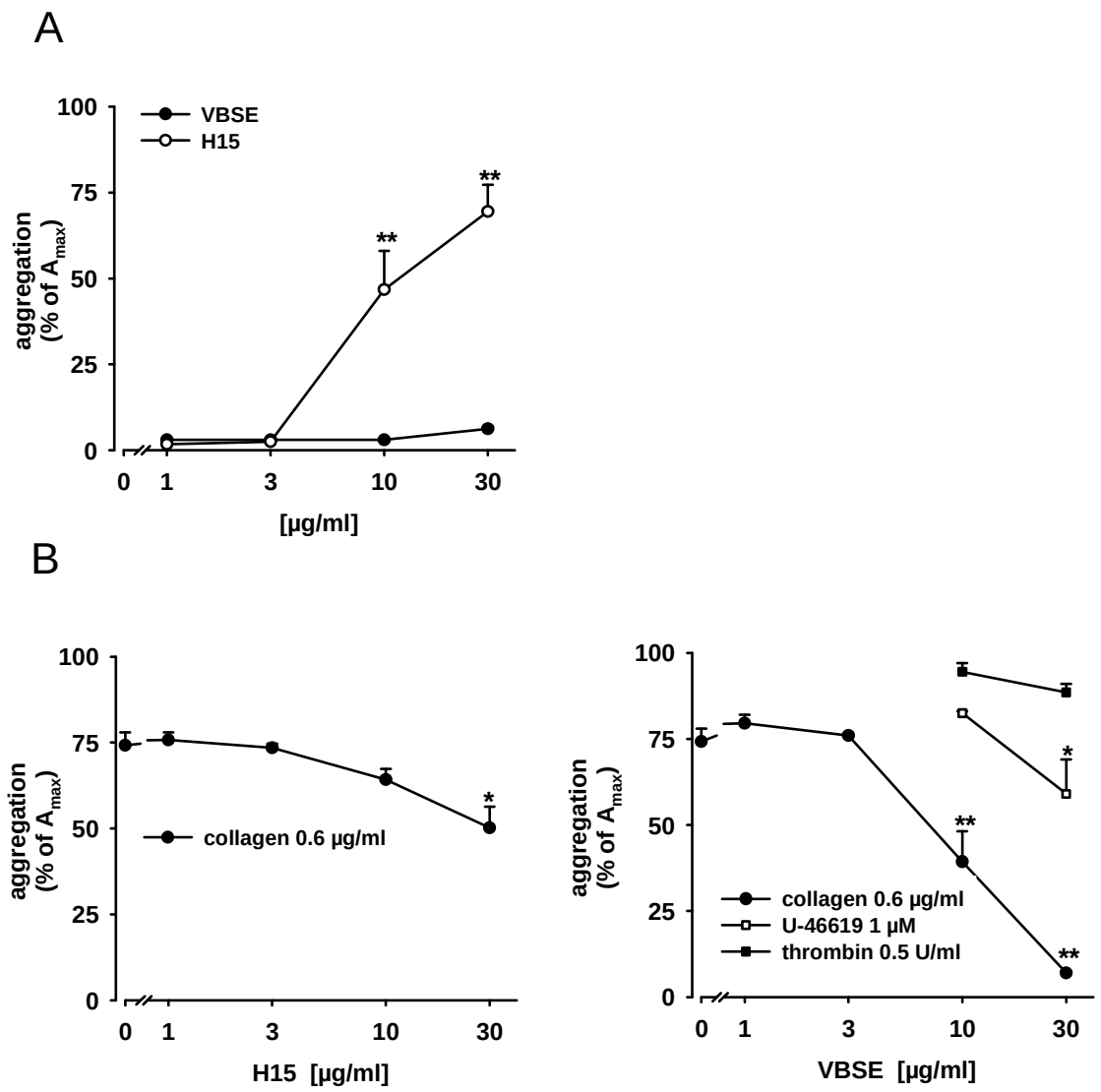

Figure 4.35: Differential effects of *B. serrata* extracts on platelet aggregation.
(**A**) Human washed platelets (2×10^8/ml in Tyrode´s buffer) were supplemented with $CaCl_2$ (1 mM) right before the start of the measurement and cells were stimulated with H15® extract or VBSE extract as indicated. Then, aggregation was recorded for 5 min using a turbidimetric light-transmittance device. (**B**) Concentration-response curves for extracts of *B. serrata* extracts on agonist-induced aggregation. Cells were pre-incubated with the indicated concentrations of H15®, VBSE extract or vehicle (DMSO) for 15 min at RT and aggregation was elicited in response to the agonists as indicated. The aggregation response is displayed as percentage of the maximal light transmission A_{max}. Values are given as mean + S.E., n = 3-4. ANOVAs followed by Tukey HSD tests were applied to data related to untreated controls, **P* < 0.05 or ***P* < 0.01.

Finally, the effect of the *B. serrata* extracts on thrombin generation was investigated. H15® extract at concentrations ≥ 1 µg/ml potently induced thrombin formation in recalcified PRP (**Figure 4.36A**) and thus, acted in analogy to previous results observed for isolated 11-methylene-BAs (**Figure 4.31**). In contrast, the VBSE extract (up to 30 µg/ml) was not active and also no effect was observed on collagen-induced thrombin generation which is in line with the previous findings for 11-keto-BAs (see **4.4.4)**. Notably, that H15® extract showed cumulative effects on collagen-induced formation of thrombin (**Figure 4.36B**).

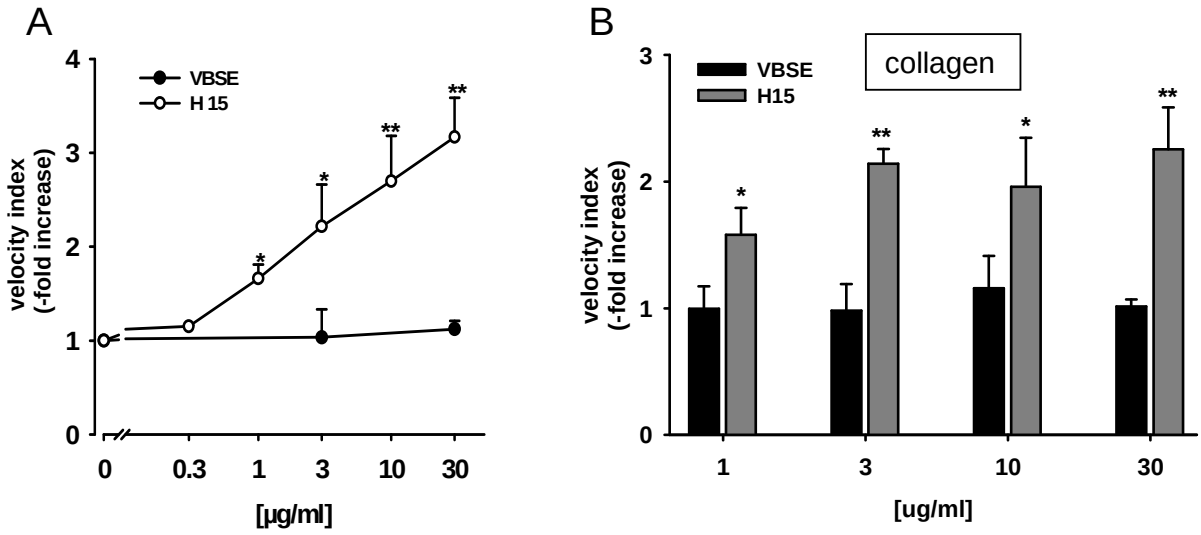

Figure 4.36: Effects of *B. serrata* extracts on thrombin generation.
Thrombin generation was assessed in recalcified PRP. (**A**) PRP and buffer containing H15®, VBSE extract or vehicle (DMSO/HEPES) as indicated were added to each well of a 96-well microtiter plate and were tested for their ability to induce thrombin generation. (**B**) Effects of H15® and VBSE extract on collagen-induced thrombin generation. PRP was pre-incubated with H15® extract, VBSE extract or vehicle for 15 min at RT and thrombin generation was induced by collagen (2 µg/ml).Data are expressed as mean (increase over unstimulated cells) + S.E., n= 3-4. One way ANOVA and Tukey HSD were performed, **P* < 0.05 or ***P* < 0.01.

In summary, this data show that BAs depending on the structure (e.g. the presence of the 11-keto- and 3-*O*-acetyl moiety) differentially modulate platelet physiology which is further influenced by the nature of the platelet agonist and the relative content of 11-methylene- and 11-keto-BAs in *B. serrata* extracts seemingly determines the overall effect on platelet functions. Nevertheless, there are additional experiments needed to define responsible molecular mechanisms in detail and to carefully evaluate the pharmacological relevance of these interactions.

5 DISCUSSION

5.1 Identification and evaluation of molecular targets of boswellic acids within the arachidonic acid cascade

5.1.1 Interaction of BAs with cyclooxygenases

Initial attempts to elucidate the molecular mechanisms underlying the anti-inflammatory properties of *B. spec.* extracts proposed 5-LO as a target of BAs because LT formation was blocked in cellular as well as in cell free assays [52-55]. Together with the fact that LTs play pivotal roles in some inflammatory and allergic reactions, it was generally accepted at that time that inhibition of LT formation by interference with 5-LO is the molecular basis of the anti-inflammatory effects of BAs. On the other hand, inhibition of the related enzymes COX-1 and p12-LO by BAs has been excluded for a long time [53]. In order to demonstrate the selectivity of BAs for 5-LO, the authors addressed the effects of BAs on COX-1 and p12-LO. However, instead of using AKBA, the Aβ-BA analogue lacking the 11-oxo moiety was utilized for this purpose [53, 280]. In fact, Aβ-BA is a poor inhibitor of COX-1 (this study) and also failed to inhibit p12-LO [8]. Additionally, previous studies reported BA-induced release of AA from human platelets but only 11-methylene-BAs (e.g. β-BA) caused further transformation to 12-H(P)ETE [8] whereas 11-keto-BAs (AKBA) were hardly effective. Indeed, AA-metabolism forming the COX-1 product 12-HHT was neglected by AKBA. Hence, it is demonstrated that AKBA is a potent blocker of COX-1 in intact human platelets as well as of the isolated COX-1 enzyme. Interestingly, the effects of BAs on cellular COX-2 product synthesis and isolated COX-2 activity were only modest (IC_{50} > 100 µM).At least in intact platelets, the 11-keto moiety plays a critical role for the interference with COX-1 product synthesis, but also the 3-*O*-acetyl group seemingly governs the potency, since KBA suppressed COX-1 activity less efficiently. Similar structure-activity relationships were observed before for other targets and biochemical actions [8-10, 56] designating AKBA as the most potent BA-analogue. Along these lines, Poeckel et al. showed that p12-LO is potently inhibited by AKBA, whereas the 11-methylene-BAs rather stimulated this enzyme [8]. Interestingly, when the potencies of AKBA for inhibition of p12-LO (IC_{50} = 17 µM [8]), COX-1 (IC_{50} = 32 µM) and 5-LO (IC_{50} = 16 [54]) in cell-free assays are compared, there are actually only small differences apparent.

For COX-1 inhibition, the efficacy of AKBA in intact cells (IC_{50} = 6 to 23 µM) was somewhat higher than in cell free assays (IC_{50} = 32 µM). It is possible that AKBA, due to its high hydrophobicity accumulates in subcellular membrane compartments of platelets where activated COX-1 resides. Moreover, in intact platelets, the efficacy of AKBA depended on the stimulus (e.g. thrombin vs. A23187), and AKBA was most efficient to inhibit COX-1 when platelets were activated by A23187 (IC_{50} = 6 µM). It is not clear why BAs lacking the 11-keto moiety (β-BA and Aβ-BA) fail to potently block COX-1 activity under these conditions. Also for inhibition of 5-LO, AKBA was most potent in cells challenged by A23187, whereas β-BA and Aβ-BA were hardly efficient [53, 63] and this thesis. Possibly, the prominent increase in $[Ca^{2+}]_i$ evoked by A23187 or A23187-induced alterations of membrane characteristics may govern the cellular uptake and/or the interference of 11-keto-BAs with COX-1 (5-LO).

Besides the inhibition of product synthesis, a direct interference of BAs with COX-1 (but not COX-2) could be visualized by the protein pull-down approach using immobilized β-BA or KBA. Since the binding was reversed by AA or ibuprofen, it is assumed that BAs bind to the active site of COX-1. In addition to COX-1, it was shown that p12-LO is efficiently precipitated by KBA-Seph [8]. Therefore, AKBA can not be regarded as a selective inhibitor of 5-LO, since it also almost equally well inhibits COX-1 and p12-LO, implying rather pleiotropic effects of BAs on enzymes within the AA cascade. Moreover, BAs were shown to inhibit the activity of various CYP450 enzymes [19] that can also metabolize AA, leading to EETs [281]. Since inhibition of COX-1 by AKBA was reduced by increasing the amount of AA, and since binding of COX-1 to immobilized KBA is prevented by AA, AKBA might be considered as a competitive COX-1 inhibitor. Regarding the chemical structure, AKBA represents a lipophilic (fatty) acid that may fit into AA-binding sites of respective enzymes. The docking results confirm the interaction of BAs with COX-1 (within the AA-binding pocket). All four BAs docked into the active site of COX-1, which might be achieved via van der Waals interactions complemented with hydrogen bonds formed by the hydroxyl or the acetyl-group with Tyr355 and Arg120. The interference with Arg120 is regarded as a common feature of NSAIDs [127]. The positive Chemscore values for the BAs indicate favorable binding to the active site of COX-1, even though they fail to explain the different IC_{50} values measured. Noteworthy, the obtained Chemscore values are smaller than for the co-crystallized structures BFL (and SC-558). Relatively higher Chemscores were obtained for binding of the BAs to COX-1 over COX-2, correlating with the rather poor inhibition of COX-2 activity by BAs (IC_{50} > 100 µM). Collectively, the docking study suggests favorable binding of BAs to COX-1.

Finally, to estimate the pharmacological relevance of the interference of BAs with COX-1 a whole blood experiment reflecting *in vitro* conditions was applied. None of the BAs tested (50 µM) essentially suppressed COX-1 product formation in human whole blood. It is widely

accepted that the potency of NSAIDs for COX inhibition is influenced by their plasma protein (mainly albumin) binding [282]. Since the amount of free drug is important for its inhibitory activity the impaired efficacy of BAs may be due to high albumin binding (also see **5.1.2**). While AKBA is regarded as a competitive and reversible inhibitor of COX-1, competition between free drug (AKBA) and substrate (AA) for COX-1-binding might be influenced by unspecific protein binding. In contrast, irreversible (aspirin) and slow reversible (indomethacin) inhibition seems to be less affected by protein binding.

In conclusion, despite the long appreciated opinion about AKBA and its selectivity for 5-LO, AKBA also interferes with COX-1, and as shown before, for other AA-metabolizing enzymes (i.e. p12-LO [8] and CYPs [19]. Comparative studies with well-recognized COX-1 inhibitors revealed that AKBA is about equipotent to ibuprofen and aspirin in COX-1 inhibition, at least in cell-free assays and isolated intact cells. The inhibitory effect of AKBA is reversible, and increased levels of AA as substrate for COX-1 impair the efficacy. Moreover, pull-down experiments using purified or COX-1 of cellular origin and docking studies indicate a favourable binding of AKBA into COX-1 active site. In contrast, COX-2 activity was less affected by BAs as compared to COX-1, and pull-down experiments as well as docking studies exclude strong affinities of BAs towards COX-2. However, the failure of AKBA to essentially inhibit COX-1 activity under physiological mimicking conditions (whole blood assay) questions the pharmacological relevance of this interference regarding the anti-inflammatory potential of AKBA-containing preparations (i.e. frankincense).

5.1.2 Interference of BAs with 5-lipoxygenase

As mentioned above, inhibition of 5-LO activity and formation of LTs was long proposed to be the major mechanism of BAs accounting for the anti-inflammatory properties of frankincense preparations [5, 53, 54]. The suppression of LT formation by BAs or frankincense extracts was analyzed so far only in cell-free assays or in isolated leukocytes from rats or guinea pigs but never in a physiological context (e.g. human whole blood assays or in humans *in vivo*) or under experimental conditions that consider pharmacologically relevant factors (i.e. plasma albumin-binding). Therefore, the pharmacological relevance of the inhibition of 5-LO by BAs *in vivo* is unclear. This study provides a detailed analysis of the interference of the major natural occurring BAs with 5-LO regarding mechanistic aspects of 5-LO inhibition, and pharmacological relevance of 5-LO as molecular target applying physiologically relevant test systems. 5-LO activity is modulated by several co-factors (lipid hydroperoxides, substrate concentration, Ca^{2+} and phospholipids [268]) that often affect the potency of pharmacological 5-LO inhibitors [232, 283]. 5-LO inhibitors are categorized as redox-type inhibitors, iron ligand-type inhibitors, and nonredox-type 5-LO inhibitors [268]. AKBA lacks antioxidant and iron-chelating properties [54] and was proposed to act directly on 5-LO at a regulatory and selective site for pentacyclic triterpenes that is different from the AA-binding site. Thus, binding of 4-azido-5-^{125}iodo-salicyloyl-β-alanyl-11-keto-boswellic acid to 5-LO was supported by Ca^{2+} (> 500 nM) but reduced by AA (10 - 50 µM), suggesting that AKBA binds 5-LO in an AA-competitive and Ca^{2+}-depending manner [55]. However, attempts to selectively precipitate 5-LO from PMNL lysates using immobilized BAs failed [8].

This study revealed that AKBA and KBA were the most potent β-configurated BA analogues (IC_{50} = 2.9 and 6.3, respectively) suppressing activity of human recombinant 5-LO but also the α-configurated αBA significantly reduced 5-LO catalysis (IC_{50} = 15.3 µM). Concerning essential factors regulating 5-LO activity, AKBA and KBA were more efficient at high AA concentrations (20 µM), and also in intact PMNL, supplementation of excess of AA (20 µM) rather improved the efficacy, excluding an AA-competitive mode of action and interference with FLAP. Moreover, Ca^{2+} did not enhance the potency against 5-LO activity but even slightly impaired it. Possibly, binding to 5-LO and inhibition of 5-LO catalytic activity is conferred by BAs at different sites of the enzyme. In fact, also classical nonredox-type 5-LO inhibitors (e.g. ZM230487) may act at two different (AA-binding) clefts on 5-LO with distinct affinities [283]. Finally, AKBA was less active in the presence of PC and when crude 5-LO in *E. coli* supernatants was analyzed, which is not readily understood but at least indicates an interference with the regulatory PC-binding C2-like domain or other putative regulatory sites [189]. When BAs were applied to cellular assays, using Ca^{2+}-ionophore stimulated human PMNL IC_{50} values

(3.2 and 8.8 µM for AKBA and KBA, respectively) were slightly higher as observed in previous studies (IC_{50} = 1.5 and 2.8 µM) using PMNL from rats [53, 54]. Species-related differences in the susceptibility of 5-LO towards BAs are likely responsible, supported by the finding that AKBA was even less potent in PMNL from guinea pigs [30]. Also by using the human cell lines MM6 and HL-60 higher IC_{50} values for AKBA (12 and 15 µM, respectively, [57]) were determined. Parameters that influence the bioactivity of test compounds *in vivo* (i.e. albumin-binding) or stimuli like LPS plus fMLP mimicking pathophysiological conditions in the body [284], were applied to estimate the efficacy of BAs as 5-LO inhibitors *in vivo.* In assays using human activated PMNL in the presence of albumin, BAs and frankincense extracts were hardly effective or completely failed to inhibit 5-LO activity. This property might account also for the failure of BAs (i.e. AKBA and KBA) to inhibit 5-LO activity in whole blood. Albumin is abundant in plasma (30-40 mg/ml), and lipophilic acids (e.g. acidic drugs such as NSAIDs, warfarin, tolbutamide) are known to be substantially bound to serum albumin [282]. Such (unspecific) protein-binding often impairs the pharmacological activity of the respective drug in whole blood assay as already shown for some LT synthesis inhibitors (e.g. MK-886) [186]. Also BAs are lipophilic acids explaining the tight binding of AKBA to albumin (> 95%) and the loss of potency in the presence of albumin. Conclusively, albumin-binding might be mainly responsible for the failure of AKBA and KBA to inhibit 5-LO product synthesis in whole blood, congruent with the lack of suppression for COX-1 product formation in this assay. Moreover, upon single administration of 800 mg frankincense extract to human volunteers the LTB_4 plasma levels were not reduced [285]. Similarly, Wildfeuer et al. failed to demonstrate suppression of LTB_4 and LTC_4 *ex-vivo* in A23187-challenged PMNL from guinea pigs treated (i.p.) with 20 mg/kg acetyl-BAs [30] which might be related also to the poor bioavailability of KBA and AKBA [16].

It is unequivocal that BAs are direct inhibitors of 5-LO with a mechanistically unique mode of action, influenced by 5-LO-modulating co-factors and by experimental assay settings. 5-LO products play pivotal roles in certain inflammatory diseases but the benefits of frankincense preparations are unlikely based on the interference of 11-keto-BAs with 5-LO. The role of LTs in asthma and allergic rhinitis is well established and anti-LTs are successfully applied in therapy. However, accumulating evidence excludes a pivotal role of LT in arthritis and inflammatory bowel diseases [198, 286]. As high effectiveness of frankincense has been reported for the treatment of Crohn`s disease, colitis and osteoarthritis [5], it is rather unlikely that the interference with LT synthesis represents a responsible mode of action.

In particular, the fairly low plasma levels of 11-keto-BAs (≤ 0.3 µM) obtained after oral administration of frankincense accompanied by the lack of reduction of LTB_4 plasma levels, and the failure of 11-keto BAs to inhibit 5-LO product formation in whole blood raises serious doubts about the pharmacological relevance of 5-LO inhibition by BAs as underlying molecular mechanism of the anti-inflammatory properties of frankincense.

5.1.3 Interference of BAs with the microsomal Prostaglandin E_2 synthase-1

PGE_2 is a key player in inflammation and pain, and the inducible, COX-2-coupled mPGES-1 is regarded as a potential target for the development of anti-inflammatory therapeutics [172]. The identification of mPGES-1 as a molecular target of BAs in this study provides evidence for a functional interaction of β-BA with mPGES-1 *in vivo* which may contribute to the potent anti-inflammatory effectiveness of administered frankincense preparations.

First of all, mPGES-1 selectively bound to immobilized BAs in a pull-down assay, and SPR spectroscopy data confirm such direct interaction. The pull-down approach using immobilized BAs selectively precipitate mPGES-1 from A549 lysates as well as captured purified mPGES-1 from an incubation mixture containing *E. coli* proteins. This confirms the suitability of this experimental strategy for target identification of BAs as previously demonstrated. SPR-based biosensors such as BIAcore® are widely used to determine biomolecular interactions in real time without labeling requirements [287], including direct binding of small molecules (e.g. BAs) to macromolecular targets (e.g. mPGES-1) [252]. Unfortunately, inconsistent binding patterns were obtained by using naturally occurring BAs as analyte, presumably due to their high lipophilicity and thus, concentration-dependent aggregation or super-stoichiometric binding behavior [288]. Even extensive changes of assay conditions failed to improve the quality. Hence, BIAcore® experiments were conducted using the more hydrophilic synthetic BA analogue ox-KBA. The SPR-based ligand-analyte studies revealed K_D values of 5.2 to 13 µM for ox-KBA, which fit well with the IC_{50} value (5 µM) of ox-KBA in the mPGES-1 cell-free assay, suggesting a direct relation between binding (measured by SPR) and interference with the catalytic activity of mPGES-1. It was demonstrated that natural occurring BAs (i.e. AKBA, KBA, and β-BA) at low micromolar concentrations inhibit mPGES-1-mediated PGE_2 formation in cell-free assays. BAs concentration-dependently block PGE_2 biosynthesis in intact cells as well but were somewhat less potent under these conditions. It should be noted that BAs (up to 100 µM) failed to reduce the formation of the COX-2-derived product 6-keto $PGF_{1\alpha}$ in a cellular assay and hardly inhibited the activity of isolated COX-2. Conclusively, suppression of cellular PGE_2 biosynthesis is the result of the interference with mPGES-1, rather then with COX-2. In particular β-BA, the

major BA present in frankincense reaching the highest plasma levels (up to 10 µM) among the BAs in frankincense-treated humans [7], suppressed PGE_2 formation in human whole blood at physiological relevant concentrations. Importantly, generation of the COX-2 derived metabolite 6-keto-$PGF_{1\alpha}$ was not affected under the same conditions and detrimental effects on COX-2 or mPGES-1 expression patterns were also excluded. In this respect, the failure of 11-keto-BAs might be related to strong albumin-binding as observed before. Notably, complete suppression of PGE_2 formation could not be achieved by β-BA up to 100 µM. Similar results were obtained for the mPGES-1 inhibitor MK-886. In contrast, the selective COX-2 blocker celecoxib was more efficient but also basal PGE_2 levels remain detectable which is probably due to the contribution of COX-1 and other PGES [289].

Moreover, at a dose of 1 mg/kg (i.p.), β-BA reduced the inflammatory reaction in two *in vivo* models of inflammation, carrageenan-induced mouse paw edema and rat pleurisy being equipotent to 5 mg/kg indomethacin. During carrageenan-induced edema formation, PGE_2 levels are significantly elevated [273, 290], and COX-inhibitors prevented the inflammatory response [291]. Results from previous studies using the carrageenan-induced paw edema (rat or mouse) and i.p. application of undefined mixtures of BAs concur with data obtained in this study, although much higher doses (e.g. 125 mg/kg) were used in the studies performed by Singh et al. [4, 292]. Also in the early phase of carrageenan-induced pleurisy PGE_2 plays a central role [293, 294]. Intriguingly, in the pleurisy model, exudates from β-BA-treated animals showed significant lower PGE_2 levels whereas the formation of 6-keto-$PGF_{1\alpha}$ and LTB_4 was not significantly altered. Moreover, eicosanoid formation in exudates from AKBA-treated animals remained unaffected reflecting the inability of AKBA to reduce PGE_2 in human whole blood. Because suppression of PGE_2 formation is the major anti-inflammatory mechanism of NSAIDs (like indomethacin), lowering PGE_2 by inhibition of mPGES-1 may contribute to the anti-inflammatory properties of β-BA. As observed in whole blood experiments, β-BA was less potent compared to indomethacin to reduce PGE_2 levels, but still efficiently suppressed exudate formation and infiltration of inflammatory cells, supporting the idea that other anti-inflammatory features of β-BA *in vivo* such as inhibition of cat G [227] may still cooperate.

In contrast to others, this study proposes β-BA as the most relevant anti-inflammatory BA that may act via inhibition of PGE_2 formation. Clinical studies with pilot character indicate therapeutic efficacy of frankincense mainly in OA and RA [5, 41]. As mentioned above, extensive studies using 5-LO inhibitors or FLAP-deficient mice exclude a role of LTs in OA or RA [198, 286]. On the other hand, in the pathophysiology of both OA and RA, PGE_2 is a key mediator, accounting for typical symptoms of these inflammatory diseases [295], which also rationalizes the frequent therapeutic use of NSAIDs. mPGES-1 is a crucial enzyme in massive PGE_2 formation from COX-2-derived PGH_2 and both COX-2 and mPGES-1 are co-ordinately

unregulated at sites of inflammation [296]. In patients suffering from RA or OA, a pivotal role for mPGES-1 was demonstrated [148, 297, 298] and data from animal arthritis models support the functionality of mPGES-1 in inflammatory joint diseases [165, 272, 273]. The pharmacological intervention with mPGES-1 in the therapy of PGE_2-mediated disorders is proposed to be a potential alternative for NSAIDs and coxibs [172, 299] supported by results from recent studies on mPGES-1 KO mice where an advantage of the gastric and cardiovascular safety versus mice lacking COX-1 or COX-2 (or mice treated with unselective NSAIDs or coxibs, respectively) was evident [166, 300]. In fact, the selective mPGES-1 inhibitor MF63 (IC_{50} = 1 nM) [162] relieved fever and inflammatory pain in animal models but did not cause NSAID-like gastrointestinal toxic effects [301]. Interestingly, BAs showed gastric ulcer protective effects in different experimental models [31], and a 90-day double blind, randomized, placebo-controlled study supports evidence for the safety of a *B. serrata* extract in OA patients accompanied by significant improvement of the disease [41].

Hence, one may speculate that the beneficial effects of frankincense preparations observed in clinical studies and animal models of OA and RA are related to the intervention of β-BA with PGE_2 synthesis due to direct inhibition of mPGES-1. Such speculations are favored by the close correlation between steady-state plasma levels of β-BA (6.35 to 10.1 µM) in humans obtained after oral administration of frankincense preparations and the effective concentrations of β-BA (≥ 3 µM) to suppress PGE_2 synthesis in human whole blood *in vitro* accompanied by its substantial anti-inflammatory potential *in vivo*.

5.2 Boswellic acids differentially modulate platelet physiology

The functional properties and the potencies of the BAs depend on their structure, in particular on the absence or presence of the 11-keto group, and indeed, AKBA is frequently the most effective analogue [8-10, 56], although in some instances the 11-methylene-BAs possess superior efficacy, depending on the target/effect and cell type [8, 64, 77, 80]. Previously, it was shown that 11-methylene-BAs augmented $[Ca^{2+}]_i$ in human platelets depending on IP3/PLC and Src kinase signaling pathways and initial analysis regarding functional platelet responses (platelet aggregation and thrombin generation) were undertaken, supporting rather agonistic properties of 11-methylene-BAs [64]. In this respect, 11-keto-BAs were hardly effective. Because of the cardiovascular and inflammatory risk evoked by an alteration in the character and function of platelets [302], the present study addressed the effects of 11-keto- and 11-methylene-BAs as well as two different *B. serrata* extracts on agonist-induced platelet physiology.

First of all, experiments using the typical platelet agonists collagen, U-46619 and thrombin [205] revealed that BAs, depending on their structure (11-keto group and/or 3-*O*-acetyl group), differentially modulate $[Ca^{2+}]_i$ which is further influenced by the nature of agonist. AKBA suppressed Ca^{2+} mobilization induced by collagen or U-46619 with almost equal potencies (IC_{50} = 6 and 8 µM), but not when thrombin was used as a stimulus. Since both agonists use rather distinct signaling pathways to elicit Ca^{2+} mobilization (see below) it is not immediately possible to relate the effects of AKBA towards one common target. Besides AKBA, also β-BA reduced U-46619- and collagen-induced Ca^{2+} mobilization, though less efficient (IC_{50} = 18 and 23 µM, respectively). This result was actually quite surprising, since 11-methylene-BAs themselves cause a transient increase of $[Ca^{2+}]_i$ in platelets (this study and [64]). Such a transient increase of $[Ca^{2+}]_i$ could probably desensitize platelets by unspecific actions (e.g. depletion of intracellular Ca^{2+} stores) and thus, be the reason for the subsequent failure of Ca^{2+} release evoked by a second agonist. In fact, elicitation of Ca^{2+} mobilization by U-46619 and subsequent stimulation of platelets with collagen or thrombin partially prevented the effects of these agonists but were slightly less pronounced as in the case of BAs. One would expect that KBA, containing an 11-keto moiety or Aβ-BA, possessing a 3-*O*-acetyl-group should be more potent than β-BA. However, KBA caused no suppression at all but rather enhanced the signals induced by all agonists and Aβ-BA was less effective than AKBA or β-BA. Thus, it is conceivable that AKBA and β-BA act at different targets which both leading to suppression of Ca^{2+} mobilization. Together, BA-modulated Ca^{2+} homeostasis in platelets seems to be rather complex and so far the puzzling effects could not be related to a discrete molecular basis.

Since elevation of $[Ca^{2+}]_i$ is a determinant for aggregation of washed platelets [204, 205] the prominent antagonistic properties of AKBA were subjected to their impact on agonist-evoked

platelet aggregation. Effective concentrations of AKBA (≤ 1 µM) significantly antagonized collagen-induced platelet aggregation. AKBA was less potent to suppress platelet aggregation induced by U-46619, and when thrombin was used to evoke these responses, AKBA failed at all. KBA (30 µM) only marginally affected platelet aggregation elicited by collagen. Apparently, the 3-*O*-acetly group and the 11-oxo moiety present in AKBA render this BA a potent inhibitor of collagen-evoked platelet aggregation implying that defined structure-activity relationships exist excluding unspecific effects of AKBA in this case. Along these lines, the effects of two separate *B. serrata* extracts, considered to contain distinct amounts of 11-keto- and 11-methylene-BAs on platelet activation were determined. The relative composition and content of 11-keto- and 11-methylene-BAs in these extracts determine their overall beneficial (platelet suppressing) or detrimental (platelet activating) effectiveness. Lower concentrations of AKBA were sufficient to suppress collagen-evoked aggregation ($IC_{50} \leq 1$ µM) as compared to those required to inhibit Ca^{2+} mobilization ($IC_{50} = 6$ µM). Moreover, AKBA was about equipotent for suppression of Ca^{2+} release in response to U-46619 as compared to collagen, but U-46619-evoked aggregation was hardly affected by AKBA ($IC_{50} = 25$ µM). Therefore, the inhibitory effects of ABKA on agonist-induced Ca^{2+} mobilization and on aggregation also might be separated. It is possible that already a minimal impairment of $[Ca^{2+}]_i$ as in the case of collagen is sufficient to substantially affect aggregation. Presumably, AKBA targets a component(s) pivotal in the signal transduction of collagen (and U-46619), which apparently is dispensable for thrombin-induced pathways leading to Ca^{2+} mobilization and platelet aggregation. It should be noted that the signal transduction pathways of collagen and U-46619 are quite distinct and, at least in part, utilize different types of signaling molecules. U-46619 binds GPCRs and signals via $G_{i/q}$ proteins and PLCβ to rapidly release of Ca^{2+} from IP_3-sensitive stores and platelet aggregation depends on G_i stimulation by ADP an other released granule contents [218]. Collagen mainly binds glycoprotein VI and slowly allows Ca^{2+} entry via Src family kinase/PLCγ2-mediated pathway [223] and evokes full platelet activation. Preliminary analysis of the phosphorylation status of collagen-activated platelets showed that AKBA even at higher concentrations (30 µM) slightly suppressed collagen-induced phosphorylation of Src familiy kinase and PLCγ2 and was less active compared to the selective Src family kinase inhibitor PP2. Note that collagen-induced platelet activation through GPVI and subsequent activation of PLCγ2 is considered to depend also on bruton`s tyrosine kinase-mediated phosphorylation [303]. This might be one explanation for the rather moderate effect on collagen-induced PLCγ2-phosphorylation by AKBA in these experiments.

In addition, the previously reported dependence of Ca^{2+} mobilization of 11-methylene-BAs on Src-family kinase-/PLC-mediated pathways [64] was extended to platelet aggregation. Both, β-BA and Aβ-BA significantly ($EC_{50} \leq 10$ µM) evoked platelet aggregation which was sensitive to

unselective PLC blockade (U-73121) as well as to selective Src family kinase inhibitors SU6656 and PP2. In parallel to platelet activation an increase of tyrosine phosphorylation is apparent [278] and such effects were observed for β-BA, being equipotent to collagen. Preincubation with PP2 partially underlined the role of Src-family kinase for β-BA signaling but additional experiments remains to identify the accurate molecular basis.

Because thrombin is the major trigger for stable plug formation and functions as a potent platelet activator it was challenging to examine the impact of platelet-modulating agents on thrombin formation [304]. 11-methylene-BAs themselves strongly and concentration-dependently induced thrombin generation which concurs with previous findings [64]. Moreover, they potentiate the effect of collagen- and U-46619-induced thrombin generation, accounting for a rather pro-thrombotic potential [305]. In contrast, thrombin generation itself or agonist-induced thrombin formation was not essentially altered by 11-keto-BAs. Despite the prominent role of $[Ca^{2+}]_i$ as an important signaling step modulating various platelet responses (aggregation, thrombin formation, granule secretion), also Ca^{2+}-independent mechanisms in platelets exist. Thus, PKC pathways [306, 307] or PI3K transduction have been demonstrated to participate in platelet activation while $[Ca^{2+}]_i$ was absence [308]. It is feasible that such mechanisms may account for the puzzling effects in BA platelet signaling.

In summary, depending on their structurally variety BAs differentially modulate platelet physiology. While 11-metylene BAs (in particular β-BA) mainly mediated platelet activation reflected by pronounced Ca^{2+} mobilization, platelet aggregation and thrombin generation, 11-keto-BAs showed rather alleviative effects. In this regard, the efficient and selective inhibition on collagen-induced platelet aggregation by AKBA is of particular interest. At least some of the effects observed, were evoked by concentrations of BAs which could be physiologically relevant after oral intake of substantial amounts of adequate frankincense preparations. In this respect, the versatile properties of isolated BAs could be transferred to two distinct *B. serrata* extracts differing in their total amount of 11-methylene- and 11-keto-BAs. Conclusively, the overall pharmacological actions on platelets evoked by isolated BAs or frankincense preparations should be taken into account when administering them to patients.

6 SUMMARY

Extracts of *Boswellia species* (*B. spec.*) gum resin have been traditionally used for centuries in the folk medicine of India and China to treat inflammatory disorders, and also immunmodulatory and anti-cancer properties were reported. Since there is a growing demand in the western society for natural- and especially plant-derived remedies, the scientific community initially focused on frankincense in the early seventies and expanded their studies in the late eighties until today. Promising beneficial results were obtained in pilot clinical trials, demonstrating efficacy of diverse frankincense preparations in asthma, osteoarthritis and inflammatory bowel diseases. Today, only one approved medicine derived from *B. serrata* gum resin is available on the market (H15® Gufic), and its distribution is restricted to India and a part of Switzerland. Based on the assumption that boswellic acids (BAs) are the main pharmacological principles of frankincense extracts, numerous studies were carried out to elucidate molecular and cellular mechanisms of BAs responsible for the anti-inflammatory potential of frankincense applied in humans. Most studies focused on AKBA or KBA as pharmacological principles and several targets including 5-lipoxygenase (5-LO), platelet-type 12-LO, human leukocyte elastase, IκB kinases, cytochrome P450 enzymes and topoisomerases have been proposed, but their interaction *in vivo* has been largely neglected. Thus, the pharmacological relevance of the interference of BAs with these targets is still unclear.

Following this line, the present work describes the identification of novel molecular targets of BAs and evaluates the interference with important key players involved in inflammatory processes. The protein fishing technique, using a BA affinity matrix, identified cyclooxygenase (COX)-1 as a molecular target of BAs. Subsequent functional analysis revealed AKBA as a potent inhibitor of COX-1 product formation in human platelets (IC_{50} 6 - 17 µM) as well as of the isolated enzyme. In contrast, 11-methylene-BAs (i.e. β-BA and Aβ-BA) and related pentacyclic triterpenes such as α-amyrin were virtually inactive. The mode of inhibition by AKBA was reversible and most likely competitive. Further characterizations favored direct binding of AKBA to the active side of COX-1 and excluded strong interference with COX-2. Interestingly, switching from cellular assays to more physiological conditions (i.e. whole blood experiments) strongly impaired COX-1 inhibition by AKBA, indicating a limited pharmacological relevance of this interaction.

The knowledge about the proposed interaction of 5-LO with BAs was incomplete and therefore suppression of leukotriene (LT) biosynthesis as a molecular basis for the anti-inflammatory potential of BA-containing preparations was re-evaluated. So far, studies analyzed suppression of LTs only in cell-free assays or in neutrophils from rats (but not human cells) and these studies partially ignored the complex regulation of 5-LO or the inclusion of important physiological parameters (i.e. albumin binding or whole blood assays). Among the natural occurring BAs tested, AKBA and KBA were most potent to suppress 5-LO product formation in human neutrophils as well as the activity of isolated 5-LO with IC_{50} values of 2.8 - 8.8 µM. Again, 11-methylene-BAs were hardly effective (IC_{50} > 30 µM) but for the first time an inhibition of LT formation for α-BA (IC_{50} = 15.3 -23.1 µM) was demonstrated. Factors influencing 5-LO activity (i.e., Ca^{2+}, phospholipids, substrate concentration) were shown to modulate the potency of 11-keto-BAs to inhibit 5-LO. High substrate concentrations improved the efficacy of AKBA and KBA towards 5-LO, while the presence of Ca^{2+} seems to be negligible. An impaired potency of 11-keto-BAs was observed when phospholipids (i.e. phosphatidylcholine) were present or crude 5-LO in supernatants of *E. coli* was analyzed. The most interesting observation in this study was the failure of 11-keto-BAs to suppress 5-LO product formation in test systems that reflect physiological conditions *in vivo* such as inclusion of albumin in neutrophil incubations or in human whole blood assays, presumably caused by extensive binding of AKBA to albumin (> 95%). Moreover, oral administration of frankincense extracts to human healthy volunteers failed to reduce LTB_4 plasma levels. Together, this data show that BAs (in particular 11-keto-BAs) are direct 5-LO inhibitors that efficiently suppress 5-LO product synthesis in common *in vitro* test models but the pharmacological relevance of such interference *in vivo* seems questionable.

Turning the focus again to prostanoids, it was demonstrated that BAs concentration-dependently blocked prostaglandin (PG)E_2 synthesis *in vitro* and *in vivo*. PGE_2 is a key player in the pathophysiology of many inflammatory disorders (e.g., rheumatoid arthritis, osteoarthritis, pain, fever) and the beneficial effects of NSAIDs are essentially due to suppression of PGE_2 formation. First of all, the suitable application of the fishing construct indicated an interaction of BAs with mPGES-1 derived from crude A549 cell lysates. Direct interference was confirmed by additional fishing experiments, using isolated mPGES-1 in surface plasmon resonance (SPR) analysis. The SPR-based ligand-analyte studies with the synthetic derivative 3-*O*-oxaloyl-KBA revealed a K_D in the low micromolar range which fairly well correlates with the IC_{50} (5 µM) in the mPGES-1 cell-free assay. Potent concentration-dependent suppression of conversion of PGH_2 to PGE_2 in the cell-free assay was demonstrated for AKBA (IC_{50} = 3 µM), β-BA (IC_{50} = 5 µM) and KBA (IC_{50} = 10 µM). Aβ-BA was less active and α-amyrin completely failed in this respect. BAs also reduced formation of PGE_2 in cellular-based assays, although higher

concentration were needed as in cell-free experiments (IC_{50} = 20 µM). In human whole blood, β-BA remarkably prevented lipopolysaccharide-induced PGE_2 formation at 10 µM by almost 50%, whereas all other BAs tested were virtually inactive. Notably, the required concentration for β-BA to provoke this effect is in the range of achievable steady-state plasma levels in humans (6.4 to 10.1 µM) after oral administration of medical frankincense preparations, thus implying a physiological relevance of these findings. A detrimental effect on the formation of the COX-2-derived metabolite 6-keto-$PGF_{1\alpha}$ in human whole blood experiments by β-BA was excluded, underlying the selectivity of the interference with mPGES-1. Finally, intraperitoneal (i.p.) administration of low-dose β-BA (1 mg/kg, compared to 5 mg/kg indomethacin) reduced the development of carrageenan-induced paw edema in mice as well as pleurisy in rats, accompanied by substantially reduced PGE_2 levels but without significant effects on 6-keto-$PGF_{1\alpha}$ and LTB_4 formation. In this regard, no significant effects by AKBA (i.p. 1 mg/kg) were observed. Conclusively, the selective interference of β-BA, as a major ingredient of frankincense, with mPGES-1 is very likely to contribute to the anti-inflammatory effectiveness and provides a solid biochemical basis for the beneficial effects of frankincense in the treatment of inflammation.

Since previous studies indicated that 11-methylene-BAs stimulate platelets, the effect on platelet physiology by all β-configurated BAs from frankincense was investigated in more detail. BAs lacking the 11-keto moiety (i.e. β-BA and Aβ-BA) were found to be platelet activators in a concentration-dependent manner, displayed by robust Ca^{2+} mobilization, platelet aggregation and thrombin generation. The effective concentrations were determined at 3-10 µM. Here, it is shown, that β-BA induces platelet aggregation which partially involves Src kinase familiy as putative signaling transducers towards phospholipase (PL)C and potentiates agonist-evoked thrombin formation. Surprisingly, β-BA was also able to impair Ca^{2+} mobilization when U-46619 was used as agonist and to a minor extent when platelets were challenged with collagen. In contrast, 11-keto analogues (i.e. AKBA and KBA) showed rather “silencing” effects on platelet physiology. They are poor inducers of Ca^{2+} mobilization and essentially failed to evoke platelet aggregation and thrombin formation. In fact, when collagen was used as a stimulus for platelet activation pronounced antagonistic properties of AKBA were demonstrated. Remarkably, AKBA exerted a prominent detrimental effect on collagen-induced platelet aggregation ($IC_{50} \leq 1$ µM). Attempts to elucidate putative interaction partners or signaling pathways point to the Src kinase family/PLCγ2 route. In addition, the effects of two *B. serrata* extracts containing different amounts of BAs on platelet functions were investigated.

Together, one may conclude that 11-methylene-BAs stimulate platelet biochemistry and induce select platelet functions whereas 11-keto-BAs prevent activation of human platelets. In view of

the low effective BA concentrations necessary to modulate platelet physiology, these findings might be of pharmacological relevance for patients applying frankincense preparations.

In summary, the data presented in this work provide substantial additional information about BAs and their effects on molecular and cellular aspects of inflammatory processes. Therefore, the object of research was focused on enzymes within the arachidonic acid cascade and platelet physiology. Detailed investigations yielded new insights on the influence of BAs on intracellular signaling and functional characteristics of platelets. Application of the BA-fishing construct discovered two novel molecular targets of BAs, namely COX-1 and mPGES-1. Moreover, extensive functional analysis considering important physiological parameters critically examined the interference of BAs with COX enzymes, 5-LO and mPGES-1 in view of their *in vivo* relevance and the findings rather exclude suppression of COX and 5-LO product formation as responsible anti-inflammatory mechanisms. In fact, the interference of β-BA with mPGES-1, lowering pathophysiological PGE_2 levels *in vitro* and *in vivo* represents a more reasonable molecular basis contributing to the anti-inflammatory potential of BA-containing frankincense preparations in humans.

7 ZUSAMMENFASSUNG

Die traditionelle Phytomedizin in Indien und China verwendet bereits seit Jahrhunderten Extrakte verschiedener Weihrauchspezies (*B. spec.*) zur Behandlung entzündlicher Erkrankungen. Darüber hinaus finden sich Berichte, die eine immunmodulierende und anticancerogene Wirkung von *B. spec.* beschreiben. Nicht zuletzt wegen der stetig wachsenden Nachfrage und Akzeptanz hinsichtlich pflanzlicher Arzneimittel beschäftigen sich Wissenschaftler bereits seit über 30 Jahren mit Weihrauch. Neben den empirischen Daten lieferten initiale klinische Studien aussichtsreiche Ergebnisse, die eine Wirksamkeit verschiedener Weihrauchextrakte zur Behandlung von Asthma, Osteoarthritis und entzündlichen Darmerkrankungen indizieren. Bis heute ist jedoch nur ein aus *B. serrata* gewonnenes Weihrauchpräparat (H15® Gufic) als Arzneimittel erhältlich, dessen Zulassung sich allerdings auf Indien und einen Kanton in der Schweiz beschränkt.

Auf der Annahme basierend, dass Boswelliasäuren (BAs) die pharmakologisch relevanten Wirkstoffe von Weihrauchextrakten darstellen, wurde eine Vielzahl pharmakologischer Studien zur Klärung molekularer bzw. zellulärer Wirkmechanismen von BAs durchgeführt. Mit Hilfe dieser Daten sollte eine rationale Basis für die heilsamen Effekte von Weihrauchextrakten im Menschen geschaffen werden, die eine effektive und sichere Therapie mit Weihrauchpräparaten oder einzelnen definierten BAs in Aussicht stellt. Die Mehrzahl der Untersuchungen fokussierte sich nahezu ausschließlich auf die Effekte von AKBA oder KBA und es wurden molekulare Wechselwirkungen mit 5-Lipoxygenase (5-LO), Plättchen-Typ 12-LO, humaner Leukozyten Elastase, IκB Kinasen, Topoisomerasen und Cytochrom P450 Enzymen postuliert. Eine Beurteilung dieser Interaktionen unter physiologisch relevanten Versuchsbedingungen ist bisher stark vernachlässigt worden und im Hinblick auf die z. T. sehr hohen benötigten Hemmkonzentrationen *in vitro* und den relativ niedrigen Plasmaspiegel von BAs erscheint eine pharmakologische Relevanz *in vivo* fraglich.

Vor diesem Hintergrund beschreibt die vorliegende Arbeit die Identifizierung neuer molekularer Targets von BAs und untersucht die Beeinflussung zentraler Komponenten innerhalb entzündlicher Prozesse. Durch den Einsatz eines Pulldown-Verfahrens, welches sich eine BA-Affinitätsmatrix zu Nutze macht, gelang die Identifizierung der Cyclooxygenase (COX)-1 als molekularem Bindungspartner von BAs. Die sich anschließende funktionelle Charakterisierung dieser Interaktion bestätigt AKBA als einen potenten Inhibitor der zellulären COX-1 Produktbildung (IC_{50} 6-17 µM) sowie der katalytischen Aktivität des isolierten Enzyms. 11-Methylen-BAs und strukturverwandte pentazyklische Triterpene wie z.B. α-Amyrin hingegen weisen keine oder eine nur äußerst geringe Aktivität auf (IC_{50} >> 50 µM). Mechanistische

Studien zeigen für AKBA eine reversible und von der Substratkonzentration abhängige Hemmung, die sich mit dem Profil des bekannten COX-1–Hemmers Ibuprofen vergleichen lässt. Zusätzliche Untersuchungen belegen eine direkte Bindung von AKBA im aktiven Zentrum der COX-1 und schließen eine maßgebliche Interferenz mit der COX-2 aus (IC_{50} >> 50 µM). Eine Variation der experimentellen Bedingungen von zellulären zu mehr physiologischen Systemen (wie .z.B. Vollblutassays) hat eine drastische Verminderung der COX-1 Inhibition durch AKBA zur Folge, was die pharmakologische Relevanz dieser molekularen Wechselwirkung limitiert.

Die postulierte Interaktion der 5-LO mit BAs ist teilweise unvollständig untersucht worden. Deshalb wurde in dieser Arbeit die Hemmung der LT-Biosynthese als molekularer Wirkmechanismus BA-haltiger Präparationen re-evaluiert. Die bislang durchgeführten Studien analysierten die Suppression der LT-Bildung nur in zellfreien Systemen oder in isolierten Neutrophilen von Ratten (kaum jedoch in menschlichen Zellen). Weiterhin wurde die komplexe Regulation der 5-LO sowie die Berücksichtigung physiologischer Versuchsparameter (Proteinbindung oder Vollbluttestsysteme) in diesen Studien stark vernachlässigt. In der aktuellen Untersuchung wurde gezeigt, dass von den natürlich vorkommenden β-konfigurierten BAs vor allem AKBA und KBA (11-Keto-BAs) die 5-LO Produktbildung in menschlichen Neutrophilen sowie die Aktivität humaner rekombinanter 5-LO mit IC_{50} Werten von 2,8 - 8,8 µM hemmen. BAs ohne 11-Keto-Funktion zeigen deutlich schwächere Wirksamkeit (IC_{50} > 30 µM). Darüber hinaus konnte zum ersten Mal eine Hemmung der zellulären und zellfreien 5-LO Aktivität für eine α-konfigurierte BA, α-BA (IC_{50} = 15,3 - 23,1 µM) gezeigt werden. Des Weiteren wurde für Faktoren, welche die 5-LO Aktivität modulieren (Ca^{2+}, Phospholipide, Substratkonzentrationen) eine Beeinflussung auf die 11-Keto-BA-vermittelte 5-LO Inhibition demonstriert. Hohe Substratkonzentrationen verbessern die Wirkstärke von AKBA und KBA, wobei die Anwesenheit von Ca^{2+} nur einen marginalen Einfluss ausübt. Eine deutlich verminderte Potenz für AKBA und KBA wurde in der Gegenwart von Phospholipiden (Phosphatidylcholin) und bei Aktivitätsbestimmungen in *E. coli* Überständen hinsichtlich der 5-LO Produktbildung festgestellt. Die wohl auffälligste Beobachtung in dieser Studie war, dass 11-Keto-BAs nicht in der Lage sind, die 5-LO Produktbildung unter physiologisch relevanten Testbedingungen (wie z.B. in der Anwesenheit von Albumin im zellulären System oder in Vollblutassays) zu vermindern. Eine hinreichende Erklärung für dieses Phänomen wurde in der starken Bindung von AKBA an Albumin (> 95%) gefunden. Außerdem konnte gezeigt werden, dass die orale Applikation eines definierten Weihrauchextraktes (800 mg/Tag) bei gesunden Probanden nicht zu einer Reduktion von LTB_4-Plasmaspiegeln führt.

Zusammenfassend liefern diese Ergebnisse klare Hinweise darauf, dass es sich bei BAs (im Besonderen 11-Keto-BAs) um direkte Inhibitoren der 5-LO handelt, die in standardisierten *in*

vitro Testmodellen eine effiziente Hemmung der 5-LO Produktbildung hervorrufen. Allerdings, ist eine pharmakologische Relevanz dieser Interaktion *in vivo* sehr fragwürdig.

Interessanterweise konnte eine BA-vermittelte konzentrationsabhängige Hemmung der Prostaglandin (PG)E_2 Synthese *in vitro* und *in vivo* ermittelt werden. PGE_2 nimmt eine Schlüsselrolle in der Pathophysiologie vieler entzündlicher Zustände (wie z.B. rheumatoider Arthritis, Osteoarthritis, Schmerz und Fieber) ein und die nutzbringenden Effekte nichtsteroidaler Antiphlogistika in der Therapie solcher Krankheitszustände kommt im Wesentlichen durch eine Reduktion der PGE_2 Bildung zustande. Zunächst indizierte die Anwendung der Pulldown-Methode in A549 Zelllysaten die mikrosomale PGE_2 Synthase (mPGES)-1 als molekularen Bindungspartner von BAs, und die Bestätigung einer direkten Interaktion zwischen BAs und isolierter mPGES-1 gelang anschließend mittels Oberflächen-Plasmon-Resonanz Spektroskopie (SPR). Die SPR-Bindungsstudien mit dem synthetischen Derivat 3-*O*-oxaloyl-KBA ergaben K_D Werte im unteren mikromolaren Bereich (5-13 µM) und korrelieren mit dem IC_{50} Wert (5 µM) der in einem zellfreien mPGES-1 Aktivitätsassay ermittelt wurde. Eine potente konzentrationsabhängige Suppression der katalytischen mPGES-1 Aktivität in einem zellfreien Testsystem wurde für AKBA (IC_{50} = 3 µM), β-BA (IC_{50} = 5 µM) und KBA (IC_{50} = 10 µM) nachgewiesen, wohingegen Aβ-BA (IC_{50} > 30 µM) deutlich schwächer aktiv und das strukturverwandte pentazyklische Triterpen α-Amyrin (IC_{50} > 100 µM) praktisch unwirksam war. Die zelluläre PGE_2 Bildung wird ebenfalls von BAs (AKBA, β-BA und KBA) reduziert (IC_{50} = 20 µM), obwohl höhere Konzentrationen zur Inhibition benötigt werden als im zellfreien System. In Vollblutexperimenten zeigt β-BA (10 µM) ein erhebliches inhibitorisches Potential und supprimiert die Lipopolysaccharid-vermittelte PGE_2 Bildung um 50%. Alle anderen getesteten BAs waren praktisch unwirksam. Beachtenswert ist, dass die zur PGE_2 Hemmung benötigte Konzentration von β-BA im Rahmen erreichbarer steady-state Plasmaspiegel *in vivo* (6,4 – 10 µM) liegt und der Befund der PGE_2 Hemmung physiologische Relevanz aufweist. Wie bereits in zellfreien und zellulären Experimenten gezeigt, konnte auch im Vollblut ein Einfluss auf die COX-2-vermittelte 6-Keto-$PGF_{1\alpha}$-Synthese durch β-BA ausgeschlossen und dadurch die Selektivität der Wechselwirkung mit mPGES-1 unterstrichen werden. Schlussendlich reduziert die intraperitoneale (i.p.) Applikation von β-BA (1 mg/kg) die Entwicklung eines Carrageninduzierten Pfötchenödems in der Maus sowie eine Brustfellentzündung in der Ratte. Dabei wurden signifikant verminderte PGE_2 Level im Brustfell-Exsudat der Ratte festgestellt, während eine wesentliche Veränderung der gebildeten 6-keto $PGF_{1\alpha}$- sowie LTB_4-Mengen ausblieb. AKBA (i.p., 1mg/kg) war in diesem Zusammenhang nicht aktiv.

Zusammenfassend implizieren diese Daten, dass die selektive Interaktion von β-BA mit der mPGES-1 eine signifikante entzündungshemmende Potenz aufweist und somit einen

molekularen und pharmakologisch relevanten Wirkmechanismus darstellt, der unter anderem einen wesentlichen Beitrag zur Klärung der Mechanismen der anti-inflammatorischen Effizienz von Weihrauchextrakten liefern kann.

Da initiale Studien in Thrombozyten auf stimulierende Effekte von 11-Methylen-BAs hinwiesen, wurden in der vorliegenden Arbeit die Einflüsse der in Weihrauch vorkommender β-konfigurierten BAs auf physiologische Prozesse humaner Thrombozyten im Detail analysiert. In diesen Experimenten konnte gezeigt werden, dass BAs ohne 11-Keto Funktion (β-BA und Aβ-BA) grundsätzlich als Aktivatoren einzelner zellulärer Funktionen aufzufassen sind und konzentrationsabhängig eine Ca^{2+}-Mobilisierung, Thrombozytenaggregation und Thrombinbildung induzieren ($EC_{50} \geq 3\ \mu M$). Mit Hilfe pharmakologischer Inhibitoren konnte bei der β-BA-vermittelten Aggregation humaner Thrombozyten eine partielle Beteiligung der intrazellulären Signaltransduktionskette Src Kinasen/PLC festgestellt werden. Interessanterweise war β-BA ebenfalls in der Lage, die U-46619- und Kollagen-induzierte Ca^{2+}-Mobilisierung zu verringern. Im Gegensatz zu 11-Methylen-BAs verursachen 11-Keto-BAs (AKBA und KABA) eine äußerst schwache Ca^{2+}-Mobilisierung und induzieren weder Thrombozytenaggregation noch Thrombingenerierung. Vielmehr lässt sich bei einer Vorbehandlung von Thrombozyten mit 11-Keto-BAs eine hemmende Wirkung auf Agonist-stimulierte Zellen beobachten. So bewirkt die Vorinkubation mit AKBA eine potente Inhibition der Kollagen-induzierten Aggregation humaner Thrombozyten ($IC_{50} \leq 1\ \mu M$), wohingegen der Thrombin-vermittelte Effekt nicht moduliert wurde. Versuche, diesen markanten antagonistischen Effekt möglichen Interaktionspartnern bzw. Signaltransduktionswegen zu zuordnen, deuten auf eine Beteiligung der Src Kinasen-/PLCγ2-Route hin. Zusätzlich wurden die Einflüsse zweier unterschiedlicher *B. serrata* Extrakte hinsichtlich ihrer modulativen Eigenschaften auf Thrombozytenfunktionen getestet.

Aufgrund dieser Resultate kann man schlussfolgern, dass 11-Methylen-BAs eine aktivierende Wirkung auf die Physiologie sowie auf einzelne funktionelle Eigenschaften humaner Thrombozyten ausüben, während 11-Keto-BAs diesbezüglich eher antagonistische Effekte vermitteln. Im Hinblick auf die zur Modulation benötigten effektiven Konzentration von BAs kann eine pharmakologische Relevanz dieser Interaktionen während einer Einnahme der Standarddosis von Weihrauchpräparaten nicht ausgeschlossen werden.

Zusammenfassend liefert diese Arbeit wesentliche Erkenntnisse über BAs und ihre Effekte auf molekulare und zelluläre Aspekte entzündlicher Prozesse, erstmals auch unter dem Aspekt der pharmakologischen Relevanz. Der Forschungsschwerpunkt wurde diesbezüglich auf Enzyme der Arachidonsäurekaskade und Plättchenphysiologie gelegt. Die Untersuchungen ergaben neue Einblicke in die durch BAs beeinflussten intrazellulären Signalwege und funktionelle

Eigenschaften humaner Thrombozyten. Die Anwendung moderner Identifizierungsstrategien (Pulldown-Methode und SPR-Studien) führte zur Entdeckung von COX-1 und mPGES-1 als neue molekulare Targets von BAs. Durch detaillierte funktionelle Charakterisierung unter Berücksichtigung wesentlicher physiologischer Parameter wurde die Wechselwirkung von BAs mit COX-1/2, 5-LO und mPGES-1 hinsichtlich einer möglichen biologischen Relevanz *in vivo* überprüft. Bedingt durch diese Ergebnisse sind die Wechselwirkungen von BAs (im speziellen AKBA) mit COX-1 und 5-LO als verantwortliche anti-entzündliche Wirkprinzipien auszuschließen. Vielmehr repräsentiert die Hemmung der pathophysiologischen PGE_2 Bildung *in vitro* und *in vivo* über die β-BA-vermittelte Inhibition der mPGES-1 einen adäquaten molekularen Mechanismus der mit großer Sicherheit zur anti-inflammatorischen Effektivität von BAs und Weihrauchpräparationen im Menschen beiträgt.

8 REFERENCES

[1] Diamandopoulos AA. Organic and inorganic cosmetics in the preclassical Eastern Mediterranean. Int J Dermatol 1996;35:751-6.

[2] Martinez D LK, Janzen J. Weihrauch und Myrrhe. Kulturgeschichte und wirtschaftliche Bedeutung.: Wissenschaftliche Verlagsgesellschaft Stuttgart, 1989.

[3] Menon MK, Kar A. Analgesic and psychopharmacological effects of the gum resin of Boswellia serrata. Planta Med 1971;19:333-41.

[4] Singh GB, Atal CK. Pharmacology of an extract of salai guggal ex-Boswellia serrata, a new non-steroidal anti-inflammatory agent. Agents Actions 1986;18:407-12.

[5] Ammon HP. Boswellic acids in chronic inflammatory diseases. Planta Med 2006;72:1100-16.

[6] Poeckel D, Werz O. Boswellic acids: biological actions and molecular targets. Curr Med Chem 2006;13:3359-69.

[7] Buchele B, Simmet T. Analysis of 12 different pentacyclic triterpenic acids from frankincense in human plasma by high-performance liquid chromatography and photodiode array detection. J Chromatogr B Analyt Technol Biomed Life Sci 2003;795:355-62.

[8] Poeckel D, Tausch L, Kather N, Jauch J, Werz O. Boswellic acids stimulate arachidonic acid release and 12-lipoxygenase activity in human platelets independent of Ca2+ and differentially interact with platelet-type 12-lipoxygenase. Mol Pharmacol 2006;70:1071-8.

[9] Altmann A, Fischer L, Schubert-Zsilavecz M, Steinhilber D, Werz O. Boswellic acids activate p42(MAPK) and p38 MAPK and stimulate Ca(2+) mobilization. Biochem Biophys Res Commun 2002;290:185-90.

[10] Poeckel D, Tausch L, George S, Jauch J, Werz O. 3-O-acetyl-11-keto-boswellic acid decreases basal intracellular Ca2+ levels and inhibits agonist-induced Ca2+ mobilization and mitogen-activated protein kinase activation in human monocytic cells. J Pharmacol Exp Ther 2006;316:224-32.

[11] Siemoneit U, Hofmann B, Kather N, Lamkemeyer T, Madlung J, Franke L, et al. Identification and functional analysis of cyclooxygenase-1 as a molecular target of boswellic acids. Biochem Pharmacol 2008;75:503-13.

[12] Shargel LY, A.B. . Applied biopharmaceutics & pharmacokinetics: New York: McGraw-Hill, 1999.

[13] Sharma S, Thawani V, Hingorani L, Shrivastava M, Bhate VR, Khiyani R. Pharmacokinetic study of 11-Keto beta-Boswellic acid. Phytomedicine 2004;11:255-60.

[14] Tawab MA, Kaunzinger A, Bahr U, Karas M, Wurglics M, Schubert-Zsilavecz M. Development of a high-performance liquid chromatographic method for the determination of 11-keto-beta-boswellic acid in human plasma. J Chromatogr B Biomed Sci Appl 2001;761:221-7.

[15] Sterk V, Buchele B, Simmet T. Effect of food intake on the bioavailability of boswellic acids from a herbal preparation in healthy volunteers. Planta Med 2004;70:1155-60.

[16] Kruger P, Daneshfar R, Eckert GP, Klein J, Volmer DA, Bahr U, et al. Metabolism of boswellic acids in vitro and in vivo. Drug Metab Dispos 2008;36:1135-42.

[17] Weber CC, Reising K, Muller WE, Schubert-Zsilavecz M, Abdel-Tawab M. Modulation of Pgp function by boswellic acids. Planta Med 2006;72:507-13.

[18] Kruger P, Kanzer J, Hummel J, Fricker G, Schubert-Zsilavecz M, Abdel-Tawab M. Permeation of Boswellia extract in the Caco-2 model and possible interactions of its constituents KBA and AKBA with OATP1B3 and MRP2. Eur J Pharm Sci 2009;36:275-84.

[19] Frank A, Unger M. Analysis of frankincense from various Boswellia species with inhibitory activity on human drug metabolising cytochrome P450 enzymes using liquid chromatography mass spectrometry after automated on-line extraction. J Chromatogr A 2006;1112:255-62.

[20] Cuaz-Perolin C, Billiet L, Bauge E, Copin C, Scott-Algara D, Genze F, et al. Antiinflammatory and antiatherogenic effects of the NF-kappaB inhibitor acetyl-11-keto-beta-boswellic acid in LPS-challenged ApoE-/- mice. Arterioscler Thromb Vasc Biol 2008;28:272-7.

[21] Reddy GK, Dhar SC. Effect of a new non-steroidal anti-inflammatory agent on lysosomal stability in adjuvant induced arthritis. Ital J Biochem 1987;36:205-17.

[22] Reddy GK, Dhar SC, Singh GB. Urinary excretion of connective tissue metabolites under the influence of a new non-steroidal anti-inflammatory agent in adjuvant induced arthritis. Agents Actions 1987;22:99-105.

[23] Sharma ML, Bani S, Singh GB. Anti-arthritic activity of boswellic acids in bovine serum albumin (BSA)-induced arthritis. Int J Immunopharmacol 1989;11:647-52.

[24] Krieglstein CF, Anthoni C, Rijcken EJ, Laukotter M, Spiegel HU, Boden SE, et al. Acetyl-11-keto-beta-boswellic acid, a constituent of a herbal medicine from Boswellia serrata resin, attenuates experimental ileitis. Int J Colorectal Dis 2001;16:88-95.

[25] Anthoni C, Laukoetter MG, Rijcken E, Vowinkel T, Mennigen R, Muller S, et al. Mechanisms underlying the anti-inflammatory actions of boswellic acid derivatives in experimental colitis. Am J Physiol Gastrointest Liver Physiol 2006;290:G1131-7.

[26] Kiela PR, Midura AJ, Kuscuoglu N, Jolad SD, Solyom AM, Besselsen DG, et al. Effects of Boswellia serrata in mouse models of chemically induced colitis. Am J Physiol Gastrointest Liver Physiol 2005;288:G798-808.

[27] Latella G, Sferra R, Vetuschi A, Zanninelli G, D'Angelo A, Catitti V, et al. Prevention of colonic fibrosis by Boswellia and Scutellaria extracts in rats with colitis induced by 2,4,5-trinitrobenzene sulphonic acid. Eur J Clin Invest 2008;38:410-20.

[28] Y J, Kamath JV, Asad M. Effect of hexane extract of Boswellia serrata oleo-gum resin on chemically induced liver damage. Pak J Pharm Sci 2006;19:129-33.

[29] Safayhi H, Mack T, Ammon HP. Protection by boswellic acids against galactosamine/endotoxin-induced hepatitis in mice. Biochem Pharmacol 1991;41:1536-7.

[30] Wildfeuer A, Neu IS, Safayhi H, Metzger G, Wehrmann M, Vogel U, et al. Effects of boswellic acids extracted from a herbal medicine on the biosynthesis of leukotrienes and the course of experimental autoimmune encephalomyelitis. Arzneimittelforschung 1998;48:668-74.

[31] Singh S, Khajuria A, Taneja SC, Khajuria RK, Singh J, Johri RK, et al. The gastric ulcer protective effect of boswellic acids, a leukotriene inhibitor from Boswellia serrata, in rats. Phytomedicine 2008;15:408-15.

[32] Buchele B, Zugmaier W, Estrada A, Genze F, Syrovets T, Paetz C, et al. Characterization of 3alpha-acetyl-11-keto-alpha-boswellic acid, a pentacyclic triterpenoid inducing apoptosis in vitro and in vivo. Planta Med 2006;72:1285-9.

[33] Winking M, Sarikaya S, Rahmanian A, Jodicke A, Boker DK. Boswellic acids inhibit glioma growth: a new treatment option? J Neurooncol 2000;46:97-103.

[34] Bishnoi M, Patil CS, Kumar A, Kulkarni SK. Potentiation of antinociceptive effect of NSAIDs by a specific lipooxygenase inhibitor, acetyl 11-keto-beta boswellic acid. Indian J Exp Biol 2006;44:128-32.

[35] Pandey RS, Singh BK, Tripathi YB. Extract of gum resins of Boswellia serrata L. inhibits lipopolysaccharide induced nitric oxide production in rat macrophages along with hypolipidemic property. Indian J Exp Biol 2005;43:509-16.

[36] Pungle P, Banavalikar M, Suthar A, Biyani M, Mengi S. Immunomodulatory activity of boswellic acids of Boswellia serrata Roxb. Indian J Exp Biol 2003;41:1460-2.

[37] Kavitha JV, Rosario JF, Chandran J, Anbu P, Bakkiyanathan. Hypoglycemic and other related effects of Boswellia glabra in alloxan-induced diabetic rats. Indian J Physiol Pharmacol 2007;51:29-39.

[38] Ernst E. Frankincense: systematic review. BMJ 2008;337:a2813.

[39] Kimmatkar N, Thawani V, Hingorani L, Khiyani R. Efficacy and tolerability of Boswellia serrata extract in treatment of osteoarthritis of knee--a randomized double blind placebo controlled trial. Phytomedicine 2003;10:3-7.

[40] Kulkarni RR, Patki PS, Jog VP, Gandage SG, Patwardhan B. Treatment of osteoarthritis with a herbomineral formulation: a double-blind, placebo-controlled, cross-over study. J Ethnopharmacol 1991;33:91-5.

[41] Sengupta K, Alluri KV, Satish AR, Mishra S, Golakoti T, Sarma KV, et al. A double blind, randomized, placebo controlled study of the efficacy and safety of 5-Loxin for treatment of osteoarthritis of the knee. Arthritis Res Ther 2008;10:R85.

[42] Sontakke S TV, Pimpalkhute S, Kabra P, Babhulkar S, Hingorani L. Indian J Pharmacol Open, randomized, controlled clinical trial of Boswellia serrata extract as compared to valdecoxib in osteoarthritis of knee. Indian J Pharmacol 2007;39:27-9.

[43] Sander O, Herborn G, Rau R. [Is H15 (resin extract of Boswellia serrata, "incense") a useful supplement to established drug therapy of chronic polyarthritis? Results of a double-blind pilot study]. Z Rheumatol 1998;57:11-6.

[44] Gerhardt H, Seifert F, Buvari P, Vogelsang H, Repges R. [Therapy of active Crohn disease with Boswellia serrata extract H 15]. Z Gastroenterol 2001;39:11-7.

[45] Gupta I, Parihar A, Malhotra P, Singh GB, Ludtke R, Safayhi H, et al. Effects of Boswellia serrata gum resin in patients with ulcerative colitis. Eur J Med Res 1997;2:37-43.

[46] Madisch A, Miehlke S, Eichele O, Mrwa J, Bethke B, Kuhlisch E, et al. Boswellia serrata extract for the treatment of collagenous colitis. A double-blind, randomized, placebo-controlled, multicenter trial. Int J Colorectal Dis 2007;22:1445-51.

[47] Gupta I, Gupta V, Parihar A, Gupta S, Ludtke R, Safayhi H, et al. Effects of Boswellia serrata gum resin in patients with bronchial asthma: results of a double-blind, placebo-controlled, 6-week clinical study. Eur J Med Res 1998;3:511-4.

[48] Janssen G, Bode U, Breu H, Dohrn B, Engelbrecht V, Gobel U. Boswellic acids in the palliative therapy of children with progressive or relapsed brain tumors. Klin Padiatr 2000;212:189-95.

[49] Streffer JR, Bitzer M, Schabet M, Dichgans J, Weller M. Response of radiochemotherapy-associated cerebral edema to a phytotherapeutic agent, H15. Neurology 2001;56:1219-21.

[50] Basch E, Boon H, Davies-Heerema T, Foppo I, Hashmi S, Hasskarl J, et al. Boswellia: an evidence-based systematic review by the Natural Standard Research Collaboration. J Herb Pharmacother 2004;4:63-83.

[51] Burlando B, Parodi A, Volante A, Bassi AM. Comparison of the irritation potentials of Boswellia serrata gum resin and of acetyl-11-keto-beta-boswellic acid by in vitro cytotoxicity tests on human skin-derived cell lines. Toxicol Lett 2008;177:144-9.

[52] Ammon HP, Mack T, Singh GB, Safayhi H. Inhibition of leukotriene B4 formation in rat peritoneal neutrophils by an ethanolic extract of the gum resin exudate of Boswellia serrata. Planta Med 1991;57:203-7.

[53] Safayhi H, Mack T, Sabieraj J, Anazodo MI, Subramanian LR, Ammon HP. Boswellic acids: novel, specific, nonredox inhibitors of 5-lipoxygenase. J Pharmacol Exp Ther 1992;261:1143-6.

[54] Safayhi H, Sailer ER, Ammon HP. Mechanism of 5-lipoxygenase inhibition by acetyl-11-keto-beta-boswellic acid. Mol Pharmacol 1995;47:1212-6.

[55] Sailer ER, Schweizer S, Boden SE, Ammon HP, Safayhi H. Characterization of an acetyl-11-keto-beta-boswellic acid and arachidonate-binding regulatory site of 5-lipoxygenase using photoaffinity labeling. Eur J Biochem 1998;256:364-8.

[56] Sailer ER, Subramanian LR, Rall B, Hoernlein RF, Ammon HP, Safayhi H. Acetyl-11-keto-beta-boswellic acid (AKBA): structure requirements for binding and 5-lipoxygenase inhibitory activity. Br J Pharmacol 1996;117:615-8.

[57] Werz O, Schneider N, Brungs M, Sailer ER, Safayhi H, Ammon HP, et al. A test system for leukotriene synthesis inhibitors based on the in-vitro differentiation of the human leukemic cell lines HL-60 and Mono Mac 6. Naunyn Schmiedebergs Arch Pharmacol 1997;356:441-5.

[58] Safayhi H, Rall B, Sailer ER, Ammon HP. Inhibition by boswellic acids of human leukocyte elastase. J Pharmacol Exp Ther 1997;281:460-3.

[59] Ying QL, Rinehart AR, Simon SR, Cheronis JC. Inhibition of human leucocyte elastase by ursolic acid. Evidence for a binding site for pentacyclic triterpenes. Biochem J 1991;277 (Pt 2):521-6.

[60] Park YS, Lee JH, Bondar J, Harwalkar JA, Safayhi H, Golubic M. Cytotoxic action of acetyl-11-keto-beta-boswellic acid (AKBA) on meningioma cells. Planta Med 2002;68:397-401.

[61] Takada Y, Ichikawa H, Badmaev V, Aggarwal BB. Acetyl-11-keto-beta-boswellic acid potentiates apoptosis, inhibits invasion, and abolishes osteoclastogenesis by suppressing NF-kappa B and NF-kappa B-regulated gene expression. J Immunol 2006;176:3127-40.

[62] Gayathri B, Manjula N, Vinaykumar KS, Lakshmi BS, Balakrishnan A. Pure compound from Boswellia serrata extract exhibits anti-inflammatory property in human PBMCs and mouse macrophages through inhibition of TNFalpha, IL-1beta, NO and MAP kinases. Int Immunopharmacol 2007;7:473-82.

[63] Altmann A, Poeckel D, Fischer L, Schubert-Zsilavecz M, Steinhilber D, Werz O. Coupling of boswellic acid-induced Ca2+ mobilisation and MAPK activation to lipid metabolism and peroxide formation in human leucocytes. Br J Pharmacol 2004;141:223-32.

[64] Poeckel D, Tausch L, Altmann A, Feisst C, Klinkhardt U, Graff J, et al. Induction of central signalling pathways and select functional effects in human platelets by beta-boswellic acid. Br J Pharmacol 2005;146:514-24.

[65] Syrovets T, Buchele B, Krauss C, Laumonnier Y, Simmet T. Acetyl-boswellic acids inhibit lipopolysaccharide-mediated TNF-alpha induction in monocytes by direct interaction with IkappaB kinases. J Immunol 2005;174:498-506.

[66] Roy S, Khanna S, Shah H, Rink C, Phillips C, Preuss H, et al. Human genome screen to identify the genetic basis of the anti-inflammatory effects of Boswellia in microvascular endothelial cells. DNA Cell Biol 2005;24:244-55.

[67] Sharma ML, Khajuria A, Kaul A, Singh S, Singh GB, Atal CK. Effect of salai guggal ex-Boswellia serrata on cellular and humoral immune responses and leucocyte migration. Agents Actions 1988;24:161-4.

[68] Kapil A, Moza N. Anticomplementary activity of boswellic acids--an inhibitor of C3-convertase of the classical complement pathway. Int J Immunopharmacol 1992;14:1139-43.

[69] Badria FA, Mikhaeil BR, Maatooq GT, Amer MM. Immunomodulatory triterpenoids from the oleogum resin of Boswellia carterii Birdwood. Z Naturforsch [C] 2003;58:505-16.

[70] Chevrier MR, Ryan AE, Lee DY, Zhongze M, Wu-Yan Z, Via CS. Boswellia carterii extract inhibits TH1 cytokines and promotes TH2 cytokines in vitro. Clin Diagn Lab Immunol 2005;12:575-80.

[71] Jing Y, Xia L, Han R. Growth inhibition and differentiation of promyelocytic cells (HL-60) induced by BC-4, an active principle from Boswellia carterii Birdw. Chin Med Sci J 1992;7:12-5.

[72] Shao Y, Ho CT, Chin CK, Badmaev V, Ma W, Huang MT. Inhibitory activity of boswellic acids from Boswellia serrata against human leukemia HL-60 cells in culture. Planta Med 1998;64:328-31.

[73] Hoernlein RF, Orlikowsky T, Zehrer C, Niethammer D, Sailer ER, Simmet T, et al. Acetyl-11-keto-beta-boswellic acid induces apoptosis in HL-60 and CCRF-CEM cells and inhibits topoisomerase I. J Pharmacol Exp Ther 1999;288:613-9.

[74] Liu JJ, Huang B, Hooi SC. Acetyl-keto-beta-boswellic acid inhibits cellular proliferation through a p21-dependent pathway in colon cancer cells. Br J Pharmacol 2006;148:1099-107.

[75] Jing Y, Nakajo S, Xia L, Nakaya K, Fang Q, Waxman S, et al. Boswellic acid acetate induces differentiation and apoptosis in leukemia cell lines. Leuk Res 1999;23:43-50.

[76] Zhao W, Entschladen F, Liu H, Niggemann B, Fang Q, Zaenker KS, et al. Boswellic acid acetate induces differentiation and apoptosis in highly metastatic melanoma and fibrosarcoma cells. Cancer Detect Prev 2003;27:67-75.

[77] Glaser T, Winter S, Groscurth P, Safayhi H, Sailer ER, Ammon HP, et al. Boswellic acids and malignant glioma: induction of apoptosis but no modulation of drug sensitivity. Br J Cancer 1999;80:756-65.

[78] Hostanska K, Daum G, Saller R. Cytostatic and apoptosis-inducing activity of boswellic acids toward malignant cell lines in vitro. Anticancer Res 2002;22:2853-62.

[79] Huang MT, Badmaev V, Ding Y, Liu Y, Xie JG, Ho CT. Anti-tumor and anti-carcinogenic activities of triterpenoid, beta-boswellic acid. Biofactors 2000;13:225-30.

[80] Syrovets T, Buchele B, Gedig E, Slupsky JR, Simmet T. Acetyl-boswellic acids are novel catalytic inhibitors of human topoisomerases I and IIalpha. Mol Pharmacol 2000;58:71-81.

[81] Liu JJ, Nilsson A, Oredsson S, Badmaev V, Duan RD. Keto- and acetyl-keto-boswellic acids inhibit proliferation and induce apoptosis in Hep G2 cells via a caspase-8 dependent pathway. Int J Mol Med 2002;10:501-5.

[82] Xia L, Chen D, Han R, Fang Q, Waxman S, Jing Y. Boswellic acid acetate induces apoptosis through caspase-mediated pathways in myeloid leukemia cells. Mol Cancer Ther 2005;4:381-8.

[83] Bhushan S, Kumar A, Malik F, Andotra SS, Sethi VK, Kaur IP, et al. A triterpenediol from Boswellia serrata induces apoptosis through both the intrinsic and extrinsic apoptotic pathways in human leukemia HL-60 cells. Apoptosis 2007;12:1911-26.

[84] Liu JJ, Nilsson A, Oredsson S, Badmaev V, Zhao WZ, Duan RD. Boswellic acids trigger apoptosis via a pathway dependent on caspase-8 activation but independent on Fas/Fas ligand interaction in colon cancer HT-29 cells. Carcinogenesis 2002;23:2087-93.

[85] Lu M, Xia L, Hua H, Jing Y. Acetyl-keto-beta-boswellic acid induces apoptosis through a death receptor 5-mediated pathway in prostate cancer cells. Cancer Res 2008;68:1180-6.

[86] Yuan HQ, Kong F, Wang XL, Young CY, Hu XY, Lou HX. Inhibitory effect of acetyl-11-keto-beta-boswellic acid on androgen receptor by interference of Sp1 binding activity in prostate cancer cells. Biochem Pharmacol 2008;75:2112-21.

[87] Syrovets T, Gschwend JE, Buchele B, Laumonnier Y, Zugmaier W, Genze F, et al. Inhibition of IkappaB kinase activity by acetyl-boswellic acids promotes apoptosis in androgen-independent PC-3 prostate cancer cells in vitro and in vivo. J Biol Chem 2005;280:6170-80.

[88] Kunnumakkara AB, Nair AS, Sung B, Pandey MK, Aggarwal BB. Boswellic acid blocks signal transducers and activators of transcription 3 signaling, proliferation, and survival of multiple myeloma via the protein tyrosine phosphatase SHP-1. Mol Cancer Res 2009;7:118-28.

[89] Serhan CN, Chiang N, Van Dyke TE. Resolving inflammation: dual anti-inflammatory and pro-resolution lipid mediators. Nat Rev Immunol 2008;8:349-61.

[90] Nathan C. Points of control in inflammation. Nature 2002;420:846-52.

[91] Serhan CN. Resolution phase of inflammation: novel endogenous anti-inflammatory and proresolving lipid mediators and pathways. Annu Rev Immunol 2007;25:101-37.

[92] Khan WA, Blobe GC, Hannun YA. Arachidonic acid and free fatty acids as second messengers and the role of protein kinase C. Cell Signal 1995;7:171-84.

[93] Soberman RJ, Christmas P. The organization and consequences of eicosanoid signaling. J Clin Invest 2003;111:1107-13.

[94] Burke JE, Dennis EA. Phospholipase A2 biochemistry. Cardiovasc Drugs Ther 2009;23:49-59.

[95] Clark JD, Milona N, Knopf JL. Purification of a 110-kilodalton cytosolic phospholipase A2 from the human monocytic cell line U937. Proc Natl Acad Sci U S A 1990;87:7708-12.

[96] Kramer RM, Roberts EF, Manetta J, Putnam JE. The Ca2(+)-sensitive cytosolic phospholipase A2 is a 100-kDa protein in human monoblast U937 cells. J Biol Chem 1991;266:5268-72.

[97] Leslie CC, Voelker DR, Channon JY, Wall MM, Zelarney PT. Properties and purification of an arachidonoyl-hydrolyzing phospholipase A2 from a macrophage cell line, RAW 264.7. Biochim Biophys Acta 1988;963:476-92.

[98] Takayama K, Kudo I, Kim DK, Nagata K, Nozawa Y, Inoue K. Purification and characterization of human platelet phospholipase A2 which preferentially hydrolyzes an arachidonoyl residue. FEBS Lett 1991;282:326-30.

[99] Uozumi N, Shimizu T. Roles for cytosolic phospholipase A2alpha as revealed by gene-targeted mice. Prostaglandins Other Lipid Mediat 2002;68-69:59-69.

[100] Lambeau G, Gelb MH. Biochemistry and physiology of mammalian secreted phospholipases A2. Annu Rev Biochem 2008;77:495-520.

[101] Balsinde J, Bianco ID, Ackermann EJ, Conde-Frieboes K, Dennis EA. Inhibition of calcium-independent phospholipase A2 prevents arachidonic acid incorporation and phospholipid remodeling in P388D1 macrophages. Proc Natl Acad Sci U S A 1995;92:8527-31.

[102] Bao S, Bohrer A, Ramanadham S, Jin W, Zhang S, Turk J. Effects of stable suppression of Group VIA phospholipase A2 expression on phospholipid content and composition, insulin secretion, and proliferation of INS-1 insulinoma cells. J Biol Chem 2006;281:187-98.

[103] Bao S, Li Y, Lei X, Wohltmann M, Jin W, Bohrer A, et al. Attenuated free cholesterol loading-induced apoptosis but preserved phospholipid composition of peritoneal macrophages from mice that do not express group VIA phospholipase A2. J Biol Chem 2007;282:27100-14.

[104] Hiraoka M, Abe A, Shayman JA. Structure and function of lysosomal phospholipase A2: identification of the catalytic triad and the role of cysteine residues. J Lipid Res 2005;46:2441-7.

[105] Stafforini DM, Rollins EN, Prescott SM, McIntyre TM. The platelet-activating factor acetylhydrolase from human erythrocytes. Purification and properties. J Biol Chem 1993;268:3857-65.

[106] Ghosh M, Tucker DE, Burchett SA, Leslie CC. Properties of the Group IV phospholipase A2 family. Prog Lipid Res 2006;45:487-510.

[107] Mosior M, Six DA, Dennis EA. Group IV cytosolic phospholipase A2 binds with high affinity and specificity to phosphatidylinositol 4,5-bisphosphate resulting in dramatic increases in activity. J Biol Chem 1998;273:2184-91.

[108] Pettus BJ, Bielawska A, Subramanian P, Wijesinghe DS, Maceyka M, Leslie CC, et al. Ceramide 1-phosphate is a direct activator of cytosolic phospholipase A2. J Biol Chem 2004;279:11320-6.

[109] Hirabayashi T, Shimizu T. Localization and regulation of cytosolic phospholipase A(2). Biochim Biophys Acta 2000;1488:124-38.

[110] Vane JR, Botting RM. Mechanism of action of nonsteroidal anti-inflammatory drugs. Am J Med 1998;104:2S-8S; discussion 21S-2S.

[111] Rouzer CA, Marnett LJ. Cyclooxygenases: structural and functional insights. J Lipid Res 2008.

[112] Wallace JL, Bak A, McKnight W, Asfaha S, Sharkey KA, MacNaughton WK. Cyclooxygenase 1 contributes to inflammatory responses in rats and mice: implications for gastrointestinal toxicity. Gastroenterology 1998;115:101-9.

[113] Morita I. Distinct functions of COX-1 and COX-2. Prostaglandins Other Lipid Mediat 2002;68-69:165-75.

[114] Grosser T, Fries S, FitzGerald GA. Biological basis for the cardiovascular consequences of COX-2 inhibition: therapeutic challenges and opportunities. J Clin Invest 2006;116:4-15.

[115] Lipsky PE, Brooks P, Crofford LJ, DuBois R, Graham D, Simon LS, et al. Unresolved issues in the role of cyclooxygenase-2 in normal physiologic processes and disease. Arch Intern Med 2000;160:913-20.

[116] Hersh EV, Lally ET, Moore PA. Update on cyclooxygenase inhibitors: has a third COX isoform entered the fray? Curr Med Res Opin 2005;21:1217-26.

[117] Smith CH, Larner J. Differential aggregation of the totally converted D and I forms of rabbit muscle glycogen synthase. Biochim Biophys Acta 1972;264:224-8.

[118] Landino LM, Crews BC, Gierse JK, Hauser SD, Marnett LJ. Mutational analysis of the role of the distal histidine and glutamine residues of prostaglandin-endoperoxide synthase-2 in peroxidase catalysis, hydroperoxide reduction, and cyclooxygenase activation. J Biol Chem 1997;272:21565-74.

[119] Smith WL, Garavito RM, DeWitt DL. Prostaglandin endoperoxide H synthases (cyclooxygenases)-1 and -2. J Biol Chem 1996;271:33157-60.

[120] Kozak KR, Rowlinson SW, Marnett LJ. Oxygenation of the endocannabinoid, 2-arachidonylglycerol, to glyceryl prostaglandins by cyclooxygenase-2. J Biol Chem 2000;275:33744-9.

[121] Kulmacz RJ, Pendleton RB, Lands WE. Interaction between peroxidase and cyclooxygenase activities in prostaglandin-endoperoxide synthase. Interpretation of reaction kinetics. J Biol Chem 1994;269:5527-36.

[122] Smith WL. Nutritionally essential fatty acids and biologically indispensable cyclooxygenases. Trends Biochem Sci 2008;33:27-37.

[123] Luong C, Miller A, Barnett J, Chow J, Ramesha C, Browner MF. Flexibility of the NSAID binding site in the structure of human cyclooxygenase-2. Nat Struct Biol 1996;3:927-33.

[124] Morita I, Schindler M, Regier MK, Otto JC, Hori T, DeWitt DL, et al. Different intracellular locations for prostaglandin endoperoxide H synthase-1 and -2. J Biol Chem 1995;270:10902-8.

[125] Murakami M, Kambe T, Shimbara S, Kudo I. Functional coupling between various phospholipase A2s and cyclooxygenases in immediate and delayed prostanoid biosynthetic pathways. J Biol Chem 1999;274:3103-15.

[126] Murakami M, Nakatani Y, Tanioka T, Kudo I. Prostaglandin E synthase. Prostaglandins Other Lipid Mediat 2002;68-69:383-99.

[127] Smith WL, DeWitt DL, Garavito RM. Cyclooxygenases: structural, cellular, and molecular biology. Annu Rev Biochem 2000;69:145-82.

[128] Forman BM, Chen J, Evans RM. The peroxisome proliferator-activated receptors: ligands and activators. Ann N Y Acad Sci 1996;804:266-75.

[129] Funk CD. Prostaglandins and leukotrienes: advances in eicosanoid biology. Science 2001;294:1871-5.

[130] Laneuville O, Breuer DK, Dewitt DL, Hla T, Funk CD, Smith WL. Differential inhibition of human prostaglandin endoperoxide H synthases-1 and -2 by nonsteroidal anti-inflammatory drugs. J Pharmacol Exp Ther 1994;271:927-34.

[131] DeWitt DL. Cox-2-selective inhibitors: the new super aspirins. Mol Pharmacol 1999;55:625-31.

[132] Marnett LJ, Rowlinson SW, Goodwin DC, Kalgutkar AS, Lanzo CA. Arachidonic acid oxygenation by COX-1 and COX-2. Mechanisms of catalysis and inhibition. J Biol Chem 1999;274:22903-6.

[133] Serhan CN, Clish CB, Brannon J, Colgan SP, Chiang N, Gronert K. Novel functional sets of lipid-derived mediators with antiinflammatory actions generated from omega-3 fatty acids via cyclooxygenase 2-nonsteroidal antiinflammatory drugs and transcellular processing. J Exp Med 2000;192:1197-204.

[134] Rainsford KD. Anti-inflammatory drugs in the 21st century. Subcell Biochem 2007;42:3-27.

[135] Walker MC, Kurumbail RG, Kiefer JR, Moreland KT, Koboldt CM, Isakson PC, et al. A three-step kinetic mechanism for selective inhibition of cyclo-oxygenase-2 by diarylheterocyclic inhibitors. Biochem J 2001;357:709-18.

[136] McGettigan P, Han P, Jones L, Whitaker D, Henry D. Selective COX-2 inhibitors, NSAIDs and congestive heart failure: differences between new and recurrent cases. Br J Clin Pharmacol 2008;65:927-34.

[137] Serhan CN, Levy B. Success of prostaglandin E2 in structure-function is a challenge for structure-based therapeutics. Proc Natl Acad Sci U S A 2003;100:8609-11.

[138] Dinarello CA, Gatti S, Bartfai T. Fever: links with an ancient receptor. Curr Biol 1999;9:R147-50.

[139] Moonen P, Buytenhek M, Nugteren DH. Purification of PGH-PGE isomerase from sheep vesicular glands. Methods Enzymol 1982;86:84-91.

[140] Ogino N, Miyamoto T, Yamamoto S, Hayaishi O. Prostaglandin endoperoxide E isomerase from bovine vesicular gland microsomes, a glutathione-requiring enzyme. J Biol Chem 1977;252:890-5.

[141] Tanioka T, Nakatani Y, Semmyo N, Murakami M, Kudo I. Molecular identification of cytosolic prostaglandin E2 synthase that is functionally coupled with cyclooxygenase-1 in immediate prostaglandin E2 biosynthesis. J Biol Chem 2000;275:32775-82.

[142] Jakobsson PJ, Thoren S, Morgenstern R, Samuelsson B. Identification of human prostaglandin E synthase: a microsomal, glutathione-dependent, inducible enzyme, constituting a potential novel drug target. Proc Natl Acad Sci U S A 1999;96:7220-5.

[143] Watanabe K, Kurihara K, Suzuki T. Purification and characterization of membrane-bound prostaglandin E synthase from bovine heart. Biochim Biophys Acta 1999;1439:406-14.

[144] Tanikawa N, Ohmiya Y, Ohkubo H, Hashimoto K, Kangawa K, Kojima M, et al. Identification and characterization of a novel type of membrane-associated prostaglandin E synthase. Biochem Biophys Res Commun 2002;291:884-9.

[145] Vazquez-Tello A, Fan L, Hou X, Joyal JS, Mancini JA, Quiniou C, et al. Intracellular-specific colocalization of prostaglandin E2 synthases and cyclooxygenases in the brain. Am J Physiol Regul Integr Comp Physiol 2004;287:R1155-63.

[146] Murakami M, Nakashima K, Kamei D, Masuda S, Ishikawa Y, Ishii T, et al. Cellular prostaglandin E2 production by membrane-bound prostaglandin E synthase-2 via both cyclooxygenases-1 and -2. J Biol Chem 2003;278:37937-47.

[147] Kojima F, Naraba H, Sasaki Y, Beppu M, Aoki H, Kawai S. Prostaglandin E2 is an enhancer of interleukin-1beta-induced expression of membrane-associated prostaglandin E synthase in rheumatoid synovial fibroblasts. Arthritis Rheum 2003;48:2819-28.

[148] Kojima F, Naraba H, Sasaki Y, Okamoto R, Koshino T, Kawai S. Coexpression of microsomal prostaglandin E synthase with cyclooxygenase-2 in human rheumatoid synovial cells. J Rheumatol 2002;29:1836-42.

[149] Stichtenoth DO, Thoren S, Bian H, Peters-Golden M, Jakobsson PJ, Crofford LJ. Microsomal prostaglandin E synthase is regulated by proinflammatory cytokines and glucocorticoids in primary rheumatoid synovial cells. J Immunol 2001;167:469-74.

[150] Thoren S, Jakobsson PJ. Coordinate up- and down-regulation of glutathione-dependent prostaglandin E synthase and cyclooxygenase-2 in A549 cells. Inhibition by NS-398 and leukotriene C4. Eur J Biochem 2000;267:6428-34.

[151] Korotkova M, Helmers SB, Loell I, Alexanderson H, Grundtman C, Dorph C, et al. Effects of immunosuppressive treatment on microsomal prostaglandin E synthase 1 and cyclooxygenases expression in muscle tissue of patients with polymyositis or dermatomyositis. Ann Rheum Dis 2008;67:1596-602.

[152] Korotkova M, Westman M, Gheorghe KR, af Klint E, Trollmo C, Ulfgren AK, et al. Effects of antirheumatic treatments on the prostaglandin E2 biosynthetic pathway. Arthritis Rheum 2005;52:3439-47.

[153] Kamei D, Yamakawa K, Takegoshi Y, Mikami-Nakanishi M, Nakatani Y, Oh-Ishi S, et al. Reduced pain hypersensitivity and inflammation in mice lacking microsomal prostaglandin e synthase-1. J Biol Chem 2004;279:33684-95.

[154] Ouellet M, Falgueyret JP, Ear PH, Pen A, Mancini JA, Riendeau D, et al. Purification and characterization of recombinant microsomal prostaglandin E synthase-1. Protein Expr Purif 2002;26:489-95.

[155] Thoren S, Weinander R, Saha S, Jegerschold C, Pettersson PL, Samuelsson B, et al. Human microsomal prostaglandin E synthase-1: purification, functional characterization, and projection structure determination. J Biol Chem 2003;278:22199-209.

[156] Lazarus M, Kubata BK, Eguchi N, Fujitani Y, Urade Y, Hayaishi O. Biochemical characterization of mouse microsomal prostaglandin E synthase-1 and its colocalization with cyclooxygenase-2 in peritoneal macrophages. Arch Biochem Biophys 2002;397:336-41.

[157] Lazarus M, Munday CJ, Eguchi N, Matsumoto S, Killian GJ, Kubata BK, et al. Immunohistochemical localization of microsomal PGE synthase-1 and cyclooxygenases in male mouse reproductive organs. Endocrinology 2002;143:2410-9.

[158] Jegerschold C, Pawelzik SC, Purhonen P, Bhakat P, Gheorghe KR, Gyobu N, et al. Structural basis for induced formation of the inflammatory mediator prostaglandin E2. Proc Natl Acad Sci U S A 2008;105:11110-5.

[159] Ikeda-Matsuo Y, Ota A, Fukada T, Uematsu S, Akira S, Sasaki Y. Microsomal prostaglandin E synthase-1 is a critical factor of stroke-reperfusion injury. Proc Natl Acad Sci U S A 2006;103:11790-5.

[160] Kamei D, Murakami M, Nakatani Y, Ishikawa Y, Ishii T, Kudo I. Potential role of microsomal prostaglandin E synthase-1 in tumorigenesis. J Biol Chem 2003;278:19396-405.

[161] Murakami M, Kudo I. Recent advances in molecular biology and physiology of the prostaglandin E2-biosynthetic pathway. Prog Lipid Res 2004;43:3-35.

[162] Friesen RW, Mancini JA. Microsomal prostaglandin E2 synthase-1 (mPGES-1): a novel anti-inflammatory therapeutic target. J Med Chem 2008;51:4059-67.

[163] Engblom D, Ek M, Andersson IM, Saha S, Dahlstrom M, Jakobsson PJ, et al. Induction of microsomal prostaglandin E synthase in the rat brain endothelium and parenchyma in adjuvant-induced arthritis. J Comp Neurol 2002;452:205-14.

[164] Engblom D, Saha S, Engstrom L, Westman M, Audoly LP, Jakobsson PJ, et al. Microsomal prostaglandin E synthase-1 is the central switch during immune-induced pyresis. Nat Neurosci 2003;6:1137-8.

[165] Trebino CE, Stock JL, Gibbons CP, Naiman BM, Wachtmann TS, Umland JP, et al. Impaired inflammatory and pain responses in mice lacking an inducible prostaglandin E synthase. Proc Natl Acad Sci U S A 2003;100:9044-9.

[166] Wang M, Zukas AM, Hui Y, Ricciotti E, Pure E, FitzGerald GA. Deletion of microsomal prostaglandin E synthase-1 augments prostacyclin and retards atherogenesis. Proc Natl Acad Sci U S A 2006;103:14507-12.

[167] Quraishi O, Mancini JA, Riendeau D. Inhibition of inducible prostaglandin E(2) synthase by 15-deoxy-Delta(12,14)-prostaglandin J(2) and polyunsaturated fatty acids. Biochem Pharmacol 2002;63:1183-9.

[168] Riendeau D, Aspiotis R, Ethier D, Gareau Y, Grimm EL, Guay J, et al. Inhibitors of the inducible microsomal prostaglandin E2 synthase (mPGES-1) derived from MK-886. Bioorg Med Chem Lett 2005;15:3352-5.

[169] Koeberle A, Siemoneit U, Buhring U, Northoff H, Laufer S, Albrecht W, et al. Licofelone suppresses prostaglandin E2 formation by interference with the inducible microsomal prostaglandin E2 synthase-1. J Pharmacol Exp Ther 2008;326:975-82.

[170] Koeberle A, Zettl H, Greiner C, Wurglics M, Schubert-Zsilavecz M, Werz O. Pirinixic acid derivatives as novel dual inhibitors of microsomal prostaglandin E2 synthase-1 and 5-lipoxygenase. J Med Chem 2008;51:8068-76.

[171] Cote B, Boulet L, Brideau C, Claveau D, Ethier D, Frenette R, et al. Substituted phenanthrene imidazoles as potent, selective, and orally active mPGES-1 inhibitors. Bioorg Med Chem Lett 2007;17:6816-20.

[172] Samuelsson B, Morgenstern R, Jakobsson PJ. Membrane prostaglandin E synthase-1: a novel therapeutic target. Pharmacol Rev 2007;59:207-24.

[173] Evans JF, Ferguson AD, Mosley RT, Hutchinson JH. What's all the FLAP about?: 5-lipoxygenase-activating protein inhibitors for inflammatory diseases. Trends Pharmacol Sci 2008;29:72-8.

[174] Ford-Hutchinson AW, Bray MA, Doig MV, Shipley ME, Smith MJ. Leukotriene B, a potent chemokinetic and aggregating substance released from polymorphonuclear leukocytes. Nature 1980;286:264-5.

[175] Radmark O, Shimizu T, Jornvall H, Samuelsson B. Leukotriene A4 hydrolase in human leukocytes. Purification and properties. J Biol Chem 1984;259:12339-45.

[176] Gimbrone MA, Jr., Brock AF, Schafer AI. Leukotriene B4 stimulates polymorphonuclear leukocyte adhesion to cultured vascular endothelial cells. J Clin Invest 1984;74:1552-5.

[177] Goodarzi K, Goodarzi M, Tager AM, Luster AD, von Andrian UH. Leukotriene B4 and BLT1 control cytotoxic effector T cell recruitment to inflamed tissues. Nat Immunol 2003;4:965-73.

[178] Samuelsson B. Leukotrienes: a new class of mediators of immediate hypersensitivity reactions and inflammation. Adv Prostaglandin Thromboxane Leukot Res 1983;11:1-13.

[179] Funk CD. Leukotriene modifiers as potential therapeutics for cardiovascular disease. Nat Rev Drug Discov 2005;4:664-72.

[180] Erlemann KR, Rokach J, Powell WS. Oxidative stress stimulates the synthesis of the eosinophil chemoattractant 5-oxo-6,8,11,14-eicosatetraenoic acid by inflammatory cells. J Biol Chem 2004;279:40376-84.

[181] Miller TA, Ghosh J, Myers CE, Macdonald TL. 5-HETE congeners as modulators of cell proliferation. Bioorg Med Chem Lett 2000;10:1913-6.

[182] Chiang N, Arita M, Serhan CN. Anti-inflammatory circuitry: lipoxin, aspirin-triggered lipoxins and their receptor ALX. Prostaglandins Leukot Essent Fatty Acids 2005;73:163-77.

[183] McMahon B, Godson C. Lipoxins: endogenous regulators of inflammation. Am J Physiol Renal Physiol 2004;286:F189-201.

[184] Chasteen ND, Grady JK, Skorey KI, Neden KJ, Riendeau D, Percival MD. Characterization of the non-heme iron center of human 5-lipoxygenase by electron paramagnetic resonance, fluorescence, and ultraviolet-visible spectroscopy: redox cycling between ferrous and ferric states. Biochemistry 1993;32:9763-71.

[185] Radmark O. Arachidonate 5-lipoxygenase. J Lipid Mediat Cell Signal 1995;12:171-84.

[186] Werz O. 5-lipoxygenase: cellular biology and molecular pharmacology. Curr Drug Targets Inflamm Allergy 2002;1:23-44.

[187] Rouzer CA, Shimizu T, Samuelsson B. On the nature of the 5-lipoxygenase reaction in human leukocytes: characterization of a membrane-associated stimulatory factor. Proc Natl Acad Sci U S A 1985;82:7505-9.

[188] Hammarberg T, Reddy KV, Persson B, Radmark O. Calcium binding to 5-lipoxygenase. Adv Exp Med Biol 2002;507:117-21.

[189] Radmark O, Werz O, Steinhilber D, Samuelsson B. 5-Lipoxygenase: regulation of expression and enzyme activity. Trends Biochem Sci 2007;32:332-41.

[190] Hornig C, Albert D, Fischer L, Hornig M, Radmark O, Steinhilber D, et al. 1-Oleoyl-2-acetylglycerol stimulates 5-lipoxygenase activity via a putative (phospho)lipid binding site within the N-terminal C2-like domain. J Biol Chem 2005;280:26913-21.

[191] Rakonjac M, Fischer L, Provost P, Werz O, Steinhilber D, Samuelsson B, et al. Coactosin-like protein supports 5-lipoxygenase enzyme activity and up-regulates leukotriene A4 production. Proc Natl Acad Sci U S A 2006;103:13150-5.

[192] Werz O, Burkert E, Fischer L, Szellas D, Dishart D, Samuelsson B, et al. Extracellular signal-regulated kinases phosphorylate 5-lipoxygenase and stimulate 5-lipoxygenase product formation in leukocytes. FASEB J 2002;16:1441-3.

[193] Werz O, Szellas D, Steinhilber D, Radmark O. Arachidonic acid promotes phosphorylation of 5-lipoxygenase at Ser-271 by MAPK-activated protein kinase 2 (MK2). J Biol Chem 2002;277:14793-800.

[194] Werz O, Klemm J, Samuelsson B, Radmark O. 5-lipoxygenase is phosphorylated by p38 kinase-dependent MAPKAP kinases. Proc Natl Acad Sci U S A 2000;97:5261-6.

[195] Luo M, Jones SM, Flamand N, Aronoff DM, Peters-Golden M, Brock TG. Phosphorylation by protein kinase a inhibits nuclear import of 5-lipoxygenase. J Biol Chem 2005;280:40609-16.

[196] Peters-Golden M, Brock TG. 5-lipoxygenase and FLAP. Prostaglandins Leukot Essent Fatty Acids 2003;69:99-109.

[197] Mandal AK, Skoch J, Bacskai BJ, Hyman BT, Christmas P, Miller D, et al. The membrane organization of leukotriene synthesis. Proc Natl Acad Sci U S A 2004;101:6587-92.

[198] Werz O, Steinhilber D. Therapeutic options for 5-lipoxygenase inhibitors. Pharmacol Ther 2006;112:701-18.

[199] Gillard J, Ford-Hutchinson AW, Chan C, Charleson S, Denis D, Foster A, et al. L-663,536 (MK-886) (3-[1-(4-chlorobenzyl)-3-t-butyl-thio-5-isopropylindol-2-yl]-2,2 - dimethylpropanoic acid), a novel, orally active leukotriene biosynthesis inhibitor. Can J Physiol Pharmacol 1989;67:456-64.

[200] Fischer L, Hornig M, Pergola C, Meindl N, Franke L, Tanrikulu Y, et al. The molecular mechanism of the inhibition by licofelone of the biosynthesis of 5-lipoxygenase products. Br J Pharmacol 2007;152:471-80.

[201] Wagner DD, Burger PC. Platelets in inflammation and thrombosis. Arterioscler Thromb Vasc Biol 2003;23:2131-7.

[202] Jurk K, Kehrel BE. Platelets: physiology and biochemistry. Semin Thromb Hemost 2005;31:381-92.

[203] Kehrel B, Wierwille S, Clemetson KJ, Anders O, Steiner M, Knight CG, et al. Glycoprotein VI is a major collagen receptor for platelet activation: it recognizes the platelet-activating quaternary structure of collagen, whereas CD36, glycoprotein IIb/IIIa, and von Willebrand factor do not. Blood 1998;91:491-9.

[204] Heemskerk JW, Bevers EM, Lindhout T. Platelet activation and blood coagulation. Thromb Haemost 2002;88:186-93.

[205] Holmsen H. Significance of testing platelet functions in vitro. Eur J Clin Invest 1994;24 Suppl 1:3-8.

[206] Nesbitt WS, Giuliano S, Kulkarni S, Dopheide SM, Harper IS, Jackson SP. Intercellular calcium communication regulates platelet aggregation and thrombus growth. J Cell Biol 2003;160:1151-61.

[207] Savage B, Almus-Jacobs F, Ruggeri ZM. Specific synergy of multiple substrate-receptor interactions in platelet thrombus formation under flow. Cell 1998;94:657-66.

[208] Furie B, Furie BC, Flaumenhaft R. A journey with platelet P-selectin: the molecular basis of granule secretion, signalling and cell adhesion. Thromb Haemost 2001;86:214-21.

[209] Gawaz M, Langer H, May AE. Platelets in inflammation and atherogenesis. J Clin Invest 2005;115:3378-84.

[210] Henn V, Slupsky JR, Grafe M, Anagnostopoulos I, Forster R, Muller-Berghaus G, et al. CD40 ligand on activated platelets triggers an inflammatory reaction of endothelial cells. Nature 1998;391:591-4.

[211] Singbartl K, Forlow SB, Ley K. Platelet, but not endothelial, P-selectin is critical for neutrophil-mediated acute postischemic renal failure. FASEB J 2001;15:2337-44.

[212] Urbich C, Dernbach E, Aicher A, Zeiher AM, Dimmeler S. CD40 ligand inhibits endothelial cell migration by increasing production of endothelial reactive oxygen species. Circulation 2002;106:981-6.

[213] Jackson SP, Nesbitt WS, Kulkarni S. Signaling events underlying thrombus formation. J Thromb Haemost 2003;1:1602-12.

[214] Sims PJ, Wiedmer T, Esmon CT, Weiss HJ, Shattil SJ. Assembly of the platelet prothrombinase complex is linked to vesiculation of the platelet plasma membrane. Studies in Scott syndrome: an isolated defect in platelet procoagulant activity. J Biol Chem 1989;264:17049-57.

[215] Geiger J. Inhibitors of platelet signal transduction as anti-aggregatory drugs. Expert Opin Investig Drugs 2001;10:865-90.

[216] Pitchford SC. Novel uses for anti-platelet agents as anti-inflammatory drugs. Br J Pharmacol 2007;152:987-1002.

[217] Coughlin SR. Protease-activated receptors in vascular biology. Thromb Haemost 2001;86:298-307.

[218] Paul BZ, Jin J, Kunapuli SP. Molecular mechanism of thromboxane A(2)-induced platelet aggregation. Essential role for p2t(ac) and alpha(2a) receptors. J Biol Chem 1999;274:29108-14.

[219] Rhee SG, Bae YS. Regulation of phosphoinositide-specific phospholipase C isozymes. J Biol Chem 1997;272:15045-8.

[220] Nieswandt B, Watson SP. Platelet-collagen interaction: is GPVI the central receptor? Blood 2003;102:449-61.

[221] Roberts DE, McNicol A, Bose R. Mechanism of collagen activation in human platelets. J Biol Chem 2004;279:19421-30.

[222] Ozdener F, Dangelmaier C, Ashby B, Kunapuli SP, Daniel JL. Activation of phospholipase Cgamma2 by tyrosine phosphorylation. Mol Pharmacol 2002;62:672-9.

[223] Watson SP, Auger JM, McCarty OJ, Pearce AC. GPVI and integrin alphaIIb beta3 signaling in platelets. J Thromb Haemost 2005;3:1752-62.

[224] Gibbins JM. Platelet adhesion signalling and the regulation of thrombus formation. J Cell Sci 2004;117:3415-25.

[225] Altmann A. Boswelliasäuren: Modulation zellulärer Signaltransduktionsmechanismen in Leukozyten und Thrombozyten und Korrelation zu funktionellen Eigenschaften. Institut für Pharmazeutische Chemie, Johann Wolfgang Goethe-Universität, Frankfurt 2003.

[226] Poeckel D. Pharmacological actions and targets of boswellic acids in human leukocytes and platelets. Institut für Pharmazeutische Chemie, Johann Wolfgang Goethe-Universität, Frankfurt 2006.

[227] Tausch L. Novel anti-inflammatory targets and mechanisms of boswellic acids and celecoxib. Institut für Pharmazeutische Chemie, Johann Wolfgang Goethe-Universität, Frankfurt 2008.

[228] Jauch J, Bergmann J. An efficient method for the large-scale preparation of 3-O-acetyl-11-oxo-beta-boswellic acid and other boswellic acids. Eur J Org Chem 2003:4752-6.

[229] Alley MC, Scudiero DA, Monks A, Hursey ML, Czerwinski MJ, Fine DL, et al. Feasibility of drug screening with panels of human tumor cell lines using a microculture tetrazolium assay. Cancer Res 1988;48:589-601.

[230] Werz O, Burkert E, Samuelsson B, Radmark O, Steinhilber D. Activation of 5-lipoxygenase by cell stress is calcium independent in human polymorphonuclear leukocytes. Blood 2002;99:1044-52.

[231] Holinstat M, Voss B, Bilodeau ML, McLaughlin JN, Cleator J, Hamm HE. PAR4, but not PAR1, signals human platelet aggregation via Ca2+ mobilization and synergistic P2Y12 receptor activation. J Biol Chem 2006;281:26665-74.

[232] Fischer L, Szellas D, Radmark O, Steinhilber D, Werz O. Phosphorylation- and stimulus-dependent inhibition of cellular 5-lipoxygenase activity by nonredox-type inhibitors. FASEB J 2003;17:949-51.

[233] Brungs M, Radmark O, Samuelsson B, Steinhilber D. Sequential induction of 5-lipoxygenase gene expression and activity in Mono Mac 6 cells by transforming growth factor beta and 1,25-dihydroxyvitamin D3. Proc Natl Acad Sci U S A 1995;92:107-11.

[234] Schwarz D, Junge F, Durst F, Frolich N, Schneider B, Reckel S, et al. Preparative scale expression of membrane proteins in Escherichia coli-based continuous exchange cell-free systems. Nat Protoc 2007;2:2945-57.

[235] Reckel S, Durst F, Löhr F, Shirokov V A, Dötsch V and Bernhard F. Strategies for cell-free expression of membrane proteins. unpublished manuscript 2009.

[236] Knospe J, Steinhilber D, Herrmann T, Roth HJ. Picomole determination of 2,4-dimethoxyanilides of prostaglandins by high-performance liquid chromatography with electrochemical detection. J Chromatogr 1988;442:444-50.

[237] Cho H, Ueda M, Tamaoka M, Hamaguchi M, Aisaka K, Kiso Y, et al. Novel caffeic acid derivatives: extremely potent inhibitors of 12-lipoxygenase. J Med Chem 1991;34:1503-5.

[238] Kalvegren H, Andersson J, Grenegard M, Bengtsson T. Platelet activation triggered by Chlamydia pneumoniae is antagonized by 12-lipoxygenase inhibitors but not cyclooxygenase inhibitors. Eur J Pharmacol 2007;566:20-7.

[239] Dutilh CE, Haddeman E, Jouvenaz GH, Ten Hoor F, Nugteren DH. Study of the two pathways for arachidonate oxygenation in blood platelets. Lipids 1979;14:241-6.

[240] Hamberg M, Svensson J, Samuelsson B. Prostaglandin endoperoxides. A new concept concerning the mode of action and release of prostaglandins. Proc Natl Acad Sci U S A 1974;71:3824-8.

[241] Albert D, Zundorf I, Dingermann T, Muller WE, Steinhilber D, Werz O. Hyperforin is a dual inhibitor of cyclooxygenase-1 and 5-lipoxygenase. Biochem Pharmacol 2002;64:1767-75.

[242] Guichardant M, Petit F, Lagarde M. Metabolism of endogenous arachidonic acid in weakly activated platelets. Absence of leukocyte cooperative products in whole blood. Eicosanoids 1989;2:117-21.

[243] Yamamoto M, Hashimoto J, Takaba H, Miyake K. Response of the isolated human seminiferous tubule to prostaglandins F1 alpha, F2 alpha, E1 and E2. J Urol 1987;137:345-8.

[244] Capdevila JH, Morrow JD, Belosludtsev YY, Beauchamp DR, DuBois RN, Falck JR. The catalytic outcomes of the constitutive and the mitogen inducible isoforms of prostaglandin H2 synthase are markedly affected by glutathione and glutathione peroxidase(s). Biochemistry 1995;34:3325-37.

[245] Mitchell JA, Akarasereenont P, Thiemermann C, Flower RJ, Vane JR. Selectivity of nonsteroidal antiinflammatory drugs as inhibitors of constitutive and inducible cyclooxygenase. Proc Natl Acad Sci U S A 1993;90:11693-7.

[246] Asano K, Lilly CM, Drazen JM. Prostaglandin G/H synthase-2 is the constitutive and dominant isoform in cultured human lung epithelial cells. Am J Physiol 1996;271:L126-31.

[247] Koeberle A. Myrthle. Br J Pharmacol 2008.

[248] Kato K, Ohkawa S, Terao S, Terashita Z, Nishikawa K. Thromboxane synthetase inhibitors (TXSI). Design, synthesis, and evaluation of a novel series of omega-pyridylalkenoic acids. J Med Chem 1985;28:287-94.

[249] Posadas I, Bucci M, Roviezzo F, Rossi A, Parente L, Sautebin L, et al. Carrageenan-induced mouse paw oedema is biphasic, age-weight dependent and displays differential nitric oxide cyclooxygenase-2 expression. Br J Pharmacol 2004;142:331-8.

[250] Alluri PG, Reddy MM, Bachhawat-Sikder K, Olivos HJ, Kodadek T. Isolation of protein ligands from large peptoid libraries. J Am Chem Soc 2003;125:13995-4004.

[251] Hoschle B, Gnau V, Jendrossek D. Methylcrotonyl-CoA and geranyl-CoA carboxylases are involved in leucine/isovalerate utilization (Liu) and acyclic terpene utilization (Atu), and are encoded by liuB/liuD and atuC/atuF, in Pseudomonas aeruginosa. Microbiology 2005;151:3649-56.

[252] Karlsson R, Falt A. Experimental design for kinetic analysis of protein-protein interactions with surface plasmon resonance biosensors. J Immunol Methods 1997;200:121-33.

[253] Roden LD, Myszka DG. Global analysis of a macromolecular interaction measured on BIAcore. Biochem Biophys Res Commun 1996;225:1073-7.

[254] Jones G, Willett P, Glen RC. Molecular recognition of receptor sites using a genetic algorithm with a description of desolvation. J Mol Biol 1995;245:43-53.

[255] Gupta K, Selinsky BS, Kaub CJ, Katz AK, Loll PJ. The 2.0 A resolution crystal structure of prostaglandin H2 synthase-1: structural insights into an unusual peroxidase. J Mol Biol 2004;335:503-18.

[256] Kurumbail RG, Stevens AM, Gierse JK, McDonald JJ, Stegeman RA, Pak JY, et al. Structural basis for selective inhibition of cyclooxygenase-2 by anti-inflammatory agents. Nature 1996;384:644-8.

[257] Halgren T. Merck molecular force field 1. Basis, form, scope, parameterization, and performance of MMFF94. J Comput Chem 1996;1996:490-519.

[258] Jones G, Willett P, Glen RC, Leach AR, Taylor R. Development and validation of a genetic algorithm for flexible docking. J Mol Biol 1997;267:727-48.

[259] DeLano W. The PyMOL Molecular Graphics System (2002) DeLano Scientific, San Carlos, CA, USA. http://wwwpymolorg 2002 2002.

[260] Grynkiewicz G, Poenie M, Tsien RY. A new generation of Ca2+ indicators with greatly improved fluorescence properties. J Biol Chem 1985;260:3440-50.

[261] Hemker HC, Giesen PL, Ramjee M, Wagenvoord R, Beguin S. The thrombogram: monitoring thrombin generation in platelet-rich plasma. Thromb Haemost 2000;83:589-91.

[262] Laemmli UK. Cleavage of structural proteins during the assembly of the head of bacteriophage T4. Nature 1970;227:680-5.

[263] Neuhoff V, Stamm R, Pardowitz I, Arold N, Ehrhardt W, Taube D. Essential problems in quantification of proteins following colloidal staining with coomassie brilliant blue dyes in polyacrylamide gels, and their solution. Electrophoresis 1990;11:101-17.

[264] Shevchenko A, Wilm M, Vorm O, Mann M. Mass spectrometric sequencing of proteins silver-stained polyacrylamide gels. Anal Chem 1996;68:850-8.

[265] Bradford MM. A rapid and sensitive method for the quantitation of microgram quantities of protein utilizing the principle of protein-dye binding. Anal Biochem 1976;72:248-54.

[266] Zor T, Selinger Z. Linearization of the Bradford protein assay increases its sensitivity: theoretical and experimental studies. Anal Biochem 1996;236:302-8.

[267] Werz O. Inhibition of 5-lipoxygenase product synthesis by natural compounds of plant origin. Planta Med 2007;73:1331-57.

[268] Werz O, Steinhilber D. Development of 5-lipoxygenase inhibitors--lessons from cellular enzyme regulation. Biochem Pharmacol 2005;70:327-33.

[269] Burkert E, Arnold C, Hammarberg T, Radmark O, Steinhilber D, Werz O. The C2-like beta-barrel domain mediates the Ca2+-dependent resistance of 5-lipoxygenase activity against inhibition by glutathione peroxidase-1. J Biol Chem 2003;278:42846-53.

[270] Reddy KV, Hammarberg T, Radmark O. Mg2+ activates 5-lipoxygenase in vitro: dependency on concentrations of phosphatidylcholine and arachidonic acid. Biochemistry 2000;39:1840-8.

[271] Karlsson R, Kullman-Magnusson M, Hamalainen MD, Remaeus A, Andersson K, Borg P, et al. Biosensor analysis of drug-target interactions: direct and competitive binding assays for investigation of interactions between thrombin and thrombin inhibitors. Anal Biochem 2000;278:1-13.

[272] Claveau D, Sirinyan M, Guay J, Gordon R, Chan CC, Bureau Y, et al. Microsomal prostaglandin E synthase-1 is a major terminal synthase that is selectively up-regulated during cyclooxygenase-2-dependent prostaglandin E2 production in the rat adjuvant-induced arthritis model. J Immunol 2003;170:4738-44.

[273] Guay J, Bateman K, Gordon R, Mancini J, Riendeau D. Carrageenan-induced paw edema in rat elicits a predominant prostaglandin E2 (PGE2) response in the central nervous system associated with the induction of microsomal PGE2 synthase-1. J Biol Chem 2004;279:24866-72.

[274] Hanke JH, Gardner JP, Dow RL, Changelian PS, Brissette WH, Weringer EJ, et al. Discovery of a novel, potent, and Src family-selective tyrosine kinase inhibitor. Study of Lck- and FynT-dependent T cell activation. J Biol Chem 1996;271:695-701.

[275] Hunter T. A tail of two src's: mutatis mutandis. Cell 1987;49:1-4.

[276] Bleasdale JE, Thakur NR, Gremban RS, Bundy GL, Fitzpatrick FA, Smith RJ, et al. Selective inhibition of receptor-coupled phospholipase C-dependent processes in human platelets and polymorphonuclear neutrophils. J Pharmacol Exp Ther 1990;255:756-68.

[277] Blake RA, Broome MA, Liu X, Wu J, Gishizky M, Sun L, et al. SU6656, a selective src family kinase inhibitor, used to probe growth factor signaling. Mol Cell Biol 2000;20:9018-27.

[278] Feinstein MB, Pumiglia K, Lau LF. Tyrosine phosphorylation in platelets: its regulation and possible roles in platelet functions. Adv Exp Med Biol 1993;344:129-48.

[279] Wegert W, Graff J, Kaiser D, Breddin HK, Klinkhardt U, Harder S. Effects of antiplatelet agents on platelet-induced thrombin generation. Int J Clin Pharmacol Ther 2002;40:135-41.

[280] Ammon HP, Safayhi H, Mack T, Sabieraj J. Mechanism of antiinflammatory actions of curcumine and boswellic acids. J Ethnopharmacol 1993;38:113-9.

[281] Fleming I. Epoxyeicosatrienoic acids, cell signaling and angiogenesis. Prostaglandins Other Lipid Mediat 2007;82:60-7.

[282] Warner TD, Vojnovic I, Bishop-Bailey D, Mitchell JA. Influence of plasma protein on the potencies of inhibitors of cyclooxygenase-1 and -2. FASEB J 2006;20:542-4.

[283] Werz O, Szellas D, Henseler M, Steinhilber D. Nonredox 5-lipoxygenase inhibitors require glutathione peroxidase for efficient inhibition of 5-lipoxygenase activity. Mol Pharmacol 1998;54:445-51.

[284] Surette ME, Palmantier R, Gosselin J, Borgeat P. Lipopolysaccharides prime whole human blood and isolated neutrophils for the increased synthesis of 5-lipoxygenase products by enhancing arachidonic acid availability: involvement of the CD14 antigen. J Exp Med 1993;178:1347-55.

[285] Siemoneit U. PC, Jazzar B., Northoff H., Skarke C., Jauch J. and Werz O. On the interference of boswellic acids with 5-lipoxygenase: Mechanistic studies *in vitro* and pharmacological relevance. Eur J Pharmacol 2009;in press.

[286] Peters-Golden M, Henderson WR, Jr. Leukotrienes. N Engl J Med 2007;357:1841-54.

[287] Rich RL, Myszka DG. Advances in surface plasmon resonance biosensor analysis. Curr Opin Biotechnol 2000;11:54-61.

[288] Giannetti AM, Koch BD, Browner MF. Surface plasmon resonance based assay for the detection and characterization of promiscuous inhibitors. J Med Chem 2008;51:574-80.

[289] Park JY, Pillinger MH, Abramson SB. Prostaglandin E2 synthesis and secretion: the role of PGE2 synthases. Clin Immunol 2006;119:229-40.

[290] Harada Y, Tanaka K, Uchida Y, Ueno A, Oh-Ishi S, Yamashita K, et al. Changes in the levels of prostaglandins and thromboxane and their roles in the accumulation of exudate in rat carrageenin-induced pleurisy--a profile analysis using gas chromatography-mass spectrometry. Prostaglandins 1982;23:881-95.

[291] Gemmell DK, Cottney J, Lewis AJ. Comparative effects of drugs on four paw oedema models in the rat. Agents Actions 1979;9:107-16.

[292] Singh S, Khajuria A, Taneja SC, Khajuria RK, Singh J, Qazi GN. Boswellic acids and glucosamine show synergistic effect in preclinical anti-inflammatory study in rats. Bioorg Med Chem Lett 2007;17:3706-11.

[293] Kawamura M, Hatanaka K, Saito M, Ogino M, Ono T, Ogino K, et al. Are the anti-inflammatory effects of dexamethasone responsible for inhibition of the induction of enzymes involved in prostanoid formation in rat carrageenin-induced pleurisy? Eur J Pharmacol 2000;400:127-35.

[294] Willis D, Moore AR, Willoughby DA. Heme oxygenase isoform expression in cellular and antibody-mediated models of acute inflammation in the rat. J Pathol 2000;190:627-34.

[295] Hardy MM, Seibert K, Manning PT, Currie MG, Woerner BM, Edwards D, et al. Cyclooxygenase 2-dependent prostaglandin E2 modulates cartilage proteoglycan degradation in human osteoarthritis explants. Arthritis Rheum 2002;46:1789-803.

[296] Murakami M, Kudo I. Prostaglandin E synthase: a novel drug target for inflammation and cancer. Curr Pharm Des 2006;12:943-54.

[297] Li X, Afif H, Cheng S, Martel-Pelletier J, Pelletier JP, Ranger P, et al. Expression and regulation of microsomal prostaglandin E synthase-1 in human osteoarthritic cartilage and chondrocytes. J Rheumatol 2005;32:887-95.

[298] Westman M, Korotkova M, af Klint E, Stark A, Audoly LP, Klareskog L, et al. Expression of microsomal prostaglandin E synthase 1 in rheumatoid arthritis synovium. Arthritis Rheum 2004;50:1774-80.

[299] Jachak SM. PGE synthase inhibitors as an alternative to COX-2 inhibitors. Curr Opin Investig Drugs 2007;8:411-5.

[300] Cheng Y, Wang M, Yu Y, Lawson J, Funk CD, Fitzgerald GA. Cyclooxygenases, microsomal prostaglandin E synthase-1, and cardiovascular function. J Clin Invest 2006;116:1391-9.

[301] Xu D, Rowland SE, Clark P, Giroux A, Cote B, Guiral S, et al. MF63 [2-(6-chloro-1H-phenanthro[9,10-d]imidazol-2-yl)-isophthalonitrile], a selective microsomal prostaglandin E synthase-1 inhibitor, relieves pyresis and pain in preclinical models of inflammation. J Pharmacol Exp Ther 2008;326:754-63.

[302] Ruggeri ZM. Platelets in atherothrombosis. Nat Med 2002;8:1227-34.

[303] Quek LS, Bolen J, Watson SP. A role for Bruton's tyrosine kinase (Btk) in platelet activation by collagen. Curr Biol 1998;8:1137-40.

[304] Dangas G, Marmur JD, King TE, De Leon J, Sharma SK, Vidhun R, et al. Effects of platelet glycoprotein IIb/IIIa inhibition with abciximab on thrombin generation and activity during percutaneous coronary intervention. Am Heart J 1999;138:49-54.

[305] Chesebro JH, Zoldhelyi P, Badimon L, Fuster V. Role of thrombin in arterial thrombosis: implications for therapy. Thromb Haemost 1991;66:1-5.

[306] Quinton TM, Kim S, Dangelmaier C, Dorsam RT, Jin J, Daniel JL, et al. Protein kinase C- and calcium-regulated pathways independently synergize with Gi pathways in agonist-induced fibrinogen receptor activation. Biochem J 2002;368:535-43.

[307] Quinton TM, Ozdener F, Dangelmaier C, Daniel JL, Kunapuli SP. Glycoprotein VI-mediated platelet fibrinogen receptor activation occurs through calcium-sensitive and PKC-sensitive pathways without a requirement for secreted ADP. Blood 2002;99:3228-34.

[308] Le Blanc K, Berg A, Palmblad J, Samuelsson J. Defective platelet aggregation in polycythaemia vera is not caused by impaired calcium signaling, phospholipase D activation or decreased amounts of focal adhesion proteins. Eur J Haematol 2000;65:322-30.

9 PUBLICATIONS

9.1 Original publications

1. Tausch L., **Siemoneit U**., Henkel A., Poeckel D., Kather N., Franke L., Hofmann B., Schneider G., Angioni C., Geisslinger G., Skarke C., Holtmeier W., Beckhaus T., Karas M., Jauch J. and Werz O. *Identification of human cathepsin G as a functional target of boswellic acids from the anti-inflammatory remedy frankincense.* J Immunol 2009 (in revision)

2. Koeberle A., **Siemoneit U**., Northoff H., Hofmann B., Schneider G. and Werz O. *MK-886, an inhibitor of the 5-lipoxygenase-activating protein, inhibits cyclooxygenase-1 activity and suppresses platelet aggregation*. Eur J Pharmacol 2009 (in press)

3. **Siemoneit U**., Pergola A., Jazzar B., Northoff H., Skarke C., Jauch J. and Werz O. *On the interference of boswellic acids with 5-lipoxygenase: Mechanistic studies in vitro and pharmacological relevance*. Eur J Pharmacol 2009 (in press)

4. Koeberle A., **Siemoneit U**., Bühring U., Laufer S., Albrecht W. and Werz O. *Licofelone suppresses prostaglandin E_2 formation by interference with the inducible microsomal prostaglandin E_2 synthase-1*. J Pharmacol Exp Ther 2008, Sep; 326(3):975-82

5. **Siemoneit U**., Hofmann B., Kather N., Lamkemeyer T., Madlung J., Franke L., Schneider G., Jauch J., Poeckel D., and Werz O. *Identification and functional analysis of cyclooxygenase-1 as a molecular target of boswellic acids*. Biochem Pharmacol. 2008, Jan; 75(2):503-13

6. **Siemoneit U**., Schmitt C., Alvarez-Lorenzo C., Luzardo A., Otero-Espinar F., Concheiro A. and Blanco-Mendez J. *Acrylic/cyclodextrin hydrogels with enhanced drug loading and sustained release capability*. Int J Pharm 2006; 312(1-2):66-74

7. **Siemoneit U**., Koeberle A., Rossi A., Reckel S., Maier TJ., Jauch J., Northoff H., Doetsch V., Sautebin L., and Werz O. *Boswellic acids from the anti-inflammatory remedy frankincense interact with the inducible microsomal prostaglandin E_2 synthase-1 and inhibit prostaglandin E_2 formation in-vitro and in-vivo*. Manuscript

8. **Siemoneit U**., Tausch L., Jauch J., and Werz O. *3-O-acetyl-11-keto-β-boswellic acid potently impairs agonist-induced Ca^{2+} mobilization and aggregation of washed human platelets*. Manuscript

9.2 Patents

1. **Siemoneit U**. and Werz O. *Preparations comprising boswellic acids for inhibiting the synthesis of prostaglandin E_2.* International patent (WO2008058514 20080522)

2. **Siemoneit U**., Henkel A., Jauch J. and Werz O. *Synthetic derivatives of boswellic acids for inhibiting microsomal prostaglandin E_2 synthase-1 and human cathepsin G mediated pathophysiological states*. (priority date: 26.03.2008)

9.3 Poster presentations

1. **Siemoneit U**., Poeckel D. and Werz O. *Boswellic acids differentially modulate Ca^{2+} mobilization and aggregation of human platelets*. DPhG Meeting, Marburg (2006).

2. Werz O., Poeckel D., Hofmann B., Schneider G., Jauch J. and **Siemoneit U**. *Identification of cyclooxygenase-1 as a molecular target of boswellic acids*. DPhG Meeting, Erlangen (2007).

3. Tausch L., **Siemoneit U**., Poeckel D., Kather N., Franke L., Schneider G., Holtmeier W., Beckhaus T., Karas M., Jauch J., and Werz O. *Identification of targets and molecular modes of action of boswellic acids*. DPhG Weihrauch Symposium, Tübingen (2008).

9.4 Oral presentations

1. **Siemoneit U**. and Werz O. *Boswellic acids from the anti-inflammatory remedy frankincense: Identification and functional analysis of novel molecular targets within the arachidonic acid cascade*. 7th Joint Meeting of AFERP, ASP, GA, PSE & SIF, Athens, Greece (2008).

10 ACKNOWLEDGEMENTS

Bei Herrn Prof. Dr. O. Werz möchte ich mich sehr herzlich für die Überlassung des spannenden Themas, eine exzellente Betreuung, optimale Arbeitsbedingungen, die unermüdliche Unterstützung, stete Diskussionsbereitschaft sowie erfolgreiche Zusammenarbeit bedanken.

Herrn Prof. Dr. S. Laufer danke ich für die Übernahme des Zweitgutachtens.

Besonderer Dank gebührt der Transfusionsmedizin des Universitätsklinikums Tübingen (Prof. Dr. H. Northoff und seinen Mitarbeiterinnen Frau Kotchoubey und Frau Listner) für die freundliche Bereitstellung von Vollblut und Buffy-Coats.

Herrn Prof. Dr. Alfred Nordheim und dem Proteom-Center Tübingen danke ich für die wertvolle Kooperation bezüglich der MS-Analytik.

Bei Frau Prof. Dr. L. Sautebin und Dr. Antonietta Rossi (Universität Neapel) bedanke ich mich für die erfolgreiche Zusammenarbeit im Rahmen der Tierexperimente.

Für die Bereitstellung des BIAcore® X Gerätes bedanke ich mich bei Prof. Dr. A. Steinle.

Dem stetig wachsenden „AK Werz“ danke ich für eine angenehme und kollegiale Arbeitsatmosphäre. Ein besonderer Dank geht an: die Ersten ihrer Zunft Dagmar Blaesius und Andreas Köberle; meinen Labornachbarn und Computerexperten Arne Henkel; die „DAB-ler“ Ulrike Bühring und Moritz Verhoff und den einzig verbliebenen Fußballfan Carlo Pergola.

Bei Bianca Jazzar und Gertrud Kleefeld sowie Hanne Braun bedanke ich mich für die hilfreiche Unterstützung im Labor- bzw. Uni-Alltag.

Herzlich gedankt sei auch Katharina Bauer, Gerd Helms, Holger Kahnt und dem AK Schulz für die unkomplizierte Starthilfe in den Anfängen des AK Werz in Tübingen.

Den Doktores Daniel Poeckel und Lars Tausch danke ich für die Einarbeitung und produktive Diskussionen rund ums Thema Weihrauch.

Meinen Freunden und „Pharmazeutischen Wegbegleitern“ in Heidelberg und Tübingen: Holger Weiß, Timm Krätzig, Bobby, Martin Bubik, Conny Witt, Uta Schneiders, Volker Dangel, Jutta Braun und Patrick Rother möchte ich für die schöne Zeit in- und außerhalb der Uni danken.

Ein besonders herzliches Dankeschön geht an meine Familie, für jedwede Unterstützung und das vorbehaltlose Vertrauen in den vergangenen fast 30 Jahren.

Der größtmögliche und herzlichste Dank gebührt meiner Frau Anett, die einen nicht unwesentlichen Anteil am Gelingen dieser Arbeit hat, für ihr Verständnis, ihre Geduld und große Nachsicht. Vor allem aber danke ich ihr für all die Dinge, die das Leben lebenswert machen.

11 AKADEMISCHE LEHRER

Meine akademischen Lehrer an der Ruprecht-Karls Universität Heidelberg waren:

Prof. Dr. Michael Eisenhut

Prof. Dr. Gert Fricker

Prof. Dr. Ulrich Hilgenfeldt

Prof. Dr. Andres Jäschke

Prof. Dr. Horst Ludwig

Prof. Dr. Nils Metzler-Nolte

Dr. Gabriele Reich

Prof. Dr. Jürgen Reichling

Prof. Dr. Manfred Wießler

Prof. Dr. Michael Wink

12 CURRICULUM VITAE

Persönliche Daten

Name	Ulf Siemoneit
Geburtsdatum, -ort	22.06.1979, Lingen (Ems)
Staatsangehörigkeit	deutsch
Familienstatus	verheiratet

Ausbildung

Seit 09/2005	Durchführung der Promotionsarbeit am Institut für Pharmazeutische Chemie der Eberhard Karls Universität, Tübingen
06/2005	Approbation als Apotheker und 3. Staatsexamen
11/2004 – 04/2005	2. Hälfte des Praktischen Jahres in der Kurfürstenapotheke, Heidelberg
05/2004 – 10/2004	1. Hälfte des Praktischen Jahres an der Universität Santiago de Compostela, Spanien, Institut für Pharmazeutische Technologie und Biopharmazie
10/1999 - 04/2004	Pharmaziestudium an der Ruprecht-Karls Universität, Heidelberg, 1. und 2. Staatsexamen
09/1995 – 06/1998	Allgemeine Hochschulreife, Gymnasium Johanneum, Lingen

Berufliche Tätigkeiten, Praktika, Weiterbildung und Lehrtätigkeit

Seit 09/2005	Stellvertretender Praktikumsleiter “Pharmazeutische Chemie II, Arzneibuchanalytik”, Studiengang Pharmazie, Universität Tübingen
Seit 09/2005	Weiterbildung zum Fachapotheker für Pharmazeutische Analytik, LAK Baden-Württemberg
09/2005 – 12/2008	Apotheker in der Römerapotheke, Rottenburg am Neckar
09/2002 – 10/2002	Praktikum am Biomedical Research Center, Guadalajara, Mexiko

Wehrersatzdienst

08/1998 – 8/1999	St. Bonifatius Hospital, Lingen

Fähigkeiten und Kenntnisse

Sprachen	Englisch, fließend
	Spanisch, fortgeschritten
EDV	MS Office, Sigma Plot, GrapdPad Software

Mitgliedschaften

Seit 2004	Deutsche Pharmazeutische Gesellschaft (DPhG)
Seit 2008	Gesellschaft für Arzneipflanzen- und Naturstoff-Forschung e.V.